

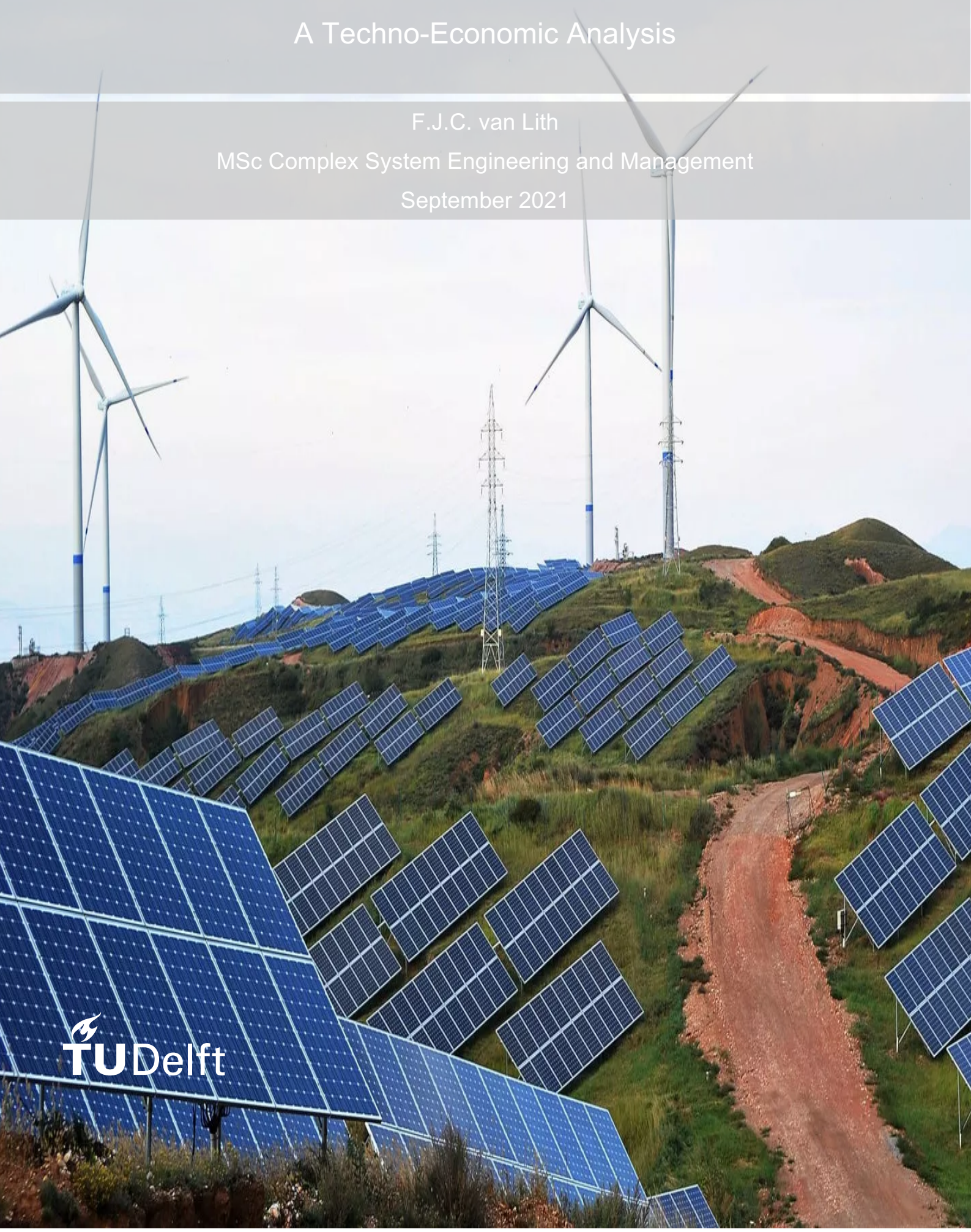
Renewable Energy Integration in the Jamali Power System

A Techno-Economic Analysis

F.J.C. van Lith

MSc Complex System Engineering and Management

September 2021



Renewable Energy Integration in the Jamali Power System

A Techno-Economic Analysis

by

F.J.C. van Lith

Master thesis submitted to Delft University of Technology
in partial fulfilment of the requirements for the degree of

MASTER OF SCIENCE

in Complex System Engineering and Management
Faculty Technology, Policy and Management

To be defended publicly on Wednesday September 15, 2021 at 15:00.

Student number: 5174570
Project duration: February 17, 2021 – September 15, 2021
Thesis committee: Prof. dr. K. Blok, Chair, Industry & Energy
Dr. Ir. P. W. Heijnen, First Supervisor, Industry & Energy
Dr. D. J. Scholten, Second Supervisor, Economics of Technology and Innovation
Msc. J. K. A. Langer, Advisor, Industry & Energy

Preface

Dear Reader,

Completing this thesis concludes my master Complex System Engineering and Management at Delft University of Technology. The thesis project has been a challenging endeavor, which was both exhausting and satisfying at the same time. However, before moving to the next chapter, I would like to express my gratitude to all that have supported me in the last half year.

First, I wish to express my gratitude to my graduation committee. Thank you Dr.ir. Petra Heijnen for the numerous meetings, time and interest in my thesis project. Throughout the meetings you challenged me to substantiate my research decisions, structure them and remain critical. Thereby, I want to express my gratitude to Prof.dr. Kornelis Blok who has provided constructive feedback on the project and provided me with new insights based on his expertise. Also, I would like to thank Dr. Daniel Scholten for your advice to see the bigger picture and not to get lost in the modeling. To Msc. Jannis Langer I want to express my gratitude for all the meetings, engagement in the project, discussions and understanding my doubts.

Furthermore, I would like to thank my family and my parents in particular for their unyielding support throughout my studies and more specifically during the last six months. Also, I want to thank my girlfriend, roommates and friends for their patience and refreshing moments during the project.

EJ.C. van Lith
Amsterdam, September 2021

Summary

With the release of the sixth IPCC report climate change has become more pressing than ever before, but catastrophic consequences can be prevented if the global community acts fast. Through industrial reform developing countries experience large economic growth. However, this growth has a dangerous side, the associated carbon emissions. Therefore, developing countries face a unprecedented challenge, namely, reducing greenhouse gas emissions while striving for significant economic growth. In the power sector emission reductions can be realized by transitioning from conventional generators to renewable sources. The challenge, also, comes with opportunities, because there will be a need for new power plant capacity as a consequence of the growth in electricity demand.

The Indonesian electricity demand has experienced a growth of 8.4% between 2009 and 2019. At the same time, its power sector depends mainly on coal power plants for electricity production. Therefore, the government has set a target of increasing new and renewable energy sources in the energy mix by 23% in 2030 and 31% in 2050. The country has abundant renewable energy sources, which are largely untouched. Integration of renewable energy technologies requires adaptation of the existing infrastructure, because potentials are in different locations than the existing conventional generators. And their production is driven (for most technologies) by weather occurrences, which makes them not dispatchable. Therefore, flexibility options such as electricity storage have to be developed and efficiently operated for a secure continuous supply of electricity.

This thesis has investigated the effect that different carbon emission reduction limits have on the power system design of Indonesia's largest electricity system, the Java-Madura-Bali (Jamali) system. This was done by studying the potential of various promising renewable energy technologies (solar photovoltaics, on- and off-shore wind, Ocean Thermal Energy Conversion (OTEC), geothermal and hydropower) in combination with short- and long-term storage (lithium-ion batteries and hydrogen storage) and grid expansions to mitigate renewable variability. For this purpose a techno-economic model was developed that optimizes operation and capacities of generation, storage and network simultaneously. The model simulates the system dynamics in the Jamali system in 2050 and was implemented in Python for Power System Analysis (PyPSA) and optimized with the Gurobi commercial solver.

In this thesis renewable energy potentials were collected or estimated, it was found that there are abundant renewable energy sources in and around Java and Bali. There is, in particular, a strong business case for solar photovoltaics, because of its relatively low costs and constant availability throughout the modeled year. Especially, when taking into consideration technology cost reductions as a result of technological learning. Thereby, lithium-ion batteries complement solar electricity production in high carbon reduction scenarios by mitigating their diurnal variability. It was found that there is an exponential relationship between system costs and carbon emission reductions in the Jamali power system. Additionally, only moderate system cost increases were found up to 80% emission reductions compared to the reference scenario with no emission mitigation efforts. At higher carbon reduction scenarios the solar capacities reach their maximum installable capacities. As a result, system cost increase exponentially due to the need for OTEC and offshore wind capacities.

In low carbon scenarios high battery capacities were found and network expansion is limited. It can be concluded that the Jamali network cannot smooth the variability of wind throughout the power system, therefore, without storage capacities the system cost almost double. On the other hand, the network remains important to transport electricity from rich renewable regions to large demand centers. In low carbon scenarios very high battery capacities were found, a possible link to the transport sector has been proposed for future research, which potentially can cover the high battery capacities found in this thesis.

OTEC, an ocean renewable energy technology in its early development stage, is deployed as a baseload power plant in the model. It was found that it is deployed in the Jamali power system at 90% carbon reductions and higher. However, it was also found that OTEC investments depend on the utilization, installable potentials and the costs of other technologies in the system. Thereby, with the site specific data the spatial investment

decisions of the model were shown, which demonstrates the need for consideration of spatial-economic detail in power system models.

In fact, the uniform fixed costs of offshore wind together with the coarse spatial resolution (25 by 25 km²) and aggregation of the renewable potentials to the energy regions are the main limitations of the study. As a result, OTEC investments may have been overestimated, whereas offshore wind capacities were underestimated.

This study developed a model with a temporal and spatial dimension of the Jamali power system, which provided insights into the system dynamics by 2050 and the effect of carbon emission reduction targets on the system design. Based on the results three recommendations were made. First, a reconsideration/reformulation of the present energy targets set for 2050 is recommended based on the low system costs of carbon reductions up to 60% found in this thesis. Second, a reconsideration of the strategy to achieve the renewable energy target in 2050 is suggested, in which solar energy in combination with short-term storage should have a more prominent role considering its importance in the cost-optimal low carbon scenarios. Also, planning and operation of flexibility options (storage and network expansion) should receive sufficient attention in the strategy. Thirdly, policy instruments supporting coal should be reconsidered and policy instruments should be designed and applied to stimulate the use of solar and batteries, because with the cost assumptions in this thesis most renewables will not outperform unsubsidized coal in 2050.

Contents

Summary	ii
List of Figures	vii
List of Tables	viii
1 Introduction	1
1.1 Indonesian Power System	1
1.2 Renewable Energy Transition in Indonesia	1
1.3 Problem Definition and Research Objective	2
1.4 Research Approach	3
1.5 Modeling Tool	3
1.6 Scope	4
1.7 Alignment to Complex System Engineering and Management	4
1.8 Thesis Outline	5
2 Literature Review	6
2.1 Literature Search and Selection Methodology	6
2.2 Literature Table and Findings	6
2.2.1 Geographical Scope	7
2.2.2 Renewable Energy Technologies Considered	9
2.2.3 Future demand year and technology cost reductions	9
2.2.4 Carbon constraints	9
2.2.5 Spatial economic detail	9
2.3 Knowledge Gaps	10
2.4 Research Questions	10
2.5 Thesis Contributions	11
3 Materials and Methods	12
3.1 Conceptualization of the Jamali Power System	12
3.1.1 Topological Transmission System Data	12
3.1.2 Methodology for the Conceptualization of a Power System Graph	13
3.1.3 Electrical Components of the Transmission Lines	13
3.1.4 Methodology for Network Simplification	14
3.2 Electricity Demand, Conventional Generators and Electricity Storage	15
3.2.1 Electricity Demand	15
3.2.2 Conventional Generation	15
3.2.3 Electricity Storage	16
3.3 Renewable Energy Potentials	17
3.3.1 Ocean Thermal Energy Conversion Potentials	17
3.3.2 Hydropower Potentials	18
3.3.3 Geothermal Potentials	18
3.3.4 Solar, On- and Offshore Wind Energy Potentials	18
3.3.5 Methodology for Capacity Potential Estimation Solar and Wind	18
3.3.6 Time Series Solar and Wind	20
3.4 Technology Cost Assumptions	20
3.4.1 OTEC Site Specific Fixed Costs	21
3.4.2 Annualized Costs	21
3.4.3 Learning Curves	21
3.4.4 Variable Cost	22

3.5	Co-optimization of Generation, Network and Storage.	22
3.5.1	Linear Optimal Power Flow	23
3.5.2	Power Flow.	23
3.5.3	Constraints	26
3.6	Modeling Logic and Overview.	27
3.6.1	Model Inputs.	27
3.6.2	Decision Variables and Constraints	27
3.6.3	Global Carbon Constraint	28
3.6.4	Model Outputs.	28
3.7	Scenario Analysis and Modeling Assumptions	29
3.7.1	Simulation Approach	29
3.7.2	Reduction of the Problem Size	30
3.7.3	Greenfield Approach.	30
3.7.4	Centralised Planning Model - Competitive Market Model	30
3.7.5	Social and Technical Feasibility of the Outcomes	31
3.7.6	Grid Stability.	31
4	Results	32
4.1	Jamali Power System Conceptualized Model Results	32
4.1.1	Default Model	32
4.1.2	Network Simplification	32
4.2	Model Validation	33
4.2.1	Electricity Demand Proxy 2018.	33
4.2.2	Conventional Generators 2018.	34
4.2.3	Model Validation Results.	34
4.3	Demand and Conventional Generator Capacity Extrapolations 2050	36
4.3.1	Electricity Demand 2050.	36
4.3.2	Conventional Generator Capacity 2050	36
4.4	Renewable Energy Potentials Results	36
4.4.1	Ocean Thermal Energy Conversion Potentials	36
4.4.2	Hydropower Potentials.	37
4.4.3	Geothermal Potentials	37
4.4.4	Solar Potentials	38
4.4.5	Wind On- and Offshore Potentials	38
4.4.6	Time Series	39
4.4.7	Total Renewable Energy Potentials.	39
4.5	Simulation Results	40
4.5.1	Case 1: Technology Costs 2020.	41
4.5.2	Case 2: 2050 Forecast Cost	46
4.5.3	Case 3: The Role of OTEC	50
4.5.4	Case 4: The Role of Storage and the High Voltage Network	52
4.6	Sensitivity Analysis	54
4.6.1	Conventional Generator Capacity Constraint	55
4.6.2	100% Renewable Scenario	55
4.6.3	Solar Capital Cost	56
5	Discussion	57
5.1	Cost-Optimal Results	57
5.1.1	Comparison to Power System Models	57
5.1.2	Comparison to Jamali Models	58
5.1.3	OTEC and Offshore Wind	58
5.1.4	Battery Capacity - Transport Sector Coupling	59

5.2	Model Discussion and Uncertainties	60
5.2.1	Electricity Demand	60
5.2.2	Energy Regions.	60
5.2.3	Spatial Resolution	60
5.2.4	Availability Factors.	60
5.2.5	Spatial-Economic Resolution	61
5.2.6	Technological Learning	61
5.2.7	Weather Data	61
5.2.8	Variability OTEC and Hydropower	61
5.2.9	Technology Selection	61
5.2.10	Temporal Resolution.	62
5.2.11	Electrical Characteristics and Power Flow	62
5.3	Research Approach and Methodology.	62
5.3.1	Greenfield Optimization and Transition Pathways	62
5.3.2	Deterministic Approach and Optimization.	62
5.3.3	Consideration of Non-Technological Factors.	63
5.4	Implications for Policy Planning	63
5.4.1	Critical Appraisal.	63
5.4.2	Implications for Present Targets and Policies.	64
5.5	Reflection Contributions	65
5.5.1	Scientific Contribution.	65
5.5.2	Societal Contribution	65
6	Conclusion and Outlook	67
6.1	Research Questions Revisited	67
6.1.1	Power System Conceptualization	67
6.1.2	Renewable Energy Potentials	67
6.1.3	Effect of Technological Learning	68
6.1.4	Role of OTEC.	68
6.1.5	Network and Storage.	68
6.1.6	Effect of Carbon Reductions	69
6.2	General Conclusion and Recommendation	69
6.2.1	General Conclusion	69
6.2.2	Recommendation Power System Planning.	69
6.3	Outlook	70
6.3.1	Spatial economic Detail	70
6.3.2	Sector Coupling	70
6.3.3	Interconnecting the Indonesian Grids	70
6.3.4	Indonesian Power System Modeling and System Robustness	71
6.3.5	Combination of Methods	71
6.3.6	El Niño.	71
	Bibliography	72
A	A1	77
B	B1	78

List of Figures

3.1	Raw Transmission Data	13
3.2	Raster within provincial boundaries	19
3.3	Modeling Logic and Overview	28
3.4	Case Overview	29
4.1	Default Model	32
4.2	Energy Regions Clustering	33
4.3	Simplified Model	33
4.4	Hourly Electricity Demand Proxy	34
4.5	Electricity Demand Distribution	34
4.6	Conventional Generators	35
4.7	Model Validation - Dispatch	35
4.8	Load Duration Curves 2020/2050	36
4.9	OTEC Potential Sites	37
4.10	Solar Spatially Resolved Potentials	38
4.11	Wind Spatially Resolved Potentials	39
4.12	Aggregated Time Series	39
4.13	Aggregated Duration Curves	40
4.14	Distributed Maximum Renewable Energy Potentials	40
4.15	Case 1: Carbon Emissions	41
4.16	Case 1: Generator Capacities	42
4.17	Case 1: Network and Storage Capacities	43
4.18	Case 1: Average System Costs	44
4.19	Case 1: System Layout	45
4.20	Case 2: Carbon Emissions	46
4.21	Case 2: Generators Capacities	47
4.22	Case 2: Network and Storage Capacities	47
4.23	Case 2: Average System Costs	48
4.24	Case 2: System Layout	49
4.25	Case 3: OTEC Site Investments	50
4.26	Case 3: Average System Costs	51
4.27	Case 3: Network and Storage Capacities	52
4.28	Case 4: Average System Costs	53
4.29	Case 4: No Network Expansions	54
4.30	Case 4: No Storage + No OTEC	54
4.31	Sensitivity: No Conventional Generator Constraints	55
4.32	Sensitivity: Zero Carbon Emissions	56
4.33	Sensitivity: Solar Capital Costs	56
B.1	Offshore Wind Validation Duration Curve	78
B.2	Onshore Wind Validation Duration Curve	78
B.3	Offshore Wind Statistics	79
B.4	Onshore Validation Duration Curve	79

List of Tables

2.1 Literature Review Table	7
3.1 Electrical Characteristics Conductor	14
3.2 Power Plant Characteristics	16
3.3 Technology Cost Assumptions	23
4.1 Model Validation - Comparison	35
4.2 OTEC Potentials	37
4.3 Hydropower Potentials	37
4.4 Geothermal Potentials	38
4.5 Solar Potentials	38
4.6 Wind On- and Offshore Potentials	38

Nomenclature

α_s	Availability factor	Pd_s	Power density
\bar{F}_ℓ	Maximum installable transmission capacity	Q_n	Reactive Power
$\bar{G}_{n/c,s}$	Maximum installable generation capacity	r	Discount rate
ΔT	Temperature difference	R_ℓ	Resistance
ℓ	Edges (Transmission lines)	s	Generator and storage technologies
η_1/η_2^{-1}	Charge/discharge efficiencies	T	Technology lifetime
η_s	Thermal efficiency	t	Timesteps (hours)
$\frac{P_2}{P_1}$	Technology capacity increase	V	Voltage Magnitude
θ_n	Voltage Angle	X_ℓ	Reactance
$A_{c,s}$	Available area	$SoC_{n,s,t}$	State of charge
b	Technology experience index	A	Adjacency/Admittance matrix
B_ℓ	Susceptance	D	Degree matrix
c	Grid cell	$K_{n,\ell}$	Incidence matrix
c_ℓ	Fixed annualised transmission line costs	L	Laplacian matrix
$c_{n,s}$	Fixed annualised generator and storage costs		
C_P	Cost of technology		
CRF	Capital recovery factor		
d	Distance		
$d_{n,t}$	Electricity demand		
$E_{n,s}$	Energy capacity storage		
e_s	Specific CO2 emissions		
$f_{\ell,t}$	Power flow		
F_ℓ	Transmission line capacity		
$g_{n,s,t}$	Generator and storage dispatch		
$G_{n,s}$	Generation and storage capacity		
$h_{s,max}$	Maximum time for (dis)charge storage		
n	Nodes (Energy regions)		
$o_{n,s}$	Variable generation and storage cost		
P_n	Active Power		
P_{net}	Power capacity OTEC plant		

1

Introduction

In this chapter the topic of this thesis is introduced by discussing the Indonesian power system and its renewable energy integration targets. Thereafter, the problem definition and the research objective are formulated. Subsequently, the research approach is presented and discussed and a modeling tool is selected. The scope and boundaries of the research are addressed and the relevance of the research topic for the Master program Complex System Engineering and Management is substantiated.

1.1. Indonesian Power System

Indonesia has a population of more than 270 million people and is the fourth most populous country in the world. Electricity demand has increased with a rate of 8.4% between 2009 and 2019 [64]. Perusahaan Listrik Negara (PLN) is the state electricity company that holds exclusive rights over the transmission, distribution and supply of electricity to the public [76]. PLN is a monopolistic vertical integrated utility [83]. PLN estimates an annual electricity demand growth of 6.42% between 2019 and 2028 in their electricity procurement plan (Rencana Usaha Penyediaan Tenaga Listrik/ RUPTL) [74]. Afterwards, considerable growth is expected due to the economic and population growth and improved living standards [58].

Due to its unique topography Indonesia has a fragmented transmission grid, the archipelago has eight large isolated electricity networks. The Jamali power system is the largest network with regard to electricity produced and consumed [76]. Due to under investments in generation capacity several systems suffer from insufficient reserve margins. The Jamali system on the contrary has sufficient reserve margins, but remains prone to large blackouts [58]. Since the power systems are not interconnected this thesis focuses on the Jamali power system, because it covers about 67% of all electricity demand in Indonesia [73].

1.2. Renewable Energy Transition in Indonesia

Although, investments in coal power plants are the cheapest option to secure generation capacity in the future, the Indonesian government faces the energy trilemma [30]. Therefore, in the National Energy General Plan (Rencana Umum Energi Nasional/ RUEN) the government aims to increase the share of renewables in the electricity mix to 23% in 2025 and 31% in 2050 [48]. According to IRENA [48] the 31% target can be achieved by 2030. On the other hand, Maulidia et al. [58] doubt the feasibility of the 2025 target due to the fact that installed capacities are lower than the targets set in RUEN for the past several years. Interestingly, in RUEN the targets are to be achieved mainly by investments in large- and micro-hydropower and geothermal energy. These technologies typically have long lead up times. Thereby, solar and wind energy are becoming cost competitive in other parts of the world. For example, it is shown that with the present technology prices a low carbon European energy system is feasible and cost competitive [7].

The underlying model structure for the RUEN is based on the Long-range Energy Alternatives Planning (LEAP) tool. According to Maulidia et al. [58] the choice for renewable technologies in RUEN are proportional to total potentials estimated through a modeling exercise of the Ministry of Energy and Mineral Resources (MEMR). However, solar, wind and ocean renewable energy potentials have been found to be considerably higher in other studies than the estimates used in RUEN [45] [50] [53] [12]. Therefore, utilization of these potentials

may be more cost efficient than the plans presented in RUEN. In turn this may pave the way for higher deployment of renewable energy capacity, which contributes to managing the energy trilemma faced by the Indonesian government. Thereby, the utilization of wind and solar resources have several advantages with regard to their renewable counterparts. They have short lead-up times, are modular and require no fuels for electricity production [19]. Nevertheless, solar and wind technologies have a very small share in the present Indonesian generation mix. Maulidia et al. [58] identified several reasons for the slow renewable energy integration in Indonesia. Among these barriers is the monopolised power sector and subsidies for fossil fuels. Independent modeling practices will therefore increase the transparency in the Indonesian power sector with unbiased model inputs.

In scientific literature several efforts by independent parties have been conducted to simulate and optimize the future generation mix of the Jamali power systems [34] [85] [31]. Interestingly, cost-optimal outcomes deviate from the capacity expansion plans formulated in RUEN, although, power system models may not be one on one comparable with the LEAP model, which covers multiple sectors. However, solar and wind energy sources cannot provide the baseload power function that is traditionally provided by coal power plants in Indonesia and can be provided by hydropower and geothermal energy to a certain extent. To maintain energy security with the integration of variable renewable energy sources flexibility solutions are needed to mitigate the intermittent power generation of these renewable energy technologies.

More specifically, renewable energy technology integration in power systems requires a redesign of the entire system, because of the different spatial orientation of renewable capacities opposed to conventional generators and their intermittent output, which varies spatially and temporally [72]. To address this models ideally should have high temporal and spatial resolution. Currently, independent authors neglected the electricity network in the Jamali power system and/or did not consider realistic renewable energy potentials.

In the Indonesian Energy Outlook the LEAP tool is used in combination with the Balmorel model that optimizes the operation of multiple sectors including the electricity sector in 2050 [18]. However, generators and network capacities are closely intertwined and their joint consideration in power system planning contains advantages. Krishnan et al. [52] showed that simultaneous optimization of transmission and generation results in lower costs than decoupled solutions. Additionally, Go et al. [28] found that including energy storage next to generation and network expansion as a decision variable in the objective function results in investment deferral, which reduces the total system cost of the solution.

To meet the future electricity demand and manage the energy trilemma in Indonesia careful and accurate power system planning is of paramount importance. Taking into consideration the alarming climate change rate the utilization of renewable energy potentials in Indonesia is inevitable. It is, therefore, pivotal to study the costs and technical feasibility of low carbon configurations of the largest power system in Indonesia, the Jamali system. Optimization is an approach that is frequently applied to find the cost-optimal design of power systems. Optimization of generation, storage and network capacities and system operation simultaneously (co-optimization) ensures sufficient flexibility options for a secure system. Therefore, co-optimizing the system would provide valuable and new insights that will assist in setting transparent and quantitative targets and provide clear direction for power system planning.

1.3. Problem Definition and Research Objective

The previous section suggests a gap between renewable energy potentials in Indonesia and their inclusion in the policy targets set in RUEN. More specifically, in the policy targets emphasis is on geothermal and hydropower, whilst Indonesia has abundant solar irradiation of $4.8 \text{ kWh/m}^2/\text{day}$ on average [19] [92]. On the other hand, high wind speeds are relatively scarce, but there is considerable technical potential for on- and offshore wind development [50]. Including these potentials in an optimization model may result in different and valuable insights for adapting policy targets and direction for cost-optimal power system planning.

Considering those potentials and optimizing the power mix based on costs covers only the affordability and sustainability pillars of the energy trilemma. The Indonesian power system is fragmented and can therefore not be considered as a single system. Therefore, the choice to focus on the Jamali power system was made. Currently, the Jamali system experiences power outages, which may be prevented by sufficient flexibility solutions in the future. Therefore, the electricity network and electricity storage should also be included in power system modeling to ensure security of supply, especially, with the integration of variable renewable energy

technologies.

The main goal of this thesis is to assist to the energy transition of the Jamali power network from an independent perspective. This will be achieved by creating a model of the Jamali power system that includes the transmission network, renewable and conventional generators and short- and long-term storage. This research aims to find cost-optimal solutions under different carbon emissions of the system in 2050 with high temporal resolution. More specifically, aim of this thesis is to find the cost-optimal capacities of the network, storage and different generation technologies in 2050 as well as the hourly optimal dispatch of the system (i.e. dispatch of generators and storage and the flow of power over the transmission lines).

By conducting a scenario analysis the effect of a decreasing carbon constraint on the total cost of the system and generator, storage and network capacity will be evaluated. Also, technological learning will be included in the scenario analysis.

This thesis intends to provide insights in the role of sustainable energy technologies, the high voltage network and energy storage under different carbon constraints to support the Indonesian government in formulating energy targets and strategies for the Jamali power system. The results will contribute to the transparency of power system planning in the Jamali power network. The model can be perceived as a proof of concept and an analysis of the system dynamics rather than a detailed analysis for the development of individual components such as sustainable energy technologies, transmission line extensions or storage facilities. Additionally, with the research approach and methodology presented in this thesis other high voltage power system networks in Indonesia can be modeled.

1.4. Research Approach

This research takes a modeling approach, a techno-economic model will be developed to replicate the future state and system dynamics of the Jamali power system. The main advantage of this approach is that system interventions can be simulated and can be tested without real world consequences. However, a main limitation of using models is that they are simplifications of reality, their results depend on assumptions and input data, which follows the garbage in garbage out principle [61]. Therefore, reflection on the validity of data inputs is important to identify caveats and interpret results. The modeling approach consists of three main steps.

First, the existing Jamali high-voltage network will be conceptualized into a model consisting of nodes and edges. To this end, a methodology will be developed that preserves the geospatial orientation of the power network. Accordingly, the conceptualized high-voltage network serves as the base of the power system model that will be co-optimized. Second, georeferenced renewable energy potentials for solar, on- and offshore wind, OTEC, geothermal energy and hydropower will be collected. If the potentials are not publicly available with sufficient spatial resolution they will be estimated. Third, generation, network and storage capacities will be co-optimized in several scenarios for a single year (2050) as well as dispatch of generators and storage and power flow per time step (hourly) to meet the research objectives formulated in section 1.3 in this thesis. For the co-optimization a modeling tool will be selected, the choice is substantiated in the next section.

Based on the techno-economic model results a recommendation will be made with respect to possible direction for power system planning and the reformulation of renewable energy targets for the Jamali power system by 2050.

1.5. Modeling Tool

Energy system models can generally be divided in top-down and bottom-up models [75]. Bottom-up models capture in detail the components of energy systems and their interconnections. Such models can cover a single sector like the electricity sector as well as multiple sectors. Although, interconnections between multiple sectors such as the thermal and electricity sector provides many benefits from an economic perspective [57] [8], the modeling and data collection becomes more complicated. The focus in this thesis project is primarily on the redesign of the Jamali power system under carbon emission constraints to assist in policy planning. This thesis, thus, covers the electricity sector only. Therefore, a power system modeling tool is most suitable for the development of a techno-economic model to answer the main research question.

Pfenninger et al. [72] mentioned in their review and classification of energy models that the main function of

a power system model is to find a balance between electricity production and demand. This requires a high temporal resolution in order to capture variation in the output of generators and fluctuations in electricity demand. With the large scale integration of renewable energy technologies in power systems, the spatial resolution has become more important due to the spatially distributed potential and variable output of renewable energy generators. This is also addressed in the review on energy system models conducted by Prina et al. [75], who made a classification based on model characteristics. In this thesis several characteristics of the energy model classification were used to select an appropriate modeling tool to address the research objective.

The following characteristics were considered important criteria for the selection of a modeling tool: Geographical coverage, time resolution and methodology [75]. Geographical coverage relates to single- and multi-node approaches adopted in energy models, a single-node approach neglects the bottlenecks in transporting electricity. To capture the spatial variability of renewable energy potentials in Jamali and model transmission bottlenecks in the power system, in this thesis a multi-nodal approach will be used. To cover the temporal variability of renewable energy technologies, a high temporal resolution is needed, ideally of one hour [7]. With regard to the methodology, power system models are generally normative (optimization) or predictive (simulation) [72]. Simulation models do not necessarily find global optima and have therefore faster solving times. Optimization methods, on the other hand, often use a mathematical programming approach to find short- and/or long-term cost-optimal solutions [75]. To achieve the research objectives both short-term operation of the power system (to cover the variability of renewable energy technologies) and investments in generators, network and storage have to be considered (to ensure that there is sufficient capacity to provide affordable, reliable and secure electricity). A single-objective function is sufficient to determine the optimal balance between generation, storage and network capacities in the system.

Taking the latter criteria into consideration, from the reviews by Prina et al. [75] and Ringkjøb et al. [77] several modeling tools suffice the criteria for the selection of a modeling tool in this thesis. Eventually, three tools were considered to develop a techno-economic model of the Jamali power system to answer the main research question. The options are Python for Power System Analysis (PyPSA) [6], PLEXOS [22] and Calliope [70]. PyPSA is chosen as modeling tool for this project for the development of the Jamali model, because it is built in Python, uses Python Pandas dataframes, is open source and contains detailed documentation [6]. PLEXOS is not openly available, therefore, it was not selected. Whereas, Calliope was not selected, because it does not have the detailed electrical network characteristics PyPSA includes.

1.6. Scope

In this research only the power system in Jamali is considered, other sectors in the energy system are not taken into account, although they have potential to reduce carbon emissions and provide flexibility services to the power system through sector coupling. Thereby, the Jamali power system is assumed to remain an isolated system by 2050, no new interconnections with other power systems are included such as with the Sumatra power system.

This thesis contributes to the collaboration between IT Bandung and TU Delft on renewable energy potentials in Indonesia. Currently, research has been published on OTEC potentials [53] in Indonesia and a master thesis project on wind energy potentials in Indonesia has been successfully completed [50]. At the present time other students are conducting research on solar and hydropower potentials in Indonesia. The site specific theoretical potentials with high spatial resolution would be suitable inputs for the model that will be developed in this thesis and can be potentially be rerun with economic site specific potentials for utility solar and hydropower that are forthcoming.

1.7. Alignment to Complex System Engineering and Management

The electricity infrastructure is a socio-technical system, it includes physical elements, which are embedded in social structures. Interactions between the actors in the system and their incomplete decisions shape the evolution of the system [14]. The Jamali transmission grid is a continuously operating interconnected system that provides millions of consumers with electricity. Behaviour of the consumers and their interactions determine the global system dynamics. The changing system dynamics of the Jamali grid as a result of renewable energy penetration requires a transition of the entire socio-technical system and is considered a socio-technical problem. Among others, the redesign of the power system in a low carbon future is an es-

stantial part in such a socio-technical problem. Central in the transition towards renewable energy sources is the development of the infrastructure. Infrastructure expansion typically has longer lead times than the construction of renewable facilities. Therefore, transmission expansion planning and flexibility options should be planned in advance to maintain system robustness and ensure electricity security [10]. Many actors are involved in this process, the government, the power utility, independent power producers, system operator and consumers. Making the planning process a multi-actor problem, the techno-economic model that will be developed in this research aims at providing support to actors involved in this process to prevent lock-ins of conventional generation and stimulate the adoption of renewable energy resources and a clean energy system in Jamali.

1.8. Thesis Outline

This thesis contains six chapters, an overview and a short description per chapter is given below.

The second chapter gives a review on relevant literature that optimized generation, storage and network expansion simultaneously. With the literature review several knowledge gaps have been identified, based on the knowledge gaps the main research question was formulated as well as the subquestions.

In the third chapter the methodology is presented. The methodology contains several sections. First, the methodology for the conceptualization the existing transmission network is presented, subsequently the methodology for the creation of energy regions is discussed and the simplification of the transmission network. In the second part the focus is on the data sources for electricity demand, generation and storage. Additionally, their extrapolations for 2050 are presented. In the third part the focus is on the data sources and estimation of renewable energy potentials in and around Jamali. In the fourth part the technology cost assumptions as well as their cost reductions in 2050 is presented. In the fifth section co-optimization of generation, network and storage is explained. In the sixth section a schematic modeling logic overview is presented. In the seventh section the simulation approach is substantiated.

In the fourth chapter the results are presented. The results follow a similar structure as the methodology. First, the system conceptualization is presented. Thereafter, the model is validated. Then, the renewable energy potential results are presented. Followed by the main results from the co-optimization with which a comprehensive answer to the main research question can be formulated. Lastly, the sensitivity analysis results are presented.

In the fifth chapter the results are discussed. First, the results are compared to results of other articles that modeled different power systems. Then, model assumptions and their impacts on the results are discussed. Followed by an evaluation of the research approach and methodology. Thereafter, the implications of the results on the actual power system is discussed. Lastly, the scientific and societal contributions of this thesis are evaluated.

In the sixth chapter this thesis is concluded by revisiting the research questions. Thereafter, a general conclusion is formulated and a recommendation is proposed with regard to the future of the Jamali power system based on the results presented in this thesis. Lastly, several interesting directions for future research are proposed.

2

Literature Review

In chapter 1 the selection for a modeling tool was substantiated. In this chapter a literature review is performed and several knowledge gaps are presented. In the previous chapter the advantages of co-optimization of generation, transmission and storage were discussed opposed to optimizing the components individually. In this chapter the search methodology is presented followed by presentation of the results in a literature review table. The articles are scrutinized on geographical coverage, renewable energy technologies, modeled demand year and whether or not technological cost reductions were included. Thereafter, the findings are discussed and knowledge gaps presented. Subsequently, based on the identified knowledge gaps the research questions are formulated.

2.1. Literature Search and Selection Methodology

The article selection in this section is in line with the criteria used to select an appropriate modeling tool in this thesis, which was discussed in section 1.5. Papers selected for the review from the search developed or applied power system models that include multiple nodes, high temporal resolution and a single objective function. Reason for these criteria are the characteristics of variable renewable energy technologies, which require high spatial and temporal resolution in power system models to produce useful insights for policy planning. Furthermore, due to the advantages of co-optimization of generation, storage and network capacities and operation [52] [28] only articles that considered the latter simultaneously have been selected.

In Scopus and Google Scholar titles, keywords and abstracts were search for "Power AND System AND Model AND Renewables" and "Co-optimization AND Generation AND (Transmission OR Network) AND Storage AND Renewables". Furthermore, the modeling tools discussed in section 1.5 were included in the search. Most of the articles, thereafter, were selected through snowballing and retrieved from discussions on the 'Open-Energy Modeling Initiative' forum. Articles were selected based on the criteria presented in the previous paragraph.

2.2. Literature Table and Findings

In Table 2.1 the reviewed articles are presented. For the comparison of articles several categories were considered relevant. The first category considers the geographical power system that is modeled to find out if efforts have been made to co-optimize the Jamali power system. The second category reviews the renewable energy technologies used, which is relevant since technologies in their early development state may contribute to the energy transition of the power systems under investigation. The 'Demand Year' and 'Forecast Cost Reductions' categories were chosen to determine to what extent research anticipated expected change in model inputs. The 'Carbon Constraint' category was included to find out how research implemented policy targets.

The technology cost reductions only apply to articles that modeled a future year, because capital cost of technologies may decrease due to technological learning [51]. Articles that did not model a future year were labeled 'N/A' in the cost reduction column. Furthermore, the optimization periods used in the articles covered one year per simulation with high temporal resolution except for [44]. Huber et al. [42] and IESR [44]

modeled power systems that are currently not existent (regions modeled are currently not interconnected by electrical infrastructure).

Review Papers Simultaneous Power System Optimization: Generation, Network Expansion, Storage						
Author	Geographical Power System	Sustainable Energy Technologies	Demand Year	Modeling Tool	Forecast Cost Reductions	Carbon Reduction Target
Tröndle et al. [90]	Europe	Solar, Wind, Hydropower, Bio-energy	2020	Calliope	N/A	None (SET target)
Collins et al. [17]	Europe	Wind, Solar	2030	PLEXOS/PRIMES*	PRIMES*	None
Gils et al. [27]	Europe	Wind, Solar, Hydropower, CSP	2050	REmix	2050	None (SET target)
Horsch	Europe	Solar, Wind	2012	PyPSA-Eur	N/A	95%
Schlachtberger et al. [80] - 2017	Europe	Solar, Wind, Hydropower	2011	PyPSA-Eur	2030	95%
Schlachtberger et al. [81] - 2018	Europe	Solar, Wind, Hydropower	2011	PyPSA-Eur	2030	95%
Frysztacki et al. [24]	Europe	Solar, Wind, Hydropower	2011	PyPSA-Eur	N/A	None
Neumann and Brown [60]	Europe	Solar, Wind, Hydropower	2011	PyPSA-Eur	N/A	95%
Pfenninger and Keirstead [69]	Great Britain	Solar, Wind, Tidal Range, Stream power**	2015	Calliope	N/A	None (SET target)
Liu et al. [55]	China	Solar, Wind, Hydropower	2050	No name	2050	90%
Hörsch and Calitz [39]	South-Africa	Solar, Wind, Hydropower	2040	PyPSA-Za	No	95%
Svendsen and Spro [89]	Western-Mediterranean/Morocco	Solar, Wind, Hydropower, CSP	2030	PowerGAMA***	2050	None
Schlott et al. [82]	Vietnam	Solar, Wind, Hydropower, Bioenergy	2020/2025/2030	PyPSA-Vn	No	None
Huber et al. [42]	ASEAN	Solar, Wind, Hydropower, Bioenergy	2050	URBS-ASEAN	2050	Yes
IESR [44]	Java-Sumatra	Solar, Wind, Hydropower	2018-2027	PLEXOS	Yes	No (SET target)

Table 2.1: * PLEXOS and PRIMES were used sequentially. First PRIMES was used to model to generation mix, subsequently PLEXOS was used for dispatch.

** Tidal and stream were used as renewable baseload technologies in one scenario.

*** PowerGAMMA used fixed capacities for the transmission system and generators based on investment plans.

2.2.1. Geographical Scope

From Table 2.1 it can be seen that many articles modeled the European power system. Many of these articles used either the Pypsa-Eur model or a precursor. Pypsa-Eur is a complete open source European dataset for generation and transmission expansion studies [40]. Most of these studies apply a 95% carbon emission reduction target with demand data available at the year of modeling (demand data that was available when the article was published with a sufficient temporal resolution). An overarching effect that is found on the European continental scale is the importance of network expansion in achieving cost-optimal high renewable penetration outcomes in the European system. Schlachtberger et al. [90] studied the effect of transmission expansion constraints on the system cost and found a non-linear relationship between total system cost and transmission capacity. Similarly, Tröndle et al. [90] showed that the need for transmission expansion is two times the capacity of the present European grid in a cost-optimal solution. Interestingly, the authors also found that system designs on the regional scale are technically and economically feasible (i.e. without investments in large transmission corridors). Gils et al. [27] showed similar findings with REMix at high solar and wind penetration in the European system. Additionally, the authors showed that the differences in system cost outcomes are minor as a result of a different solar-wind capacity ratio and variations in the cost of flexibility options such as backup, storage and grid capacity. Interestingly, many different system designs are possible in a small cost range. Schlachtberger et al. [81], also, extensively searched the solution space by conducting sensitivity analyses on carbon constraints, single technology component cost reductions and weather data inputs. The previous authors except for Tröndle et al. [90] used an one node per country approach to model the European electricity network. Hörsch et al. [40] proposed a methodology for spatial clustering. Thereby, the authors examined the effect of clustering on model outcomes. Frysztacki et al. [24],

also, examined the effect of spatial clustering in more detail on total system cost and design. All authors stress the importance and implications of the results for policy planning and decision-making. Especially, with regard to the different design options available that are economically feasible. One of the drawbacks of optimization is that only one cost-optimal solution is found, whereas other solutions may score better on social criteria, which are very important in developing feasible policies. Therefore, Neumann and Brown [60] explored the near-optimal solution space. The implications for policy planning and decision-making will be addressed more specifically in the discussion and related to the results in this research.

The other authors focused on power systems in different parts of the world. In general, results are different from the results found for the European system. Differences are caused due to different topological orientation of the electricity networks, spatial availability of renewable resources and their temporal variability, diurnal and annual electricity demand patterns driven by heating or air-conditioning, system size and the correlation between the spatial distributed electricity demand and generation. Similar to the research conducted for Europe the research objectives differ.

Liu et al. [55] developed a detailed techno-economic model of the Chinese power system that included a realistic hydropower model for the estimation of hydroelectricity time series. The authors compared three different grid scenarios for which carbon reduction parameter sweeps were applied to assess the feasibility of the zero carbon system designs. The system cost start to increase exponentially after 40% carbon reductions, storage and hydro are needed to maintain acceptable costs. Additionally, the authors searched the solution space at 90% carbon reductions while constraining transmission capacities. It was found that 25% transmission capacity reduction does not increase the system costs, but demands extra long- and short-term storage. The authors attributed the differences between their results and the results of the European models for short-term storage and the effect of transmission capacity constraints to the diametric mismatch of renewable generation and electricity load in China. Pfenninger and Keirstead [69] examined the effects on the generation mix of Great Britain with different objectives (costs, emission reductions and energy security) and the effect of grid scale storage on the overall system costs. The authors found that storage significantly reduces the total system costs with higher shares of renewables in the generation mix. Thereby, with scenarios with high renewable penetrations from 80% onward, large scale storage, dispatchable renewable generators or electricity imports are required. The importance of the grid is not as prevalent as for the European case, whereas there is a need for storage or renewable baseload power plants with high renewable penetration to maintain feasible costs. However, when large interconnection capacity would be built with mainland Europe electricity imports can cover the demand, which is in line with the importance of network expansion found with the European models.

Hörsch and Calitz [39], Svendsen and Spro [89] and Schlott et al. [82] created power system models to assess the power system design under specific generation mix policy targets next to other research objectives. Schlott et al. [82], also compared two different reanalysis weather datasets and their effect on the system design. Significant differences were found between the system designs when using the different datasets. Although, not discussed specifically by the authors, from the results it was apparent that the location of renewable potentials had a considerable impact on the resulting system design. Svendsen and Spro [89] did not co-optimize generation, transmission and storage jointly, the authors used expected installed capacities for the transmission grid and generation for 2040 and assessed the impact of storage with linearised power flow in the Western-Mediterranean region and Morocco in particular. Hörsch and Calitz [39] also, focused on deep decarbonization scenarios for the South-African power system for 2040, especially, network expansion had an important role, whereas storage capacity was less relevant in these scenarios.

With regard to the power system of interest in this thesis, a study [42] and a technical report [44] developed models that covered the Indonesian power system. Both modeled power systems in different regions that are currently not interconnected. Huber et al. [42] focused on member countries of the Association of Southeast Asian Nations. Whereas, IESR [44] covered the Jamali system with an interconnection to the Sumatra power system. The main focus of the IESR was to assess whether the Jamali power system can withstand solar and wind penetration, it was found that with planned extension up to 40% can be integrated. However, the authors simplified the Jamali transmission network to 7 nodes.

No detailed power system models that allow the optimization of generation, network expansion and storage jointly currently exist for the Jamali power system. Considering the differences described in the previous

section and the differences in results between different geographical regions, it would be a scientific as well as a societal contribution to develop such a model.

2.2.2. Renewable Energy Technologies Considered

Almost all articles in Table 2.1 include solar, wind and hydropower, some also include bioenergy. Most of the authors aim to provide insights in the design of renewable configurations of the power systems of interest to provide direction in policy planning in the energy transition. Large scale highly decarbonized power systems will likely take years to develop or longer depending on the state of the system and direction that will be taken by policymakers. Within this time immature renewable technologies may develop into mature and important contributors to achieve a sustainable power system. Only Gils et al. [27] and Pfenninger and Keirstead [69] considered concentrated solar power. Pfenninger and Keirstead [69], also, included tidal range and stream power for domestic power production in Great Britain in a single scenario and found the importance of these technologies in achieving a system with high shares of renewables. Tidal energy and other immature ocean renewable technologies such as wave energy conversion and ocean thermal energy conversion have large worldwide potential and may become important sources for renewable energy production in future power systems [67]. Including such technologies in power system models will provide valuable insights with regard to their potential contributions to and role in future sustainable energy systems.

2.2.3. Future demand year and technology cost reductions

In Table 2.1 modeled electricity demand year is shown, all articles included demand as an exogenous variable. Many authors used available demand data available at the time of writing to generate insights in the design of highly decarbonized power systems. Other authors included electricity demand growth in a future year, which would provide useful insights to policy planning, because larger generation and network capacities may be required. Additionally, technology cost may develop over time due to a variety of factors, this is empirically established in technology learning curves [51]. As a result, generation mix designs may change, which in turn affects the locations and capacities of storage and transmission. In Table 2.1 the year for which technology cost are modeled is defined, this categorization is not applicable (N/A) for articles that did not model a future demand year and did therefore no include technology cost reductions. Several articles included expected cost reductions for 2030 and Gils et al. [27] for 2050, however, none of them compared the system design outcomes to designs with present technology costs. Considering the uncertainty involved in estimating cost reductions, it would be valuable to understand what effect these cost reductions have on the system design rather than solely extrapolating these costs and using them as model inputs.

2.2.4. Carbon constraints

Most articles focus on system designs with respect to generation, network expansion and storage with high share of renewable energy technologies, i.e. a highly decarbonized power system. Thereby, they focus on a single decarbonization target that has to be met at a certain year in the future. Although, for some geographical regions targets are clearly set and challenging (Europe, Great Britain and China), mainly in developing regions the future is more uncertain and a wider approach might be more useful for transparent decision-making. Only, Schlachtberger et al. [81] and Liu et al. [55] explore the carbon emission reduction parameter space to determine its effect on the total system cost. However, the spatial design of the power system is not evaluated.

2.2.5. Spatial economic detail

In the review by Prina et al. [75] apart from the categories discussed previously, techno-economic detail is included as a category to classify energy system models. This category relates to the ability of a model to include detailed power plant characteristics. This is included in the articles in Table 2.1 to varying degrees, but is not of particular interest to this thesis (this is already modeled for the Jamali system by IESR [44]). Next to techno-economic detail another category can be considered: Spatial-economic detail. Most articles use uniform prices for specific technologies, however, in particular for renewable energy technologies the capital cost may differ based on specific characteristics of a site. As a result, the co-optimized system design may change. Therefore, for highly decarbonized systems next to the spatial and temporal resolution the spatial-economic resolution may have an impact on the outcomes and should therefore also be considered.

2.3. Knowledge Gaps

From the previously discussed topics several knowledge gaps have been identified. The main research question and subquestions presented in chapter 1 are formulated based on these knowledge gaps.

1. *Absence of a Jamali high resolution power system model*

Currently to the best of the author's knowledge there is no power system model of the Jamali power system with high spatial and temporal resolution that can assess different scenarios with carbon reduction targets. As explained in section 2.2.1 there are considerable differences in the results of power system models at different regions and therefore it is societally and scientifically relevant to develop such a model for the Jamali power system.

2. *Immature renewable energy technology inclusion in power system models*

Except for tidal energy power system models do not include immature technologies (such as ocean renewable technologies) to assess under what circumstances they may contribute to a renewable power system, what role they may take in power systems and what effect they have on flexibility options such as storage and transmission.

3. *Effect of technological learning on power system model results*

The effect of cost reductions of technological learning on total system cost under carbon constraints is not compared to system designs without such developments. Also, there are to the best of the author's knowledge no articles that include technological learning as an endogenous components in power system models with multi-horizon investments that co-optimize generation, network expansion and storage.

4. *Effect of demand growth on cost-optimal power system designs*

Many of the articles presented in Table 2.1 do not include electricity demand growth. For developing countries this is highly relevant. However, it is highly uncertain whether demand growth extrapolations are accurate reflections of actual demand growth (and difficult to validate). Therefore, the effect of different demand growth rates on the system design may provide valuable insights to policymakers. Thereby, electricity demand patterns vary regionally, which is not included in any of the reviewed articles.

5. *Inclusion of spatial economic detail in power system models*

Spatial economic detail of renewables is not included in power system models that include the existing infrastructure. However, such detail may be an important factor next to the temporal, spatial and techno-economic resolution. The spatial-economic resolution may have a large impact on the cost-optimal distribution of renewable generators, which sequentially influences the location and sizing of storage and network expansion.

This thesis aims to provide answers to knowledge gap 1, 2 and 3 to a certain extent. The extent to which the identified knowledge gaps are covered will be reflected on in the discussion in chapter 6. In the next section the research questions are formulated based on the identified knowledge gaps.

2.4. Research Questions

"How do system cost and generation, network and storage capacities develop in cost-optimal configurations of a co-optimized Jamali power system under increasing carbon constraints moving to zero emissions in 2050?"

In order to answer the main research question a techno-economic model of the Jamali power system will be developed with the PyPSA modeling tool. The model will simulate the system dynamics with hourly timesteps for a single year (2050). For the development of the model and to answer the main research question five subquestions were formulated.

1. How can the Jamali power system be conceptualized? And how can the system be divided into energy regions?
2. What are spatial energy potentials of geothermal, hydropower, solar, wind and ocean thermal energy conversion in Java, Bali and Madura? And what are their hourly production profiles?
3. How may technology costs develop until 2050? What effect do they have on the cost-optimal configurations of the Jamali power system subject to carbon constraints?
4. What is the role of OTEC potentials in the cost-optimal configuration of the Jamali power system? Under what carbon constraints and at what locations does OTEC penetrate the energy mix?
5. How does the need for storage and network expansion evolve under increasing carbon constraints in 2050? And how do they affect the costs of the system?

2.5. Thesis Contributions

This thesis contributes to the existing literature in multiple ways. In this thesis a techno-economic model is developed of a power system that serves about 150 million people. The Jamali power system has not been modeled before with multiple nodes, consideration of relevant renewable energy potentials, existing transmission network and with extrapolated electricity demand and technology costs to the best of the author's knowledge, the model itself is the main contribution of this thesis. Therewith, it contributes to a class of models that were developed to model national and international power systems while considering generation, storage and the network simultaneously. Furthermore, a distinction can be made between methodological and practical contributions.

The methodological contribution of this thesis is the proposal of a simple yet efficient procedure for the transformation of a large topological power systems into a mathematical graph, while retaining the geographical layout of its electrical substations.

Furthermore, several practical contributions are made. Firstly, by means of a scenario analysis the effect of technological learning on the development of generation, storage and network capacities is examined as well as the effect on the total system costs with increasing carbon constraints. Secondly, the role of OTEC in a detailed power system model is evaluated by considering spatially resolved potentials in close proximity to Jamali. Thirdly, in this project open data sources are used, which contributes to the transparency of power system planning in Jamali and provides a basis for modeling the other large power networks in Indonesia. Lastly, this thesis shows the relevance of including a high spatial resolution and spatial-economic detail in power system models. And more specifically, in models that include power flow and network expansions.

3

Materials and Methods

In this chapter the methods used in this thesis are presented. This chapter consists of six major sections. First the data inputs and the developed methodology to conceptualize the Jamali power system is presented (i). Thereafter, the data inputs for the hourly electricity demand, conventional generators and electricity storage is discussed (ii). Thereafter, data sources for renewable energy potentials are reported. Also, methods will be presented that are used to estimate potentials of renewable energy technologies that were not openly available with sufficient spatial resolution (iii). Thereafter, cost assumptions for power system assets included in the model are discussed as well as the methodology and assumptions to estimate technology cost reductions in 2050 as a result of technological learning (iv). Subsequently, the methodology to co-optimize generation, network and storage capacities and system operation is presented together with a schematic overview of the internal model logic (v). Afterwards, the scenario analysis approach is discussed and model assumptions are explained (vi).

3.1. Conceptualization of the Jamali Power System

The Jamali electricity grid spans the islands of Java, Bali and Madura. It transports power at different voltage levels. The transmission system consists of 500kV, 150kV and 75kV and 30kV transmission lines [73]. For this research only high voltage (150kV) and extra high voltage (500kV) were considered. For the conceptualization of the system as a model, the topological design of the power system and its electrical characteristics are essential. In the following sections the data sources and methods used to conceptualize the transmission system are presented.

3.1.1. Topological Transmission System Data

The MEMR provides several open source thematic Geo Information System (GIS) maps through the ESDM One Map geoportal to support data sharing and transparent decision-making [84] [63]. Among others, a georeferenced map of the Indonesian transmission system is available in the geoportal. The map of the transmission system consists of georeferenced lines (electrical conductors) and points (electrical substations). The data solely includes topological features of the transmission grid and does not contain information with regard to its electrical properties. Figure 3.1 shows the distribution of the transmission system over Java, Bali and Madura. Throughout this thesis two Coordinate Reference Systems (CRS) were used. In general the standard geodetic WGS84 CRS (EPSG:4326) was used. For metric calculations and computations the geodetic Batavia (Jakarta) CRS (EPSG:5330) was used.

To examine how well the data represents the present transmission system in the Jamali power system, the total length of the transmission lines in the system was calculated and compared to the total kilometer circuit (kmc) reported by PLN [73]. A difference of approximately 200 kilometercircuit (kmc) was found at the 500kV level and 4000 kmc at the 150kV level. There are two likely causes for the discrepancies, the first cause is missing data. This can be observed in Figure 3.1 where several substations at the 150kV level are not connected in the dataset. The second identified cause is the accuracy of the CRS, which depends on the way the Earth is approximated.

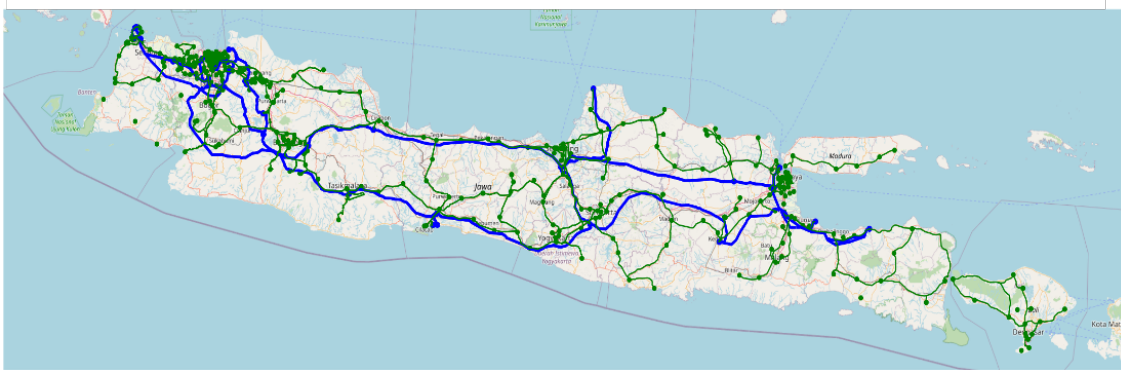


Figure 3.1: *Raw Data Jamali Transmission Network*

3.1.2. Methodology for the Conceptualization of a Power System Graph

In this thesis a methodology was developed to transform raw topological data of a power system into a mathematical graph, the methodology is presented in this section. The methodology can be adapted and used with Openstreetmap topological power network data as well. Topological electricity network data consists of georeferenced points and lines as can be observed in Figure 3.1. The points represent electrical buses. An electrical bus is a graph node in the single line diagram (graphical representation of the three phase electric power system) at which voltage, current or power flow are to be evaluated. The lines represent electrical conductors over which electricity can flow [79].

A graph is a mathematical structure that is used to model pairwise relations between objects [96]. In this thesis a graph consists of nodes that represent electrical buses and edges that represent transmission lines that interconnect these buses. Essentially, to create a graph from the topological data hundreds of transmission lines have to be connected to their adjacent electrical buses. In order to achieve this the following steps are proposed.

1. For every transmission line the coordinates of their endpoints are determined
2. Geodesic distance between an endpoint and all electrical buses is calculated
3. For every endpoint the nearest bus is found and its geometric distance is calculated and stored in a dataframe
4. Endpoints with distances to an adjacent bus of more than 1 kilometer are excluded
5. From the dataframe a graph is created with the Networkx Python package [32], which acts as the default model

Step 4 is applied, because the topological mapping contains inaccuracies (often lines do not exactly connect to a node). If distances are larger than 1 kilometer either lines are not connected to a node or lines are cut in two parts. Therefore, if there was a distance of more than 1 kilometer between the endpoint of the line and the nearest substation, the line was manually examined in Qgis. Several lines were cut in two line segments, while having the same ID, these were merged in Qgis into one line with the 'Join Multiple Lines' plugin. For reproducibility the manually merged lines are included in appendix A. Lines that did not connect to a substation (i.e. the distance between endpoint of the line and the closest substation is larger than 1 kilometer) were not included in the graph representation of the transmission system.

3.1.3. Electrical Components of the Transmission Lines

For the specific electrical components of the conductors no detailed information could be found (only thermal capacity limits and electrical reactances are of interest this will be explained in section 3.5.2). Therefore, uniform values were assumed for the transmission lines based on their voltage levels. According to Co. [16] there are three types of conductors that are used by PLN for 500kV transmission lines. In this research the thermal capacity limit of the 'GANNET' aluminium-conductor steel-reinforced cable is used. For the 150kV transmission lines no detailed technical reports were found, therefore, the thermal capacity limit of the 'AC3'

conductor reported by Hakam [33] was used, which is used in Sumatra as a 150kV conductor. For both the thermal capacity limits of both lines a power factor of 0.9 was used as in the report by Co. [16]. In the report by Co. [16] and in the paper by Hakam [33] reactances of the transmission lines were reported in 'per unit' value with no clear reference to the power and voltage base. Therefore, reactance values of typical conductors in pandaspower were converted to their equivalent reactances at 500kV according to equation 3.1, following the procedure applied in [24]. All relevant data for the transmission data is summarized in Table 3.1.

$$x'_{i,j} = x_{i,j} \left(\frac{500\text{kV}}{v_{i,j}} \right)^2 \quad (3.1)$$

Conductor Parameters					
Variables	Reactance ($x'_{i,j}$)	Thermal Capacity Limit	Standard Linetype Pandaspower	Standard Voltage ($v_{i,j}$)	Standard Reactance ($x_{i,j}$)
500 kV	0.426 Ohm/km	1786 MW	Al/St 240/40 4-bundle 380.0	380 kV	0.246 Ohm/km
150 kV	2.975 Ohm/km	401.4 MW	N2XS(FL)2Y 1x300 RM/35 64/110 kV	110 kV	0.144 Ohm/km

Table 3.1: *The values in bold are used as parameters for the transmission lines in the model.*

3.1.4. Methodology for Network Simplification

The joint optimization of transmission, storage and generation in power systems is computationally intensive due to the required spatial and temporal resolution. An hourly resolution is desirable to capture the temporal variability of wind and solar, which amounts to thousands of time steps. As a result, the spatial resolution is often reduced to different extents. The default model presented in Section 3.1.2 consists of 367 nodes and 660 edges. The default model is simplified partly following the systematic approach based on the k -means clustering methodology presented by Hörsch and Brown [38]. From these clusters energy regions are created with Voronoi partitioning.

k -Means clustering aims to partition a set of observations in k number of clusters by finding a centroid for every cluster. The position of the centroids are determined based on the geographical location of the nodes in the default model by minimizing the sum of within cluster sum of squares. The algorithm was iterated ten times. Consequently, the centroids obtained by the k -means clustering algorithm were used as new buses for the simplified model. Energy regions were created by Voronoi partitioning around the buses, which divides a region into Voronoi cells based on the closest distance to the geographical location of a bus. The model allows different number of clusters equal to or smaller than the number of nodes in Java. The islands of Madura and Bali are added automatically as separate clusters. In summary, every node/bus represents an energy region. In the model electricity demand, generation and storage in an energy region are aggregated to the equivalent node of that region.

Depending on the number of clusters, there can be several transmission lines interconnecting energy regions. Similar to the approach in [38], transmission lines interconnecting regions are replaced by a single aggregated line. The thermal capacity limit of the line equals the sum of thermal capacity limits of the replaced lines, whereas the reactance of the line equals the equivalent reactance of the lines in parallel. Additionally, length of the transmission lines are calculated by multiplying the crow-flies-distance of the lines by 1.25 [38].

Research has been carried out with regard to the impact of network resolution on optimal investment decisions in power system models [24]. Similar to other models this thesis faces the network resolution - computation time dilemma. However, compared to the European electricity grid, the Jamali power system is relatively small and isolated (not connected to other power systems). When a high number of clusters is chosen large demand centers such as Jakarta are divided in multiple energy regions in the model. Electricity flow and optimal investments within demand centers is not relevant for the research in this thesis. The regions should, on the other hand, represent the spatial distribution of renewable energy potentials such that necessary investments in transmission capacity over long distances can be identified. Taking this into consideration, 25 energy regions were selected. With 25 energy regions the demand centers are not partitioned in multiple regions and the layout of the transmission system is maintained. Implications of this approach and the choice for twenty-five energy regions will be addressed in the discussion.

3.2. Electricity Demand, Conventional Generators and Electricity Storage

In this section the data inputs for electricity demand and conventional generators are presented and their extrapolations for 2050. Thereby, electricity storage technologies included in the model are discussed.

3.2.1. Electricity Demand

Since demand and supply have to be balanced at every time step, electricity demand data with an hourly resolution is needed as input for the model. Hourly electricity demand for a year of the Jamali system is not openly available. Similar to the approach by IESR [44] in this thesis hourly electricity data from the Malaysian power system is used as a proxy for the electricity demand pattern in the Jamali system. The electricity demand of 2019 data was retrieved from the website of the Malaysian Grid Operator (GSO), the datasets contain demand data on 10 minute intervals. The data was normalized and summed to hourly intervals. Thereafter, the demand curve was scaled to the total annual electricity demand in the Jamali system in 2018.

The total electricity demand is distributed over the energy regions by the population density in each region. The population density was obtained from WorldPOP [97] and summed for every energy region separately. It is, therefore, assumed that there is no difference in the electricity demand pattern between the regions. Additionally, due to a lack of data with regard to the industrial and commercial electricity demand, these were not considered in the electricity distribution over the energy regions.

Indonesia has experienced an unprecedented electricity demand growth with an average rate of about 8.4% per year between 2009 and 2019 [64]. It was found by IESR [44] that PLN has overestimated the growth of electricity demand in Java and Bali in previous years. In the technical report by IESR [44] a more conservative demand growth for Java and Bali was estimated of 4.1% per year until 2027. Estimating the demand growth and in particular the evolution of demand patterns are studies in itself. In this thesis, therefore, an annual demand growth of 4% is assumed until 2050.

3.2.2. Conventional Generation

PLN provides detailed information in their statistics report on installed power plant types, capacities and annual generation [73]. Currently, the Jamali power system relies on five types of power plants for the generation of electricity. From largest installed capacities to smallest these are: Coal, gas, hydropower, geothermal and diesel generators. The total installed capacity in 2018 amounts to 37,721.6 MW [73]. Installed power plant capacities and locations are obtained from The Global Power Plant Database, which is an open source dataset created and maintained by the World Resource Institute [11]. The dataset does not discern between technology generator type. Installed capacities were validated with the capacities per generator type reported by PLN [73].

Power plant information characteristics are taken from an openly available catalogue for generation and storage of electricity, which is developed by the Indonesian National Energy Council in close collaboration with Energy Analyses, Danish embassy of Indonesia, the Danish Energy Agency and Indonesian Agency for the Assessment and Application of Technology. The catalogue contains data regarding technical and financial characteristics of several relevant power technologies in Indonesia with expected technological improvements and cost expectations for 2030 and 2050 [19]. As mentioned in the previous section, the Global Power Plant Database does not specify the type of power plant except for its carrier. Therefore, specific technologies have been assumed for each generator type:

- Coal: Supercritical Coal Power Plants
- Gas: Combined Cycle Gas Turbine
- Geothermal: Large System (Flash or Dry)
- Hydropower: Large System
- Oil: Diesel Generator

Technical characteristics for the present power plant technologies are included in Table 3.2. No power plant characteristics for unit commitment such as start up-, shut down- or minimal downtime are included in the model. The reason is that the capacity of power plants is a decision variable, which can therefore not be set on- or offline in the optimization.

Conventional power plants burn fuels to produce electricity, while doing so greenhouse gases are emitted. Fossil fuels contain different concentrations of carbon, therefore, carbon emission factors are used to calculate their emissions per amount of electricity produced. Power plant efficiencies are documented in Table 3.2. Emission factors per fuel type for the lower heating value are taken from Blok and Nieuwlaar [3]. Emissions per unit of electricity produced for conventional power plants are calculated by dividing the emission factor by the efficiency of the power plant. Thereafter, the emission factors are converted to metric tonnes of CO₂ per MWh, the resulting emission factors are included in Table 3.2.

Power Plant Characteristics					
Variables	Capacity Factor (p.u.)	Ramp Limits (p.u./hour)	Efficiency (p.u.)	Carbon Emissions (tonneCO ₂ /MWh)	Marginal Cost (\$/MWh)
Supercritical Coal	0.679	2.1	0.38	0.95	29.876
Combined Cycle Gas	0.665	12	0.56	0.36	45.671
Diesel	0.9	50	0.46	0.47	100.85
Geothermal	0.8	-	0.18	0	0.25
Hydropower	0.76	30	1	0	0.65

Table 3.2: Power plant characteristics and marginal prices. p.u. = per unit. Ramp limits apply to ramping up and down, values were transformed from p.u./min to p.u./hour, because the model simulates steady-state behaviour at hourly time intervals.

For 2050 the maximum installable potential of conventional power plant capacities (coal, gas and oil) is set at five times the present installed capacities at their current locations. The assumption for the locations was made based on the required infrastructure to supply the fuel for electricity production. This applies to gas in particular.

3.2.3. Electricity Storage

Electrical energy storage can assist the grid in smoothing the intermittency temporally. The storage technology stores electricity in a certain state and converts it back to electricity during periods of low demand or grid instabilities [56]. In this thesis two types of electrical energy storage technologies are included, battery energy storage (lithium-ion batteries) and hydrogen storage. Pumped hydro storage was considered, but not included due to difficulties in accurately estimating potentials in Jamali.

Pumped hydro storage has high technical maturity globally and is the most deployed storage technology in the world today [56] [47]. Considering the potential of hydropower in Jamali, there is also ample opportunity to install pumped hydro facilities. However, no openly estimated potentials were found for open-loop pumped hydro storage. On the contrary, potentials for closed-loop systems have been mapped globally [2]. For Indonesia high theoretical potentials were estimated with a storage capacity about 821 TWh [88]. These potential sites have not been validated and there exists no economic potential estimation for pumped hydro storage facilities in Indonesia. Estimation of economic pumped hydro storage potentials is out of the scope of this thesis, therefore, on closer consideration pumped hydro storage has not been considered as a storage technology in this thesis.

Rechargeable batteries are a widely used form of electrical energy storage. Batteries store electrical energy as chemical energy by an electrochemical reaction [56]. Batteries are not geographically bound like pumped hydro storage and can therefore be located at the most suitable locations for utilization [47]. Batteries system can be used for a variety of applications, this thesis focuses on their application to smooth variability of wind and solar on utility scale. Apart from bulk energy services through energy arbitrage, battery energy storage can provide for instance ancillary, transmission, distribution and energy customer services. These advantages will be discussed in more detail in the discussion in chapter 5. Lithium-ion batteries have high power/energy density and have high market share. Therefore, lithium-ion batteries will be used as battery energy storage systems in this thesis. The data in the 'Indonesian Power Technology' catalogue [19] contains global data with regard to lithium-ion batteries. For consistency the data from the storage and generation catalogue has been used for utility scale lithium-ion batteries. For lithium-ion batteries a charge and discharge efficiency of 90% is assumed, which results in a round-trip efficiency of 81%. Furthermore, the maximum discharge time of a battery is assumed to equal 4 hours in 2050 [19]. No self-discharge has been included in the modeling of lithium-ion batteries.

Initially, hydrogen was not included as an energy storage fuel in this thesis project. Mainly, because the electricity demand does not show large seasonal variations throughout the year. However, Victoria et al. [94] found that solar variability is smoothed by short-term storage and wind intermittency by hydrogen storage

and that this distribution is relatively robust to price variations of the storage technologies. Hydrogen storage systems use two separate technologies for storing and (re)producing electricity. With electrolysis electricity is converted into hydrogen, which is then stored in high pressure steel tanks or salt caverns. Thereafter, the fuel cell converts chemical energy in hydrogen back to electricity when needed [56]. No specific information on large scale hydrogen storage in Indonesia could be found, therefore, similar to other authors that used PyPSA, hydrogen characteristics and costs were obtained from Budischak et al. [9]. For power to hydrogen an efficiency of 75% is assumed, whereas for hydrogen to electricity an efficiency of 58% is used, which leads to a round-trip efficiency of about 44%. The maximum discharge efficiency of hydrogen storage is set at 168 hours.

3.3. Renewable Energy Potentials

This section starts with discussing the data sources for OTEC potentials. Subsequently, the theoretical hydropower potential data source and installable potential estimation are presented. Thereafter, the simplified estimation of geothermal installable potentials is discussed. For solar and wind theoretical potentials were estimated in this thesis based on land use maps provided by the Ministry of Environment and Forestry (MoEF) [65].

3.3.1. Ocean Thermal Energy Conversion Potentials

OTEC is a renewable energy technology in its early development stage that can be deployed as a baseload power plant in electricity systems. OTEC utilizes the temperature difference between the deep ocean and surface waters. The warm surface water is used to generate a vapor, which drives a turbine that produces electricity. The vapor condenses and is pumped back to the beginning of the cycle [46]. OTEC practical and economic potentials within Indonesian provincial boundaries are estimated by Langer et al. [53] with a novel GIS-based methodology [12] [13]. OTEC's costs will be discussed in detail in section 3.4.1. Thereby, sites located in the Exclusive Economic Zone (EEZ) are also considered in this thesis and were estimated in a forthcoming paper by Langer et al. [54]. An EEZ is an area in the sea/ocean where a sovereign state has special rights, it includes among others the possibility to deploy technologies to produce energy from water and wind resources. In this research it is assumed that each site found by Langer et al. [53] and Langer et al. [53] can be developed into a 100 MW facility by 2050. Additionally, the facilities estimated are closed loop OTEC power plants, which use a working fluid such as ammonia that completes the cycle.

OTEC facilities require specific oceanographic and climatic properties for the production of electricity. For the sites selected in Indonesia, the following technical criteria are used by Langer et al. [53] for the selection of suitable grid connected OTEC sites:

- $\Delta T \geq 20^\circ C$
Temperature difference between deep sea water and sea surface temperature of at least $20^\circ C$.
- Sea depth ~ 1000 meter
The deep sea water is extracted from a depth of around 1000 meter with a cold water pipe.
- Steep declining seabed
A steep declining seabed is needed for power production close to shore, which reduces submarine cable costs and transmission losses.

Langer et al. [53] spanned a mesh of data points 27.8km by 27.8km over the oceanic waters of Indonesia. Subsequently, the mesh of data points were filtered by sea temperature difference and sea depth constraints. Additionally, sites were excluded if located in marine protected areas.

As was already shortly mentioned, every site has a 100 MW potential. A constant capacity factor of 91.2% is assumed following [53]. However, in reality there are seasonal fluctuations in sea temperature. In this thesis it is assumed that the fluctuations are relatively small, therefore, OTEC plants will be modeled with a constant capacity factor. Transmission losses of underground cables depends on the length of the transmission lines, i.e. the distance from an OTEC site to shore. For every OTEC site in this thesis its shortest distance to shore has been calculated. Similar to the capacity factors, transmission losses for every site individually have been calculated with equation 3.2 used in [53]. Where d represents the distance from an OTEC plant to shore in kilometers.

$$\eta = (100 - 2 * 10^{-4} * d^2 - 1.99 * 10^{-2} * d) \% \quad (3.2)$$

3.3.2. Hydropower Potentials

Similar to solar and wind potentials the MEMR reports estimates on hydropower potentials, however, no georeferenced potentials are openly available. Two types of hydropower power plants can be discerned, run-of-river and reservoir facilities. Run-of-river channels flowing water through a canal, which drives a turbine. Whereas, at reservoir facilities a dam is used to store water, by releasing the water through a turbine electricity is generated. Hydropower facilities are typically categorized as large (larger than 30 MW), medium (between 30 MW and 1 MW) or mini (smaller than 1 MW) [19]. Due to the absence of openly available spatially resolved hydropower potentials in Java and Bali in this thesis high-resolution theoretical hydropower potentials were used. The gross theoretical potentials were estimated by Hoes et al. [36], the potentials are available in an open source database. Hoes et al. [36] conducted a systematic assessment to present a detailed global evaluation of exact locations and gross theoretical potentials for run-of-river hydropower. From the database all potentials within the geographic boundaries of the Jamali system were obtained with the geometry tool 'clipping' in Qgis. In this project hydropower is modeled as a baseload power plant with a constant capacity factor, therefore, the reservoir hydropower storage abilities are neglected.

Sites from the gross theoretical potential data were selected based on their size, because no detailed site analysis is conducted in this thesis to estimate the economical feasible sites. The gross theoretical potential of a location is calculated by Hoes et al. [36] with a head (larger than 1 meter) and discharge (larger than 0.1 m³/s) obtained through a Digital Elevation Model and a composite runoff dataset.

3.3.3. Geothermal Potentials

Geothermal energy is stored as thermal energy in the Earth's core. Therefore, geothermal potential sites are located at tectonic zones. Indonesia is located on the Ring of Fire and between two of the Earth's major tectonic plates (Eurasian and Pacific plate). Therefore, there are considerable potentials for geothermal power generation development in Indonesia and more specifically in Java and Bali.

Although, geothermal potentials in Indonesia have been researched and are reported in detail [64], no georeferenced maps of the potentials are openly available. High resolution mapping of renewable potentials is not the main contribution of this thesis. Nevertheless, for accurate modeling and realistic results, site locations for geothermal potentials have to be identified. Therefore, a simplified site identification approach was conducted and thereafter the total potentials were uniformly distributed over the identified sites.

Geothermal power generation facilities are located at sites with volcanic and tectonic activity [62]. The MEMR provides maps with georeferenced volcanic locations [63]. The shapefile includes polygons of volcanic areas throughout Indonesia. In Qgis the polygons were transformed into points with the 'centroid' geometry tool, each point is assumed to be a potential site for geothermal power plant development. Thereafter, the currently installed geothermal capacities [11] were added to the estimation of geothermal resources in Java and Bali [63]. The potentials were uniformly distributed over the potential sites.

3.3.4. Solar, On- and Offshore Wind Energy Potentials

For Indonesia solar and wind potentials have been estimated and reported [4] [45] [76] [91]. Only Bosch et al. [4] provides an openly available database of the estimated wind potentials. Solar photovoltaic potentials were estimated, because the existing spatially resolved potentials could not easily be aggregated to the energy regions used in this thesis. For consistency wind potentials were also estimated following the same procedure. Thereafter, power production profiles of wind and solar were created at their respective locations. In the following sections the procedure for the estimation of the potentials is explained.

3.3.5. Methodology for Capacity Potential Estimation Solar and Wind

Capacity potentials for wind and solar are restricted by land that is available for renewable energy development in Jamali. It is assumed that solar panels and wind turbines in the Jamali power system can be developed within the provincial boundaries, the borders of the provinces are shown in Figure 3.2. To estimate the potentials and production profiles the catchment was divided in grid cells with a size of 25 by 25 km². The sizes of the cells were chosen based on the resolution of grid points in the NASA MERRA-2 Reanalysis dataset, which

is explained in more detail in section 3.3.6.

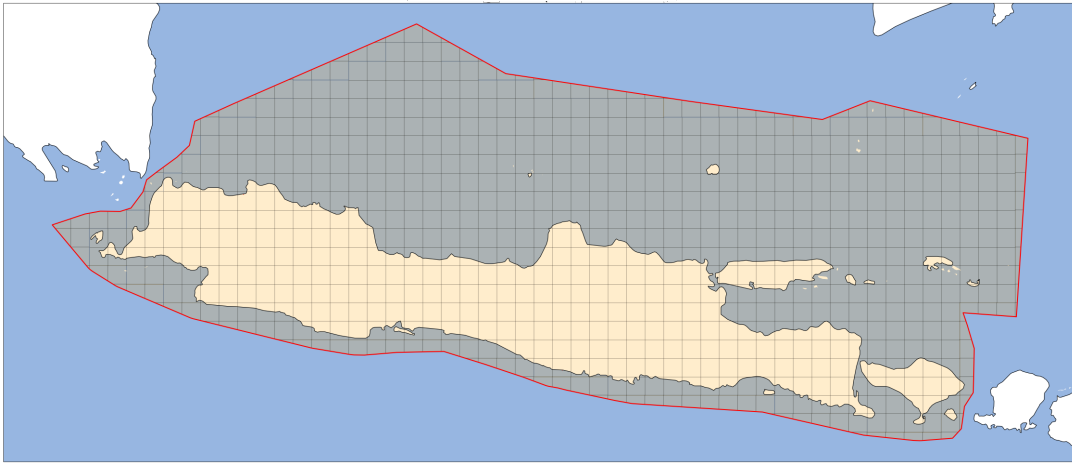


Figure 3.2: Raster that contains grid cells, which divides the catchment in equal parts.

The resulting raster is shown in Figure 3.2. The maximum installable potential per grid cell is calculated according to equation 3.3.

$$\bar{G}_{c,s} = \alpha_s \cdot Pd_s \cdot A_{c,s} \quad (3.3)$$

Where $\bar{G}_{c,s}$ represent the maximum installable potential for a grid cell c for solar or wind technology s . The share of the theoretical potential that can realistically be installed is defined as α_s for solar, on- or offshore wind. Including an availability factor next to the exclusion of land use types is conservative, however, they were included to account for uncertainty in future land development, spacing and socio-geographical concerns. Pd_s is the power density for a technology s in MW/km^2 . The power density depends on the type of solar panels and wind turbines used. $A_{c,s}$ is the area in kilometers that is available in a grid cell c for solar or wind development s . For solar photovoltaics a power density of $135 \text{ MW}/\text{km}^2$ is assumed, which is in line with a power density estimation in a forthcoming thesis on utility scale solar parks in Indonesia and lower than estimations used for Europe [40]. Furthermore, the percentage that can realistically be installed is assumed to be 5% similar to the assumption made by Hofman et al. [37]. Furthermore, solar panels were tilted according to their latitude coordinate, which is a simplification of optimal tilting [68]. For on- and offshore wind turbine technology selection and power densities the same assumptions were made as by Josef Sergio Simanjuntak [50]. The Vestas V110 2000 technology was used for onshore wind production with a power density of $1.65 \text{ MW}/\text{km}^2$. For offshore wind production Siemens SWT 4.0 130 wind turbines were chosen, with a power density of $2.37 \text{ MW}/\text{km}^2$. An availability factor of 30% was used for onshore wind similar to the assumption made in Europe [40]. Offshore wind receives less public opposition than onshore wind [29], therefore the offshore wind availability factor is assumed at 40%. It should be mentioned that such values are arbitrary due to a lack of empirical evidence, this will be addressed in the discussion. For on- and offshore wind turbines a hub height of 100 meters is employed.

The available area onshore is divided between wind and solar. Whereas, the available area offshore is attributed to wind. The available area per grid cell is determined based on a land cover assessment.

Onshore Land Cover Assessment

To determine the available area per grid cell the land cover dataset from the MoEF from 2017 was used [65]. In the dataset all land in Indonesia is classified according to different categories. First, suitable land cover types were determined for wind and solar development. Thereafter, the suitable land cover types were assigned to solar or wind. The following land types were assumed to be suitable and divided between solar and wind:

- Solar: 'Settlement', 'Openland', 'Savanna', 'Shrubs', 'Dryland Shrubs'
- Wind: 'Dryland Farming', 'Plantation'

For solar the land type 'Settlement' is included for rooftop solar. To exclude areas that are not rooftops an availability factor of 1% is assumed. Furthermore, for the solar theoretical potentials land use types without present economic activity were assigned due to land use intensity of solar photovoltaics. Onshore wind, on the other hand, occupies only a small fraction of the land and can co-exists at land that is deployed for farming [19]. It should be noted that there are better approaches in selecting land types and their division between solar and wind based on suitability factors and capacity factor distribution. This will be addressed in the discussion.

From the land types several areas were excluded, which were considered to be infeasible for renewable energy technology development. First, natural protected areas were excluded based on the data in the World Database on Protected Areas. Secondly, areas with a slope steeper than 10° were excluded [1]. Thirdly, Indonesia has many natural disaster prone areas, 'high risk' landslide and earthquake areas and volcanoes were excluded from the suitable land cover type per grid cell for wind. For solar, 'high risk' landslide and volcanic areas were excluded. Subsequently, the remaining area available for development of solar or wind per grid cell was calculated.

Offshore Surface Assessment

From the total offshore area, firstly, areas with a water depth below 50 meters were excluded from the eligible area. The exclusion is based on bathymetry maps of the National Oceanic and Atmospheric Association (NOAA). Subsequently, similar to the onshore land cover assessment natural protected areas were excluded from the eligible area. Thereafter, for every grid cell the total remaining area was calculated.

3.3.6. Time Series Solar and Wind

Production of solar panels and wind turbines depend on the availability of solar irradiance and wind speeds, which differs by location and time. Therefore, for every grid cell to determine energy production, location specific time series are needed. Renewables.Ninja is a tool that facilitates the creation of solar and wind generation profiles from the NASA MERRA-2 Reanalysis dataset [87] [71]. Reanalysis data is created with modern climate forecast models, the main advantage is that it provides global data at locations and time instants where observations are not available. The dataset has a spatial resolution of 0.5° latitude and 0.625° (50 by 50 km^2) longitude and an hourly temporal resolution [59]. Renewables.Ninja provides an interpolation method to estimate production profiles of solar and wind, which are not on a grid point. The interpolation method was used to retrieve production profiles for the desired location in this thesis. Considering the spatial resolution of the MERRA-2 dataset and the interpolation function in Renewables.Ninja, a smaller resolution than 25 by 25 km^2 was deemed not beneficial. The coarse spatial resolution will be addressed in the discussion.

First, the grid presented in Figure 3.2 was divided in an onshore and offshore grid by using the 'Clipping' and 'Overlay' features in Qgis. As a result, the surface of grid cells that include both on- and offshore land becomes smaller depending on the location of the coast line in the grid cell. The onshore grid cell contains 310 cells and the offshore grid 659 cells. For every grid cell in Figure 3.2 the coordinates of the centroid were determined. Thereafter, based on these coordinates hourly time series for the weather year 2019 were created with Renewables.Ninja for 310 locations onshore (solar and wind) and 659 locations offshore (wind). With the time series the production at a specific time instant is calculated with equation 3.4. Where $g_{c,s}$ is the hourly per unit production profile for a solar or wind technology s at a grid cell c .

$$G_{c,s}(t) = g_{c,s}(t) \cdot G_{c,s}^{max} \quad (3.4)$$

After the calculation of $G_{c,s}$ the production profiles and their equivalent installable capacity potentials onshore were aggregated and averaged to the energy regions. The offshore potentials per grid cell and their equivalent production profiles were aggregated and averaged to the energy region in which the closest point to shore is located.

3.4. Technology Cost Assumptions

Fixed costs of technologies/components in a power system include all costs that are made during investment. These costs are generally made once and cannot be incurred afterwards. In this thesis fixed costs of technologies are reported in $\$/\text{MW}$ and for transmission lines in $\$/\text{MWkm}$. Fixed costs consist of yearly recurring operation and maintenance costs and technology investment costs [93]. Technology investment cost are

lump sum payments, i.e. they are made once for the entirety of the project and have to be recovered throughout the lifetime of the technology. For inclusion in the model these values have to be converted to annual costs, because a simulation period of one single year is used. This is achieved by annuitization, which will be discussed in section 3.4.2. The capital costs of all technologies are uniform (regardless of location) except for OTEC, the cost estimation for site specific OTEC power plants is explained in the next section. In reality the costs of renewable energy technologies are location dependent, the implications of this assumption will be addressed in the discussion.

3.4.1. OTEC Site Specific Fixed Costs

The site specific cost for OTEC power plants in Indonesia were calculated following the Low-Cost assumptions and methodology by Langer et al. [53]. OTEC's capital costs can be divided in location independent and location dependent costs. The uniform costs for an OTEC plant of 100 MW equals 577 million US\$. The location dependent costs consist of heat exchangers and power transfer cost components. The heat exchangers cost depend on the temperature difference (ΔT) at a respective site, for which the cost calculations in million US\$ is described in equation 3.5.

$$\text{Heat Exchanger Costs} = (1.97 - (\Delta T - 20^\circ\text{C}) * 0.19) * P_{net} \quad (3.5)$$

The power transfer costs depend on the distance (d) to shore, which were calculated per site in section 3.3.1 and are calculated with equation 3.6 in million US\$.

$$\text{Power Transfer Costs} = (0.0497 * d + 0.304) * P_{net} \quad (3.6)$$

Together, the location independent capital cost, the capital cost of the heat exchangers and the power transfer costs make up the total capital cost of an OTEC power plant.

3.4.2. Annualized Costs

Fixed costs can be recovered by power plants by generating electricity when the market price is above their variable costs and by transmission lines by collecting congestion rent. Therefore, several technologies depending on their lifetime have more or less time to recover their fixed costs [93]. Since the model runs for a single year, these costs have to be scaled to the simulation period. This is accomplished by calculating the annualized fixed cost for every power technology. The annualized costs are calculated by multiplying the fixed cost with the capital recovery factor CRF [3]. The capital recovery factor per technology is calculated following equation 3.7.

$$CRF = \frac{r}{1 - (1 + r)^{-T}} \quad (3.7)$$

The capital recovery factor depends on the discount rate r and the lifetime T of a specific technology. For technologies that have long lifetimes the capital recovery factor approaches the discount rate [3]. The discount rate r captures the time preference of money, which describes the decrease in value of money over time. Often, the Weighted Average Capital Cost (WACC) is used as discount rate. Currently, most of the power system assets in Indonesia are in possession of PLN. Therefore, a uniform discount rate of 10% is assumed for every technology in 2050. Total investment costs in per unit of output are reported in Table 3.3.

3.4.3. Learning Curves

This thesis aims to model the Jamali power system in 2050. Similar to electricity demand, cost of technologies evolve over time due to a variety of reasons such as advances in technology, scale of production and more efficient production processes. In this thesis learning-by-doing is considered, which is independent of time and describes the cost decrease as a result of output production growth and is modeled through the learning curve approach. The learning curve expresses the fraction of technology cost reduction for each doubling of the total units produced [3] [51]. To calculate the cost reduction of a technology, the expected cumulative production in the future year and the cost reduction ratio (experience index) for that technology has to be known. learning-by-doing is not the only contributor to technological learning cost reductions. The learning curve is an empirical relation, a lot remains unclear what influences the cost reduction processes, therefore, a lot of uncertainty is involved in forecasting future technology costs.

Estimating cost reduction for all the technologies included in this project is not the main contribution and aim of this thesis. As a matter of fact, incorporating technological learning as a variable in a bottom-up model would require multi-horizon investments and results in a very large non-linear optimization problem [51], which can currently not be solved efficiently. Therefore, technology cost reductions induced by technological learning is modeled as an exogenous variable similar to electricity demand.

In this thesis technology cost reductions for 2050 estimated in the 'Indonesian Power Technology' catalogue are used [19]. The authors used an one-factor learning model to estimate technology cost reductions. To estimate the cost reductions in 2050 it is assumed that Indonesian technology costs approach international prices. The estimated accumulative capacities per technology were taken from the Stated Policies and Sustainable Development scenarios created by the International Energy Agency [43]. The Stated Policies scenarios is more conservative, whereas in the Sustainable Development scenario a larger increase in renewable energy technologies is expected. Therefore, the accumulative global capacity per technology was assumed to be the average of the accumulative capacities forecast in these scenarios. Rubin et al. [78] reviews experience indices for renewable energy technologies and found widely varying estimates. Therefore, the authors of the Indonesian Technology Catalogue [19] used a experience index of 12.5% for all technologies, except for solar photovoltaics where a rate of 20% was used due to historical observed cost reductions. For consistency in this thesis the cost reductions reported in the Indonesian Technology Catalogue [19] were used, no cost reduction with different experience indices were calculated. Although, less uniform experience indices for different technologies might be more realistic, especially for conventional power technologies. Due to time limitations specific learning rates per technology have not been included, the implications will be addressed in the discussion.

OTEC is not specifically addressed in Stated Policies and Sustainable Development scenarios scenarios. Marine technologies are, on the other hand, treated as a single technology. To discern between OTEC, wave and tidal technologies in the accumulative capacity estimation, it was assumed that half of the capacity is attributable to OTEC. Additionally, an experience index of 7% was used to calculate the capital cost reduction of OTEC by 2050 with equation 3.8, $\frac{P_2}{P_1}$ is the estimated increased capacity, b the experience index and C_{P_1} the present capital cost for OTEC.

$$C_{P_2} = C_{P_1} \cdot \left(\frac{P_2}{P_1} \right)^b \quad (3.8)$$

Hydrogen storage is not included in the catalogue. Cost estimations for lithium-ion batteries 2050 were taken from the 'Indonesian Power Technology' catalogue and included in Table 3.3. Cost for hydrogen storage were taken from [9], who extrapolated costs for 2030, which are used here as future costs, because hydrogen storage is not included in the Stated Policies or Sustainable Development scenarios.

3.4.4. Variable Cost

Fixed costs determine the design of the energy mix and the power system. However, costs are also made during the production of electricity. These costs determine when a generator is dispatched (if dispatchable) and set the price for electricity in an electricity market if the merit order of dispatch is used. If generators receive payments for the electricity produced above their marginal production cost, they make a profit that is used to cover capital expenses [93]. Generally, these costs consist of labour costs and fuel costs and are reported in \$/MWh. Cost of fuel for 2018 have been presented in section 3.2.2 and are assumed to be unchanged for 2050. Additionally, renewable energy technologies generally use no fuel and therefore their variable cost are very low or zero. Other variable costs were extrapolated in the 'Indonesian Power Technology' catalogue for 2050 and used as inputs for the model. Variable costs are reported in per unit of output per hour in Table 3.3, for conventional generators the variable costs include the cost of fuel.

3.5. Co-optimization of Generation, Network and Storage

This section elaborates on how mathematical programming is applied in this research to co-optimize generation, transmission and storage in the Jamali power system. The methods and materials described in the previous sections function as the static components in the model. The model consists of nodes and edges. The nodes are located in the centroid of their equivalent energy regions. Demand, generators and storage

Technology Cost Assumption								
Technology	Investment Cost - No learning	Investment Cost - 2050	Fixed O&M	Marginal Cost	Discount Rate	Lifetime	Estimated Cost Reduction	Experience Index
-	(\$/kW)	(\$/kW)	(%)	(\$/MWh)	(%)	(y)	(%)	(%)
Combined Cycle Gas	690	610	3.5	46.1	10	25	11	12.5
Supercritical Coal	1400	1320	3	28.4	10	30	6	12.5
Diesel	800	760	10	97.3	10	25	5	12.5
Solar PV	1190	620	1.2	0	10	25	48	20
Wind Onshore	1500	1080	4	0	10	30	28	12.5
Wind Offshore	3500	2520	2	5.5	10	30	28	12.5
Geothermal	4000	2840	1.3	0.25	10	30	29	12.5
Hydropower	2080	1850	18	0.65	10	50	11	12.5
OTEC	12745 (average)	9741 (average)	5	0	10	30	24	7
Lithium-ion Batteries	2312	628	3	2.3	10	20	73	12.5
Hydrogen Storage	1683	737	1.7	0.5	10	20	57	-
AC Lines	1065 \$/MWkm	613 \$/MWkm	2	0	10	40	42	-

Table 3.3: *Technology cost assumption overview with and without learning. The costs for OTEC are the averaged capital costs of all the sites.*

technologies are connected to the nodes. Co-optimization is applied to discover system dynamics, which cannot be deduced from the data components alone.

3.5.1. Linear Optimal Power Flow

Objective in this research is to find the cost-optimal configuration of the power system under different scenarios, which translates to the minimal annual total cost of the system. This research adopts a simulation period of one year with hourly timesteps, this results in $t = 1, 2, 3, \dots, 8760$ time periods. The objective function is defined in equation 3.9.

$$\min_{G_{n,s}, F_{\ell}, g_{n,s,t}, f_{\ell,t}} \left[\sum_{n,s} c_{n,s} G_{n,s} + \sum_{\ell} c_{\ell} F_{\ell} + \sum_{n,s,t} o_{n,s} g_{n,s,t} \right] \quad (3.9)$$

The indices n represent the nodes of the twenty-five energy regions created by clustering, the islands of Bali and Madura were added as separate regions. The indices s label the different generator and storage technologies (oil, coal, gas, solar, on- and offshore wind, OTEC, geothermal, hydropower, lithium-ion batteries and hydrogen storage) and ℓ represents the edges in the network (transmission lines). The total costs consist of the annualized fixed costs $c_{n,s}$ of generation and storage capacities $G_{n,s}$, the annualized fixed costs for transmission line capacities F_{ℓ} and of the variable costs $o_{n,s}$ of generation and storage dispatch $g_{n,s,t}$. The annualized costs are calculated by multiplying the capital recovery factor presented in section 3.7 with the fixed costs of the technologies presented in Table 3.3. The variable costs are, also, documented in Table 3.3 and are incurred at every timestep.

In this thesis generation and storage capacities $G_{n,s}$ and transmission lines capacities F_{ℓ} are decision variables, therefore, their capacities are optimized. Furthermore, the dispatch of generators and storage $g_{n,s,t}$ are decision variables is optimized at every timestep. The last decision variable is the flow of power over the transmission lines in the system $f_{\ell,t}$ at every timestep, which is a linear approximation of the complex power flow equations. Their derivation and calculation in networks is explained in the next section.

3.5.2. Power Flow

Voltage potential differences between the connection points of an electrical conductor enable a stream of charged particles between electrical buses. In a network with multiple buses and lines, the impedance of a conductor is an important property, since the current through a conductor is inversely proportional to its resistance according to Ohm's Law. The actual flow of power given certain power inputs and voltage differences on conductors in a network can be calculated with the Alternating Current (AC) method (equation 3.10) and approximated with the Direct Current (DC) method (equation 3.12) [15] [6] [79].

AC Power Flow

The AC power flow method considers the complete formulas for active power (equation 3.10) and reactive power (equation 3.11). The formula for the apparent power is non-linear quadratic and therefore numerical methods are necessary to find global optima. In equations 3.10 and 3.11, P_n is the active power injection at bus n and Q_n is the reactive power injection at bus n . N denotes the total number of buses in the network. V is the voltage magnitude at a single bus, G_{nm} is the conductance and B_{nm} is the susceptance of the conductor in the bus admittance matrix and θ is the voltage angle at the electrical buses [79].

$$P_n = \sum_{m=1}^N |V_n||V_m|(G_{nm} \cos(\theta_n - \theta_m) + B_{nm} \sin(\theta_n - \theta_m)) \quad (3.10)$$

$$Q_n = \sum_{m=1}^N |V_n||V_m|(G_{nm} \sin(\theta_n - \theta_m) - B_{nm} \cos(\theta_n - \theta_m)) \quad (3.11)$$

DC Power Flow

The DC power flow method is a linearised simplification of the AC method. The simplifications are considered reasonable for modeling power flow in transmission systems due to their specific electrical behaviour [6]. The following simplifying assumptions are made [79]:

1. $X \gg R$

Resistance R of transmission conductors are negligible compared to their reactances X . The susceptance B is the reciprocal of the resistance and is therefore assumed to be zero in equations 3.10 and 3.11.

2. $\theta \leq 30^\circ$

In steady-state operation of the transmission system the voltage angles at the electrical buses θ are very small. The sine functions at small angle is approximately equal to the angle itself. The cosine function at small angle equals 1.

3. $V = 1.0$ per unit

Voltage magnitudes V are formulated in the per unit system, as a result in transmission systems voltage magnitudes at buses are very close to 1.0. Therefore, it can be assumed that the voltage magnitude is 1.0 at all buses in the network.

From these simplifying assumptions the reactive power injection at the buses becomes very small compared to the active power injection. Therefore, the reactive power can be neglected [79]. The resulting DC approximation of the active power flow formula over a single line is defined in equation 3.12.

$$f_\ell = P_n = -P_m = \frac{(\theta_n - \theta_m)}{X_\ell} \quad (3.12)$$

The resulting flow of power between two nodes (n and m) over a single conductor ℓ is described in equation 3.12 (DC power flow). The voltage angle difference ($\theta_n - \theta_m$) at the nodes and the reactance of the line X_ℓ determine how the power will flow.

To solve the DC power flow equations in a network model the Laplacian and incidence matrix are of interest. The Laplacian matrix with n nodes is a $n \times n$ matrix, which is constructed from the degree matrix and the adjacency matrix. The degree matrix is a matrix that specifies the number of edges connected to a node on the diagonal and all other entries are 0 as defined in equation 3.13 [86].

$$D_{i,j} = \begin{cases} \deg(v_i) & \text{if } i = j \\ 0 & \text{otherwise} \end{cases} \quad (3.13)$$

The adjacency matrix defines, which vertices in a graph are connected in an unweighted graph if vertices are adjacent the cell has a 1 and 0 otherwise as defined in equation 3.14. If a graph is bidirectional, the adjacency matrix is symmetric. Without any self loops in the graph, the values on the diagonal are 0, because they are not connected [86].

$$A_{i,j} = \begin{cases} 1 & \text{if } i \text{ and } j \text{ are connected} \\ 0 & \text{otherwise} \end{cases} \quad (3.14)$$

The Laplacian matrix (L) is a combination of the degree matrix (D) and the adjacency matrix (A) as defined in equation 3.15. The Laplacian matrix has the nodal degrees on its diagonal and -1 if vertices are adjacent and 0 otherwise [86].

$$L = D - A \quad (3.15)$$

In contrast to the Laplacian matrix, the incidence matrix shows the relation between nodes and edges. The incidence matrix with n nodes and ℓ edges is a $n \times \ell$ matrix [86]. For a directed graph the matrix entries are defined as in equation 3.16.

$$K_{n,\ell} = \begin{cases} 1, & \text{if edge } \ell \text{ starts at node } n \\ -1, & \text{if edge } \ell \text{ end at node } n \\ 0, & \text{otherwise} \end{cases} \quad (3.16)$$

The incidence matrix indicates at what node an edge starts (1) and where it ends (-1), additionally the rows of the incidence matrix accumulate to 0 (an edge attaches only to two vertices). The incidence matrix is related to the Laplacian matrix, the relation is defined in equation 3.17.

$$L = K K^T \quad (3.17)$$

Every DC approximated flow of power over a conductor in a network can compactly be denoted with the incidence matrix [6], the resulting formula is defined in equation 3.18.

$$f_\ell = \frac{1}{X_\ell} \sum_n K_{n\ell} \theta_n \quad (3.18)$$

In a network nodes may have a positive or negative power balance at a given time instant. As a result of the power imbalances electricity flows through the network according to the potential differences and impedance of the transmission conductors (voltage angle differences θ and reactance X in the DC power flow approximation). Kirchhoff's circuit laws determine the electrical behaviour in real power systems and are therefore considered when modeling the flow of power. The linear equations of power flow can be solved by Kirchhoff's current law (conservation of charge) or Kirchhoff's voltage law (conservation of energy) [6] [79]. In this thesis the Kirchhoff's current law will be used to calculate the DC approximation of the power flows over conductors in a network.

Kirchhoff's current law states that at every junction in an electrical network the power imbalance equals the flows arriving at the junction and departing from that junction. It ensures power conservation at each vertex. Similar to the power flows the imbalance can be denoted with the incidence matrix, which is defined in equation 3.19. The power imbalance at a bus in the network p_n should be equal to the direct flows arriving at that bus $\sum_\ell K_{n\ell} f_\ell$ this holds for every bus in the network [6].

$$P_n = \sum_\ell K_{n\ell} f_\ell \quad \forall n \quad (3.19)$$

By substituting equation 3.18 in equation 3.19 a weighted Laplacian matrix is constructed from the relation in equation 3.17 for which the voltage angles θ can be solved and used in equation 3.17 to find the power flows over the transmission lines.

Kirchhoff's voltage law states that the sum of voltages in a cycle should be zero, which is in line with the conservation of energy. The DC power flow equations can be solved with Kirchhoff's voltage law, however, this not method will not be used in this research. For a detailed explanation of the methodology the reader is referred to Hörsch et al.

3.5.3. Constraints

The optimisation problem in equation 3.9 is subject to an equality constraint and several inequality constraints. In the model demand is assumed to be inelastic $d_{n,t}$ at every energy region and for every timestep. Therefore, the continuous balancing of electricity demand and supply becomes the power imbalance described in 3.19. Where $f_{\ell,t}$ represents the flow of power between the energy regions at timestep t and $K_{n\ell}$ is the incidence matrix of the network.

$$\sum_s g_{n,s,t} - d_{n,t} = \sum_{\ell} K_{n\ell} f_{\ell,t} \quad \forall n, t \quad (3.20)$$

The linear inequality constraints define the convex polytope solution space. The inequality constraints can be categorized as generator, storage and transmission constraints.

The absolute flow of power $|f_{\ell,t}|$ is constrained by the transmission line thermal capacity limit F_{ℓ} is formulated in equation 3.21.

$$|f_{\ell,t}| \leq F_{\ell} \quad \forall \ell, t \quad (3.21)$$

The capacity of transmission lines can also be constrained by a maximum installable capacity (\bar{F}_{ℓ}) due to for instance public acceptance issues. Thereby, the lower boundary can be set larger than zero according to for instance the installed line capacities today. In this thesis the minimum capacities are equal to the presently installed transmission line capacities between the energy regions. The investment inequality for transmission line capacities is defined in equation 3.22.

$$0 \leq F_{\ell} \leq \bar{F}_{\ell} \quad \forall \ell \quad (3.22)$$

Dispatch of all generators in the system are constrained by their nominal capacity and should be greater than zero, which is mathematically defined in equation 3.23.

$$0 \leq g_{n,s,t} \leq G_{n,s} \quad \forall n, s, t \quad (3.23)$$

The nominal output of variable renewable generators such as that of solar and wind are constrained by the solar irradiation and wind speeds at a specific timestep. For non-dispatchable renewable generators their capacity factors are multiplied by their installed capacities to come to their nominal output $G_{n,s}$ for every timestep. The per unit availability is calculated with Renewables.Ninja, which is discussed in section 3.3.6.

Additionally, generation capacity is constrained by the maximal theoretical capacity that can be installed $\bar{G}_{n,s}$ for a specific technology s at a bus n , this constraint is mathematically defined in equation 3.24. In this thesis the maximal theoretical capacities are equal to the installable potentials for renewable energy technologies at an energy region, the potentials and potential estimations were presented in section 3.3. Also, conventional generators have a maximal theoretical capacity, they were discussed in section 3.2.2.

$$0 \leq G_{n,s} \leq \bar{G}_{n,s} \quad \forall n, s \quad (3.24)$$

Storage components connect to a node in the network. Their operation depends on their state of charge, which is the part of the storage capacity that is available for discharge and is described in equation 3.25. The state of charge of a storage unit s at a node n for at a timestep depends on the charging h_{charge} and discharge $h_{\text{discharge}}$ at every timestep and the state of charge in the previous time step. η_1 and η_2 are the efficiencies for charging and discharging and prevent the storage from being used when there is no electricity oversupply or shortage in the network.

$$\text{SoC}_{n,s,t} = \text{SoC}_{n,s,t-1} + \eta_1 g_{n,s,t, \text{charge}} - \eta_2^{-1} g_{n,s,t, \text{discharge}} \quad (3.25)$$

The state of charge should not exceed the energy capacity of the storage components and cannot be smaller than zero, this constrained is described equation 3.26

$$0 \leq \text{SoC}_{n,s,t} \leq E_{n,s} \quad \forall n, s, t \quad (3.26)$$

The energy capacity $E_{n,s}$ and power capacity $G_{n,s}$ are assumed to be proportional, therefore, the energy capacity depends on the maximum amount of time $h_{s,\max}$ a storage unit can be fully charged or discharged

$$E_{n,s} = h_{s,\max} \cdot G_{n,s} \quad (3.27)$$

In order to find cost-optima of the power system in a certain setting, global constraints can be set. The global constraint is a value that can be set such that the time varying components cannot surpass the target. In this thesis the global target relates to the carbon emissions of the systems. These are calculated by their emission factors (tonneCO₂/MWh), which are divided by their efficiencies and multiplied by the total amount of electricity produced. The mathematical formulation for the global carbon constraint is formulated in equation 3.28. Additionally, this constraint can be adapted to set a maximum or desirable level of renewable energy capacity, by changing the carrier weight to the power capacity of a generator and setting the global constraint accordingly (this has not been applied in this thesis).

$$\sum_{n,s,t} \frac{1}{\eta_s} g_{n,s,t} \cdot e_s \leq CAP_{CO_2} \quad (3.28)$$

In this research the linear optimal power flow translates into a very large linear programming problem, because the model aims to cover the Jamali power system with different renewable energy and storage technologies at hourly timesteps for an entire year. As mentioned before the PyPSA free software toolbox will be used to optimize and simulate the Jamali power system, the toolbox includes models for different power system components.

For solving the large optimization problem the Gurobi commercial solver will be used under an academic licence. The algorithm used by Gurobi to find the optimum in a linear programming problem is the interior point algorithm [66].

3.6. Modeling Logic and Overview

The model contains many inputs, the theory with regard to the linear optimal power flow was presented in the previous sections. In this section a schematic overview is presented in Figure 3.3 and will be discussed accordingly. To develop a clear understanding of what is optimized, what constraints are applied and what results are generated five categories are shown in Figure 3.3: Inputs, Decision Variables, Constraints, Global Constraint and Outputs.

3.6.1. Model Inputs

The backbone of the model is the mathematical graph that contains nodes and edges that interconnect the nodes. To the nodes electricity demand, generators and storage is assigned if located in their respective energy region. Electricity demand, solar and wind production are exogenous variables and their production depends on input time series. To the generators and storage technological characteristics as well as costs are attributed. These variables form the main data inputs of the model.

3.6.2. Decision Variables and Constraints

Generator, storage and transmission line capacities are subject to optimization. Therefore, their capacities are determined in a cost minimal optimization of the system subject to several constraints. The model follows a greenfield optimization approach, it does not consider already installed capacities except for the transmission network. The minimum transmission line capacities are set according to the present installed capacities. The choice for the minimum constraint was made to find out where the present grid needs to be expanded under different scenarios and if the present high voltage grid can integrate renewables. Transmission line capacities are not constrained by a maximum. Maximum generator capacities are constrained by the renewable energy potential presented in the next chapter and cannot be negative. Furthermore, storage is available at every region and the capacities are not constrained. In turn, the capacities of the generators, transmission and storage are itself constraints to the variables that are optimized for every time step (labeled with the red dot in Figure 3.3). These decision variables are generator dispatch, storage operation and power flow. Furthermore, dispatch of storage and generation are also constrained by their operational limits, which are included in the technology data inputs and apply to every time step.

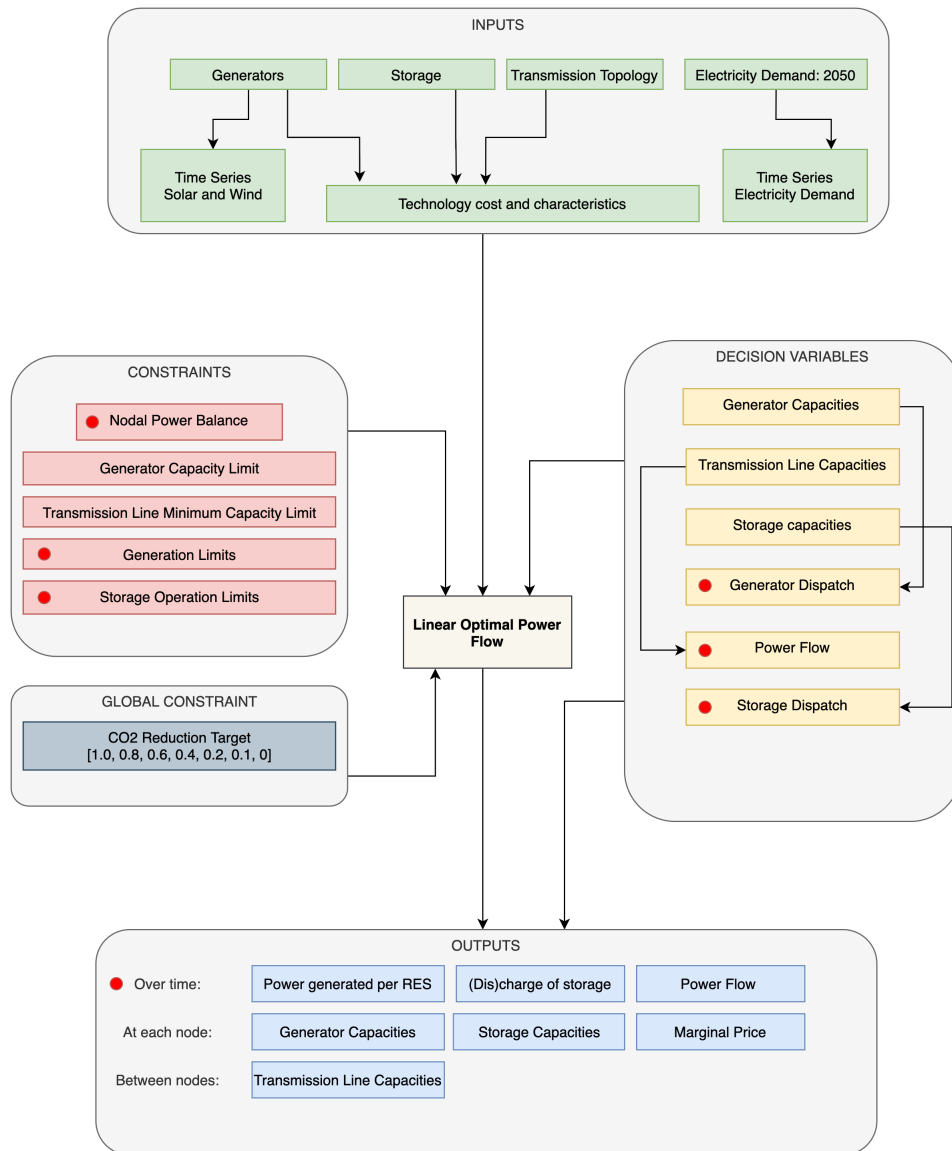


Figure 3.3: Modeling Overview and Logic. The red dot indicates that the variables, constraints or results are dynamic, i.e. that they apply to every time step or are optimized for every time step.

3.6.3. Global Carbon Constraint

The global constraint is varied throughout the scenarios, the emissions per unit of electricity produced per generator are included in their technology characteristics. The default carbon constraint is an extrapolation of the emissions of the 2018 Jamali power system proportional to the estimated demand growth. This relates to a future system with a similar energy mix as the generation mix today, but larger. The total power system emissions in 2018 were calculated by multiplying the electricity production per technology with the lower heating value emission factors presented in Table 3.2. The resulting total system carbon emissions are about 102 million tonne CO₂. The emissions were scaled to the by the annual demand growth (4%) up to 2050. This results in approximately 421 million tonne CO₂ emissions in total in 2050. The carbon constraint is varied in the scenario analysis, which will be discussed in section 3.7.1.

3.6.4. Model Outputs

With the linear optimal power flow several results are generated, which are divided in three categories. First, for every time step the power produced per generator, charge and discharge of storage and the flow of power over the transmission lines between different energy regions is calculated. At each node, the cost-minimal capacities of the generators and storage are calculated as well as the location marginal price. Also, the transmis-

sion line expansion are calculated in the cost-optimal configuration, which interconnect the energy regions and facilitate the flow of power between the regions.

3.7. Scenario Analysis and Modeling Assumptions

In order to provide a comprehensive answer the the main research question scenario analysis will be conducted. The simulation approach, i.e. what runs will be conducted with varying inputs will be presented in this section. Thereafter, the problem size and simplification are discussed. Thereafter, several generalizing assumptions have been made. Assumptions that concern the data inputs such as electricity load pattern distribution and installable potential of renewable energy technologies were addressed in the previous sections. Here generalizing assumptions that relate to model decisions are addressed, this is essential in understanding the potential of the model and its shortcomings.

3.7.1. Simulation Approach

In order to answer the research questions four cases containing several scenarios are proposed. The first two cases focus on the effect of technological learning on the cost-optimal configuration of the Jamali power system under different carbon constraints. The third case assesses the role of OTEC in the Jamali power system and the focus of the fourth case is on the effect of storage and the network on the system design and costs.

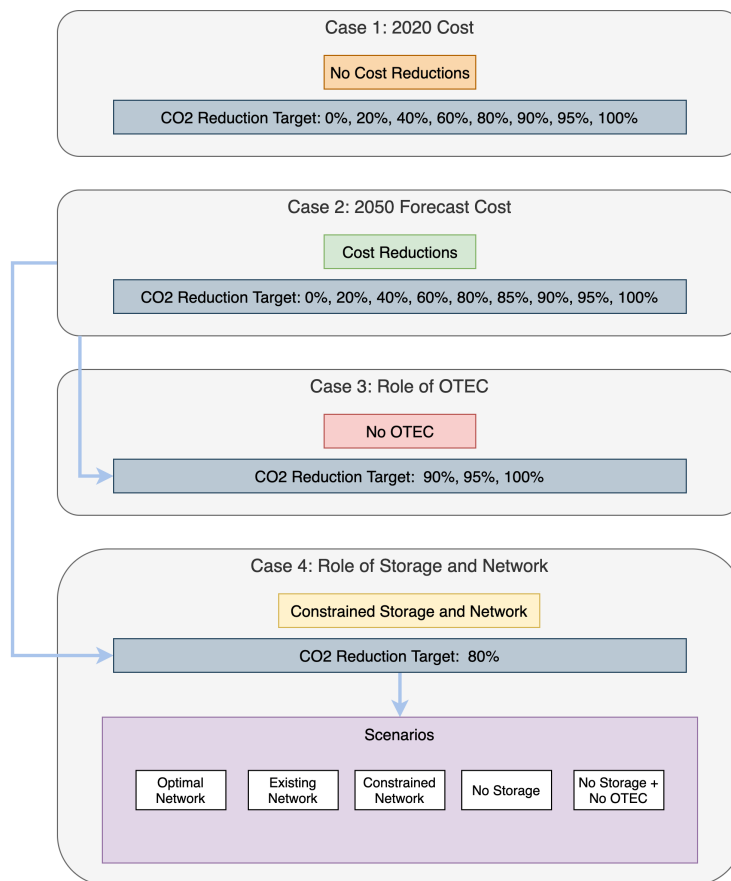


Figure 3.4: Case Overview

Due to the uncertainty involved in estimating cost reductions, the first case contains technology costs of 2020. With these costs eight scenarios with decreasing carbon emissions will be analyzed. The reduction target per scenario is shown in Figure 3.4 in the 'Case 1' box. For the second case the same scenarios are used with one additional scenario with a carbon reduction target of 85%. In this case the technology cost reductions estimated for 2050 are used as data inputs instead of the present technology costs.

The focus of the third case is on the role of OTEC on the system design and costs. From the second case scenarios are selected that deployed OTEC potentials. From these scenarios OTEC is excluded as a potential renewable energy source to determine its effect on the system cost.

In the fourth case a single scenario from the second case is selected with one carbon reduction target. Subsequently, different scenarios are executed to investigate the role of storage and the network on the system costs and design. Firstly, the minimum transmission line capacities are removed in the 'Optimal Network' scenario. In the 'Existing Network' scenario, the network capacities are not optimized to find out if and how the present grid can integrate renewables. In the 'Constrained Network' scenario the line capacities from the 'Optimal Network' are reduced by 50% to estimate their effect on the system costs. In the 'No Storage' scenario, no storage capacities are included. The 'No Storage + No OTEC' is an extension of the 'No Storage' scenario without OTEC.

Based on the model outcomes sensitivity analyses will be conducted to explore the solution space by varying parameters that are uncertain or may provide additional insights on the resulting system designs.

With 25 clusters and hourly timesteps the linear programming problem consists of approximately 4 million variables and 6.5 million constraints. Solving this problem on a Macbook Pro with 8GB RAM in Jupyter Notebook was not possible due to the computational demands. Therefore, through a student subscription a Virtual Microsoft Machine through Azure was rented. The strongest Virtual Machine (D-Series) with 28GB RAM available under a student subscription could not solve this linear programming problem. To solve the model with full resolution a machine with higher RAM memory is needed.

3.7.2. Reduction of the Problem Size

To reduce the size of the linear programming problem the temporal resolution was decreased to three hourly time steps. This resulted in a linear programming problem with approximately 1.5 million variables and 3 million constraints. The problem is solvable with 'STANDARD_D12_V2' virtual machine, the computational time varies from a couple of hours to more than ten hours. Thereby, a couple of scenarios did not converge after more than twenty-four hours. Therefore, it was decided to reduce the size of the linear programming problem even further. Simplification was performed by taking one week for every month with three hourly time steps, the time series were averaged for every three hours. This resulted in a optimization problem with 672 time steps, about 705 thousand constraints and about 343 thousand continuous variables. By comparing the reduced time series of the electricity demand to the pattern in the complete time series the fourth week of every month was selected, which includes the peak load of the original time series. For solar and wind time series the average capacity factors were compared, only small deviations were observed.

It is acknowledged that there are better methods to reduce the temporal resolution while maintaining the variability of time series as good as possible with, for instance, heuristics. However, for this thesis the reduced time series show sufficient resemblance with the full time series.

3.7.3. Greenfield Approach

Firstly, as was mentioned shortly in the previous section the model assumes that there is no installed generating capacity in 2050 and is therefore able to design a generation mix from scratch. This, also, applies to storage. For the transmission network, however, it is assumed that the current installed capacities will be there in 2050, the costs are included in the overall system cost (i.e. it is assumed that the investment cost have not been amortized). The model adopts a time horizon of a single year in 2050.

3.7.4. Centralised Planning Model - Competitive Market Model

It is assumed that there is a centralised planner or a system operator that has perfect foresight over the simulation horizon and full control over the system components and aims to maximize social welfare, thus minimize the cost of electricity. This approach generates the same results as the competitive market model in which every actor aims to maximize its profits, since the set of optimality conditions are identical [93]. Thereby, the demand as well as the availability of solar and wind are known from the beginning of the simulation, therefore, the model is deterministic. No unpredictability is included such as transmission line tripping or unexpected generator outages.

3.7.5. Social and Technical Feasibility of the Outcomes

The model is subject to several constraints, which determine whether the model is computationally feasible. However, in reality feasibility is much more dependent on specific technological characteristics, social acceptance issues and regulations, which are not considered internally. This will be mentioned in the discussion.

3.7.6. Grid Stability

The power system is analyzed in its steady-state, therefore, the model does not include and provide any information with regard the voltage and frequency stability of the high-voltage grid. Thereby, no spinning reserve is considered and also no reserve margins are included in the optimization. Only a congestion factor of 70% for transmission lines is included to prevent overestimation of the transmission line loading, which would result in tripping of the lines.

4

Results

In this chapter the results will be presented. The chapter contains five major sections and is structured as follows. First, the results of the conceptualized model will be presented (i). Thereafter, the model is validated with fixed power plant and network capacities for 2018 (ii). The model inputs consist of the demand proxy for 2018 and the present installed power plant capacities. Aim of the validation is to verify that the model makes accurate dispatch decisions. Thereafter, the results of demand and conventional generator extrapolations for 2050 are presented as well as the maximum installable renewable energy potentials (iii). Then, the optimization results are presented according to the cases presented in section 3.7.1 (iv). Lastly, the results of the sensitivity analysis are discussed (v).

4.1. Jamali Power System Conceptualized Model Results

In this section the results of the methodologies for network conceptualization and simplification discussed in section 3.1 are presented. First, the default model is shown, thereafter, the network simplification results are depicted.

4.1.1. Default Model

Based on the proposed methodology to conceptualize a topological georeferenced map of a power system the default Jamali model was created and is shown in Figure 4.1. The network contains 367 nodes and 660 edges. The 500kV (blue) transmission lines have a capacity of 1786 MW and reactance of 0.426 Ohm/km, whereas the 150kV (green) transmission lines have a capacity of 401.4 MW and reactance of 2.975 Ohm/km. the nodes and edges of the graph form the basis of the model presented in this thesis.

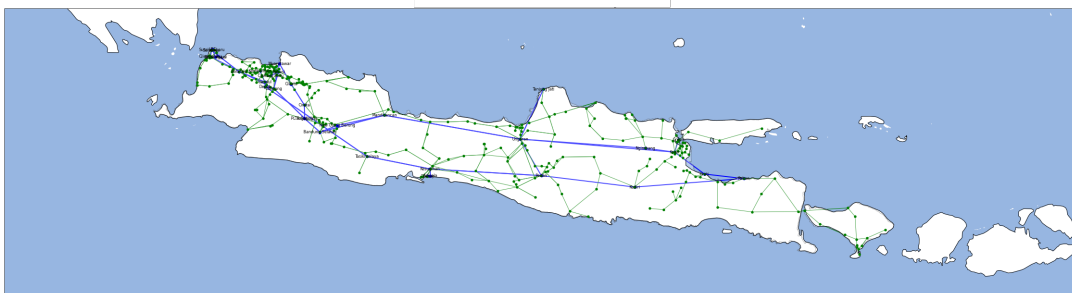


Figure 4.1: *Default Graph Representation of the Jamali transmission system. The nodes represent electrical buses, the edges symbolize transmission lines. The 150kV level is colored green, whereas the 500kV level is given the blue color. The names at the vertices are the names of the 500kV substations.*

4.1.2. Network Simplification

As explained in section 3.1.4 the default model contains too many components for computational tractability. Therefore, the default model is simplified by k -means clustering of the electrical buses. The algorithm was

iterated ten times. In Figure 4.2 the clusters are shown. The colored buses belong to the same cluster and the large red node is the centroid of a clusters. Based on the locations of the centroids Voronoi regions were created. The centroids from here on represent the equivalent electrical bus of a region. As described in section 3.1.4 Bali and Madura were added automatically as separate energy regions in the model. A main drawback of this methodology is that the regions neglect borders of provinces and regencies and may therefore wrongly aggregate generators and demand centers to specific regions, which are not connected in reality, this will be addressed in the discussion in more detail.

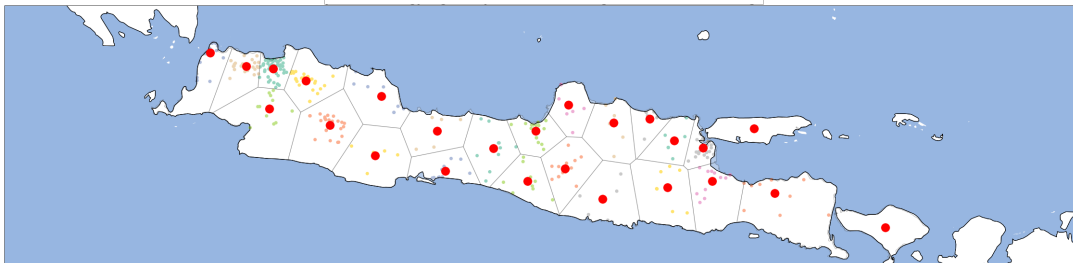


Figure 4.2: The colored points represent the nodes in the default model. In a region the nodes have the same color, because they are part of the same cluster. The red nodes represent the new buses in the simplified system and are the centroids of the clusters and Voronoi regions.

Among others, this thesis aims to find out how renewable energy integration demands changes in the existing transmission network. Therefore, the existing network is included as a lower capacity constraint in the co-optimization of generation, network and storage. Hence, the existing transmission network in the default model is adapted to the energy regions in the simplified set-up of the model following the methodology explained in section 3.1.4. The transmission lines between the energy regions are aggregated, the results is shown in Figure 4.3.

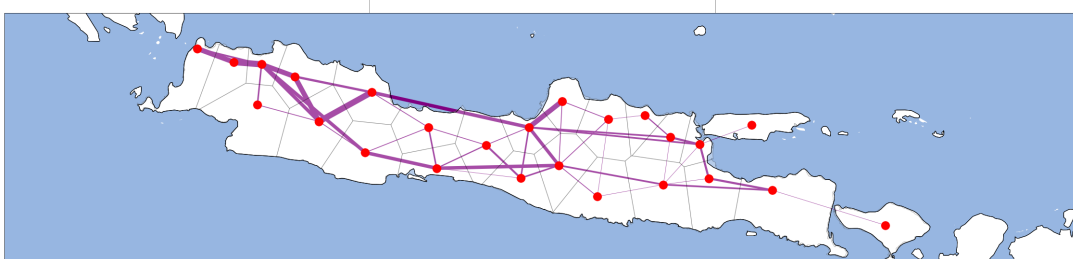


Figure 4.3: Simplified model with lower spatial resolution than the default model.

After clustering the network has 41 lines. The largest aggregated line has a capacity of about 6783.2 MW, the smallest remains unchanged (between Java and Bali and Java and Madura) with a capacity of 401.4 MW. Within the energy regions it is assumed that there is no power flow constraints (copperplate). A drawback of the clustering method is that spatial resolution is lost and therefore bottlenecks in the system, which was also found by Frysztacki et al. [24]. This will be addressed in more detail in the discussion.

4.2. Model Validation

The model is validated by comparing its outputs to the dispatch numbers published by PLN in 2018 [73]. In this validation procedure the capacities of the network, generation and storage are fixed. Therefore, the model performs an annual dispatch with hourly timesteps with 2018 input data. The input data consists of hourly demand data and generator capacities at the energy regions, which are presented the next sections.

4.2.1. Electricity Demand Proxy 2018

As explained in section 3.2.1 Malaysian electricity demand data is used as a proxy for Jamali electricity demand in this thesis. The data was scaled to the annual demand in the Jamali system in 2018. The electricity demand for all provinces in Indonesia is reported by PLN [73]. From the 'Energy Balance' Table total demand in for Java and Bali was retrieved, which is reported in the 'Electricity Consumption' column. The annual demand amounts to approximately 171 TWh with a peak load of 24.36 GW. The calculated peak load is about 2.7

GW lower than the peak load of about 27.1 GW reported by PLN [73]. Therefore, it can be concluded that the demand curves of Malaysia and Indonesia are different and the scaling procedure is not optimal. The electricity demand for an entire year is shown on the left in Figure 4.4. The demand is relatively stable throughout the year.

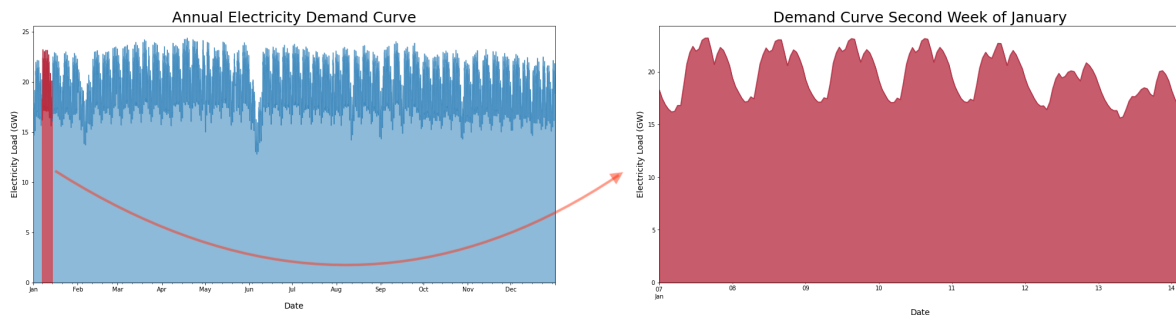


Figure 4.4: Annual hourly electricity demand proxy for the Jamali power system in 2018 in the left sub-figure. The right sub-figure shows the electricity demand pattern in a single week in January.

In Figure 4.4 on the right a single week in January is plotted. From the figure it becomes clear that there is a consistent pattern throughout the days and in a week. Electricity demand is at its highest during the afternoon and then decreases to a minimum during the night. Additionally, the height of the peaks are significantly lower during the weekend days.

The total electricity demand is distributed over the energy regions developed in section 3.1.4 by the population density in each region. The population density was obtained from WorldPOP [97] and summed for every energy region separately. It is, therefore, assumed that there is no difference in the electricity demand pattern between the regions. Additionally, due to a lack of data with regard to the industrial and commercial electricity demand, these were not considered in the electricity distribution over the energy regions. The distributed demand over the energy regions is illustrated in Figure 4.5.

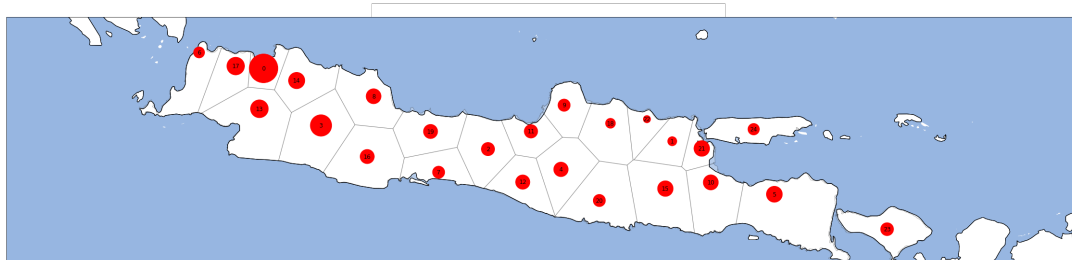


Figure 4.5: Distributed electricity demand over the energy regions, the sizes of the nodes represent their relative electricity demand.

4.2.2. Conventional Generators 2018

In Figure 4.6 the installed power plant capacities from the The Global Power Plant Database [11] are aggregated to the energy regions. Installed capacities were validated with the capacities reported by PLN [73] per generator type. The generator capacity distribution over the energy regions is illustrated in Figure 4.7.

4.2.3. Model Validation Results

The model is validated on its dispatch accuracy by comparing it to the actual dispatch of the Jamali power system. Model outputs are compared to generator dispatch per technology type in this section. The comparison is conducted to validate the results (and to identify the deviations from the real system) and verify the functioning of the model. Currently, no significant storage capacity is installed in the Jamali power system, therefore, electricity is only distributed spatially.

In Figure 4.7 the total installed capacities and their distribution per energy regions are shown. The loading of the transmission lines and the power plants dispatch differs per hour depending on the demand at that hour at the energy regions. Figure 4.7 represents one single timesteps in the simulation period. The selected time

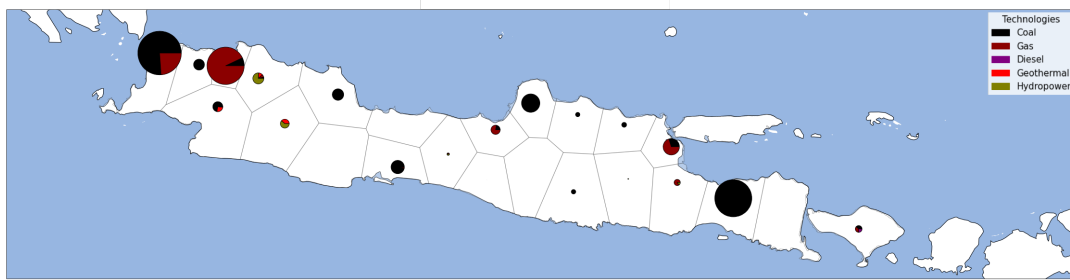


Figure 4.6: Locations and capacities of present installed power plant capacities. The largest vertex equals a capacity of approximately 6.3 GW.

instant is the 18th of April at 15:00, which is the timestep with the maximum peak load. As can be seen in the color bar, lines cannot be loaded over 70% of their total capacity to capture unforeseen losses or failures in the power system. There are several lines that are loaded at their maximum, both the conductors connecting Bali and Madura to Java are constraint by their thermal capacity limits. Although, not clearly visible in Figure 4.7, there is insufficient generation capacity at Madura to meet the estimated load. Therefore, electricity demand is not met, i.e. the load is shed. In the next section the load shedding is included in the annual dispatch results in 4.1, which are compared to the generator dispatch reported by PLN [73].

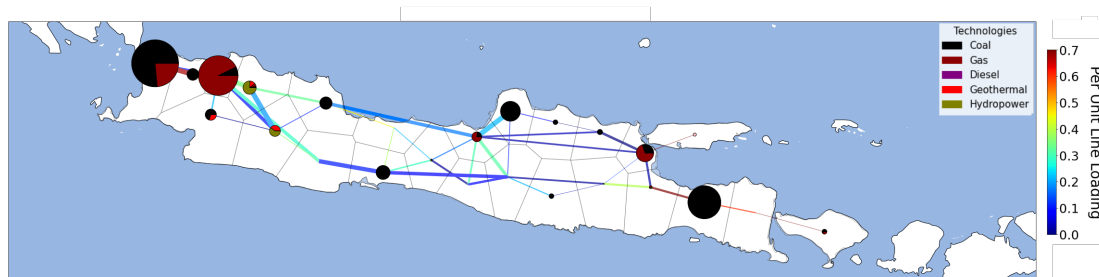


Figure 4.7: Steady-state configuration of the Jamali power system at 18/04/2018 at 15:00 (system peak load). The vertices represent the electricity generation at every region, the largest vertex equals approximately 4 GWh. Whereas, the width of the lines shows the line capacities, the thickest line has a capacity of approximately 6.8 GW. The color of the lines shows their per unit loading, which is indicated by the color bar.

The simulated power production per power plant type for 2018 is compared to the production per plant type reported by PLN [73] in the Table 'Energy Production by Type of Power Plant'. However, the total generation reported by PLN [73] is lower than the total electricity consumption and reported demand that is used in this thesis. Therefore, in Table 4.1 the generation numbers per power plant type were converted to percentages of the total power production for comparison purposes. The dispatch of coal, geothermal and hydropower are overestimated in the model. Whereas, gas production is underestimated. Thereby, in the model 0.9% of the load is not met. The load shedding happens in Madura, where there is no generation capacity and limited transmission capacity.

Comparison PyPSA Results and PLN Generation								
Variables	Coal (%)	Gas (%)	Diesel (%)	Hydropower (%)	Geothermal (%)	Shed (%)	Total Electricity Generation (TWh)	Peak Load (GW)
PLN	68.9	23.3	0.6	3.9	2	0	145.9	27.07
PyPSA	73.5	11.4	0	9.5	4.6	0.9	171	24.36

Table 4.1: Share of energy production technology comparison between model and generation reported by PLN.

Several reasons have been identified for the differences in model outputs and the values reported by PLN [73]. The most striking difference is the dispatch of gas power plants. In the model the relative dispatch of gas is significantly lower than its share in the PLN numbers. As a result, other base power plants contribute more to the total electricity production. The most obvious reason for this occurrence is the difference in peak load. Due to a lower peak load in the model, smaller peak moments occur and therefore gas power plants need to be dispatched to lesser extents.

Additionally, in the model the transmission line capacities are aggregated, which results in less transmission bottlenecks. Therefore, large (and cheaper) coal power plants can be utilized to deliver electricity to regions, which in reality are constrained by transmission capacity and are forced to use gas and/or diesel.

Also, renewable hydro and geothermal dispatch is overestimated by the model compared to PLN dispatch numbers. Currently, hydropower facilities are dispatched as peak power plants and used for ancillary services in the Jamali power system [19], which explains its lower share in the numbers reported in Table 4.1. Furthermore, uniform capacity factors have been used. In reality, capacity factors may be lower.

Lastly, the system is dispatched as a centralized planning- or competitive market model [93]. In reality, in the Jamali power system fossil fueled power plants are subsidized and the dispatch may therefore not be according to the theoretical model used in this thesis.

4.3. Demand and Conventional Generator Capacity Extrapolations 2050

In this section the results for electricity demand and the generator capacities in 2050 are presented.

4.3.1. Electricity Demand 2050

As discussed in section 3.2.1 an annual demand growth of 4% is assumed until 2050. In Figure 4.8 the load duration curve of the 2050 demand is mapped against the load duration curve in 2020. The total demand from 2018 till 2050 increases approximately with a factor 3.5. This results in a peak load of 85.4 GW and a total demand of 598.5 TWh in 2050.

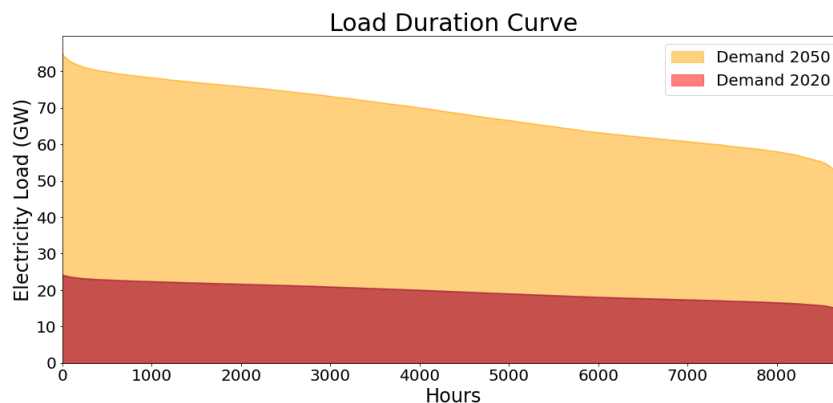


Figure 4.8: Increased electricity demand in the second week of January plotted against the demand in 2018.

4.3.2. Conventional Generator Capacity 2050

The present installed generator capacity of about 37 GW will be insufficient to meet the estimated peak demand in 2050 of approximately 85.4 GW. Therefore, generator capacity investments are required in order to ensure security of supply. As discussed in section 3.2.2 the maximum installable potential is set at five times the present installed capacities at their current locations. The largest aggregated gas capacity (in an energy region) equals about 25 GW and the total installable capacity is approximately 50 GW. For coal the maximum capacity at an energy region is 26.7 GW and the total accumulates to approximately 113.5 GW.

4.4. Renewable Energy Potentials Results

An important part of this thesis is the potential for renewable energy technologies in Jamali, data sources and potential estimations were presented in section 3.3. In this section the results will be presented in the following order: OTEC, hydropower, geothermal, solar and on- and offshore wind.

4.4.1. Ocean Thermal Energy Conversion Potentials

In this section the total OTEC potentials in close proximity to Jamali are reported in Table 4.2. The transmission efficiencies (i.e. loss of power as a result of electricity transport) are not completely accurate due to a

small error in the calculation. The efficiencies are a fraction (between 0.001 and 0.08) higher than they should be, the implications will be addressed in the discussion.

OTEC Potential Results					
Variables	Number of Sites	Plant Capacity	Capacity Factor	Average Transmission Efficiency	Total Practical Potential
Provincial Boundary	20	100 MW	0.912		2.0 GW
Exclusive Economic Zone (EEZ)	143	100 MW	0.912		14.3 GW
Total	163			0.979	16.3 GW

Table 4.2: Potential results and variables for grid connected OTEC in the Jamali system.

The sites in close proximity to Java, Bali and Madura found in [53] and [54] are shown in Figure 4.9. Similar to offshore wind potentials, it is assumed that the OTEC facilities are connected to the closest onshore energy region.

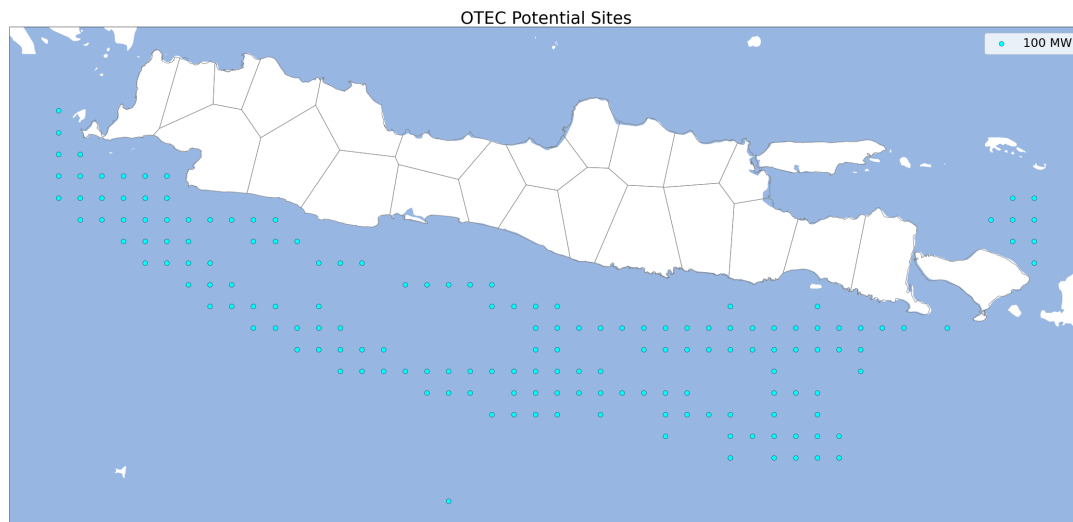


Figure 4.9: OTEC Potential sites, the dots represent practical sites with 100 MW capacity.

4.4.2. Hydropower Potentials

By the exclusion criteria presented in section 3.3.2 the total hydropower potential in Jamali amounts to about 7.6 GW, which is similar to the potentials of all hydropower types combined reported by the MEMR [19]. In particular, the constant capacity factor is a rough assumptions and a detailed hydropower model should be used for more realistic modeling of actual hydropower dispatchable capacity throughout the year, however, this is out of the scope of this thesis.

Hydropower Capacities				
Variables	Number of Sites	Plant Capacity	Capacity Factor	Total Capacity
Potentials	110	0.069 GW (Average)	0.76	7.68 GW (Resources)
Currently Installed Capacity	25	0.097 GW (Average)	0.76	2.44 GW
Total				10.1 GW (Total Capacity in the Jamali system)

Table 4.3: Total hydropower capacities considered in this thesis. The capacities are divided in presently installed facilities and potentials.

4.4.3. Geothermal Potentials

By distributing the total geothermal potentials reported by MEMR [64] spatial resolved potentials were created. The total potential, number of potential sites and the individual power plant capacities are documented in table 4.4. It should be noted that this is a rough approach and that the actual locations may differ, however, similar to estimating and locating hydropower economical potentials this is out of the scope of this thesis.

Geothermal Capacities				
Variables	Number of Sites	Plant Capacity	Capacity Factor	Total Capacity
Potentials	1007	0.024 GW	0.9	8.461 GW (Resources)
Currently Installed Capacity	7	0.16 GW (Average)	0.9	1.132 GW
Total				10.64 GW (Total Capacity in the Jamali system)

Table 4.4: Total geothermal capacities considered in this thesis. The capacities are divided in presently installed facilities and potentials.

4.4.4. Solar Potentials

The methodology presented in section 3.3.5 was applied, for all grid cells the available land was estimated and production profiles were created. The total available area, theoretical potential and installable potential are summed for all the grid cells and summarized in Table 4.5.

Solar Capacities						
Variables	Power density	Available Area	Theoretical Potential	Average Capacity Factor	Availability Factor	Installable Potential
Utility Scale	135 MW/km ²	22,133 km ²	2,988 GWp	0.183	5%	149.4 GWp
Rooftop	135 MW/km ²	15,654 km ²	2,113 GWp	0.183	1%	21.2 GWp
Total						170.6 GWp

Table 4.5: Results and variables for solar potential in Java, Bali and Madura

The exploitable solar potential is 170.6 GWp as reported in Table 4.5. In Figure 4.10 the installable potential per grid cell is shown. The potentials of the grid cells were corrected with their average capacity factor to provide insights in production potential. As can be seen highest potentials are found in the South of Java along the coast of the Indian Ocean and in Bali.

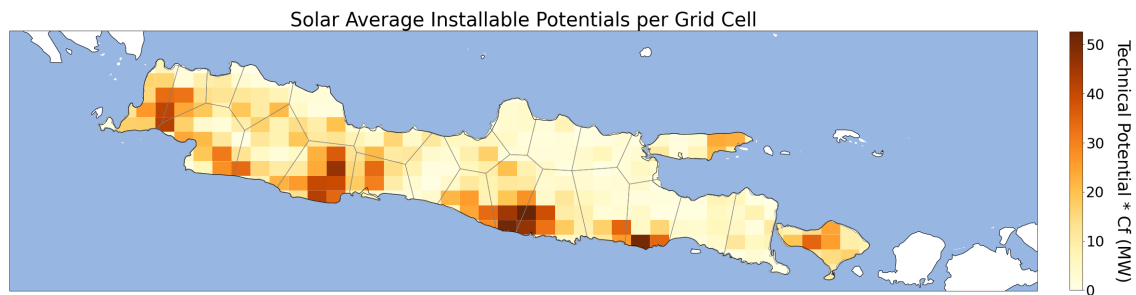


Figure 4.10: Spatially distributed solar potential in Java, Bali and Madura.

4.4.5. Wind On- and Offshore Potentials

As discussed in the methodology the same wind technologies and power densities for on- and offshore wind are used as estimated by Josef Sergio Simanjuntak [50]. The Vestas V110 2000 was used for onshore wind production with a power density of 1.65 MW/km². For offshore wind production Siemens SWT 4.0 130 wind turbines were chosen, with a power density of 2.37 MW/km². For both turbine types a hub height of 100 meter was assumed. The methodology in section 3.3.5 was applied to estimate the available area, theoretical potential, exploitable potential and hourly production per grid cell. The total results are summarized in Table 4.6. In Figure 4.11 the spatially distributed wind for on- and offshore is illustrated. The potential capacities of

Wind on- and offshore Capacities						
Variables	Power density	Available Area	Theoretical Potential	Average Capacity Factor	Percentage Available	Installable Potential
Onshore	1.65 MW/km ²	28,690 km ²	47.3 GWp	0.13	30%	14.2 GWp
Offshore	2.37 MW/km ²	135,904 km ²	322.1 GWp	0.2	40%	161.1 GWp
Total						175.3 GWp

Table 4.6: Results and variables for wind on- and offshore potential in Jamali.

the offshore grid cells are higher than the onshore potentials, which is caused by more area available for wind

technology development, a higher power density and higher average capacity factors. The capacity factors are visualized in Figure 4.12. Almost all of the offshore wind potential is located in the Java Sea, because the provincial boundaries do not extend far into the Indian Ocean, although the wind availability is better in those grid cells.

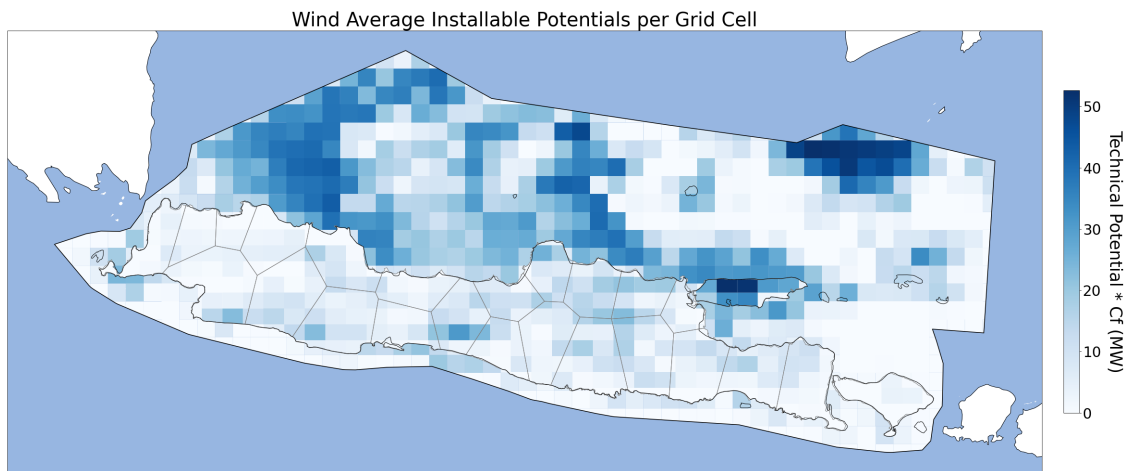


Figure 4.11: Aggregated series on- and offshore wind time of the grid cells for the Jamali system.

4.4.6. Time Series

To gain insights in the production of on- and offshore wind technologies the per unit time series created with Renewables.Ninja were aggregated and are illustrated in Figure 4.12. For the entire region solar and wind production profiles show seasonal variability. Solar, however, is relatively stable throughout the year.

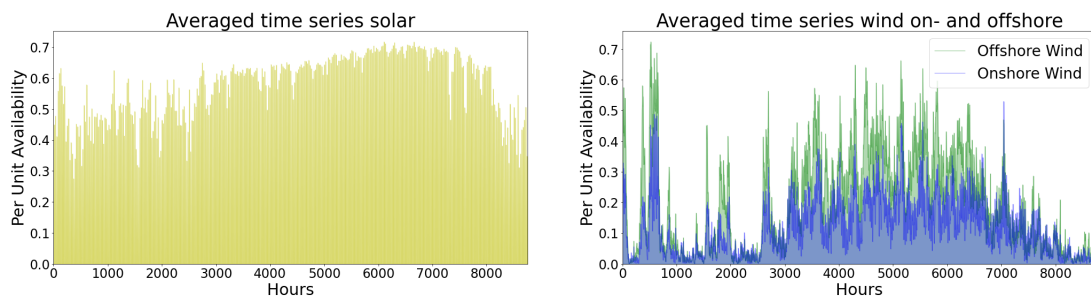


Figure 4.12: Aggregated series solar and on- and offshore wind per unit availability of the Jamali system.

From the figure it is clear that on- and offshore wind production are correlated, offshore wind production has generally a higher capacity factor (see Table 4.6). There are periods during the year with very little on- and offshore wind production, which is likely caused by the presence of similar weather systems over the geographical area. To gain more insight in the availability of wind and solar throughout the year their duration curves were created and are shown in Figure 4.13. The diurnal variation of solar is clearly observable. Thereby, there is a significant part of the year where there is very little wind production on- and offshore.

From the results of solar, on- and offshore wind potentials it can be concluded that, although, the provinces cover a large geographical area, there remain periods throughout the year with very low production of solar (during the night) and wind combined. This implies the need for peak power plants, storage and renewable baseload power plants in a low carbon Jamali power system.

4.4.7. Total Renewable Energy Potentials

In the previous sections potentials for renewable energy technologies were presented. In this section an overview of the potentials of the renewable energy technologies is given. In Figure 4.14 potentials per region are presented to give a clear overview and insight in the distribution of the potentials over the system and renewable capacity constraints, they are corrected by their average capacity factors.

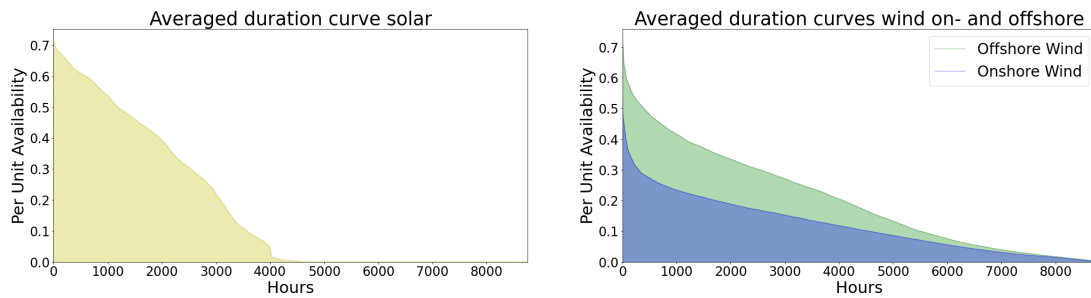


Figure 4.13: Aggregated duration curves solar and on- and offshore wind of the Jamali system.

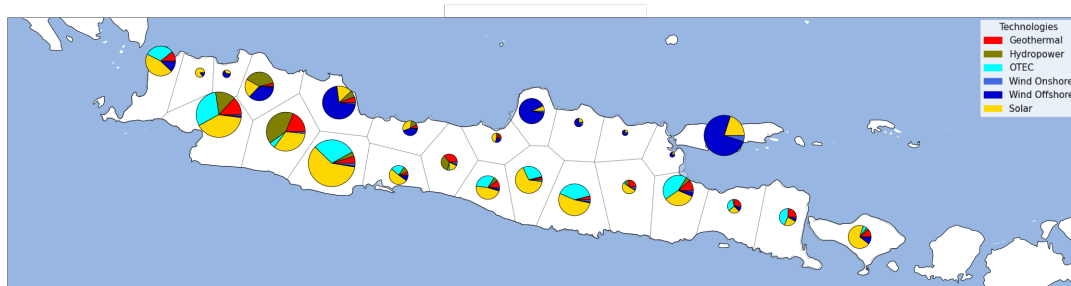


Figure 4.14: Total installable potentials mix per region. The total potential are multiplied by the average capacity factors of the renewable technologies at the specific energy region, i.e. fixed capacity factors for geothermal, hydro, OTEC. Averaged capacity factors for solar and wind.

There is a clear distribution of renewable energy potentials over the energy regions. The solar and OTEC potentials are distributed along the Southern coast of Java and in Bali, whereas the offshore wind potentials are located on the Northern coast of Java and in Madura. Onshore wind potentials are very small compared to the potentials of the other renewable energy technologies. Furthermore, there is a total of about 36.5 GW baseload capacity potential from OTEC, hydropower and geothermal in the system (technologies modeled as baseload power plants), which is less than half of the peak power demand estimated for 2050. With these results it can be concluded that in a low carbon system Jamali power system there will be a need for solar and wind, which will have to be balanced with storage.

4.5. Simulation Results

In order to answer the research questions four cases were presented in the previous chapter, in this section the results of the cases will be evaluated. As was explained in section 3.6 in chapter 3, the results presented in the previous sections function as the inputs for the optimization for which the results are presented in this section. The cases are summarized below and are analysed based on installed capacities, system costs and the spatial layout of the system.

1. Case 1: Technology Costs 2020
2. Case 2: 2050 Forecast Cost
3. Case 3: Role of OTEC
4. Case 4: Role of Storage and the High Voltage Network

The cases contain several scenarios. Scenarios are compared on their average system cost per unit of electricity produced. The average system cost serves as an indication of how much costs have to be made for a cost-optimal configuration of the system given certain simplifications. However, it is not the price of electricity and does not necessarily reflect it. For each scenario a cost-optimal configuration of the power system is sought. Especially, case 1 and 2 contain many scenarios. To provide insights into the spatial design (layout) of the power system several representative scenarios are selected and visualized for case 1 and 2. In the scenario analysis the 0% carbon reduction scenario relates to a world without efforts to reduce carbon emissions

compared to 2018, therefore, the emissions increase proportionally to the electricity demand in 2050. This scenario serves as the reference case or the 'business as usual' scenario.

4.5.1. Case 1: Technology Costs 2020

For the first case no cost reductions as a result of technological learning are included, the costs are equal to technology costs in 2020 [19]. Additionally, for every scenario the carbon constraint increases relative to the business as usual scenario as presented in the simulation approach in section 3.7.1 in chapter 3. The annual system carbon emissions as a function of carbon constraints is visualized in Figure 4.15. As can be seen, the carbon emissions are already at their maximum in the 0% carbon reduction scenario, this implies that the constraint is binding from the first scenario and that there exists a cheaper system with higher carbon emissions. The shadow price of the constraint per scenario is visualized in the right sub-figure in Figure 4.15, which gives an indication of the effect of the constraint on the system costs. Relaxing the carbon constraint in the higher carbon scenarios results in small total cost reductions, whereas, in the low carbon scenarios its impact is large. The system without constraints will be discussed in more detail in the sensitivity analysis in section 4.6. For all scenarios except the 100% carbon reduction scenario feasible cost-optimal solutions were found. In the zero carbon scenario there is insufficient renewable capacity available that can generate sufficient electricity to meet the demand at all times given the potentials presented in section 4.4.

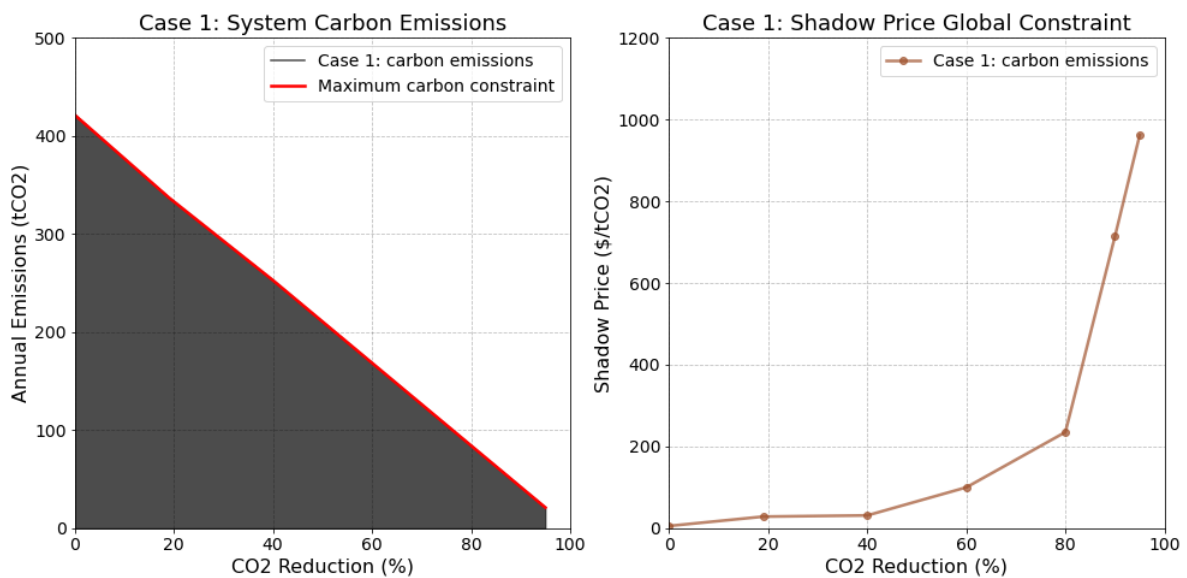


Figure 4.15: The vertical axis shows the annual system emissions in million metric tonnes, the horizontal axis represents the carbon reduction targets. The red line shows the maximum allowable emissions for the system, i.e. the global carbon constraint.

Based on the costs the capacities for generation, network and storage are optimized. The capacity development as a function of the carbon emission reductions is presented relative to their maximum installable potentials in Figure 4.16. Network and storage capacities are unconstrained and shown in Figure 4.17. Especially, in the higher carbon reduction range, maximum installable renewable potentials are an important explanatory variable when interpreting the results.

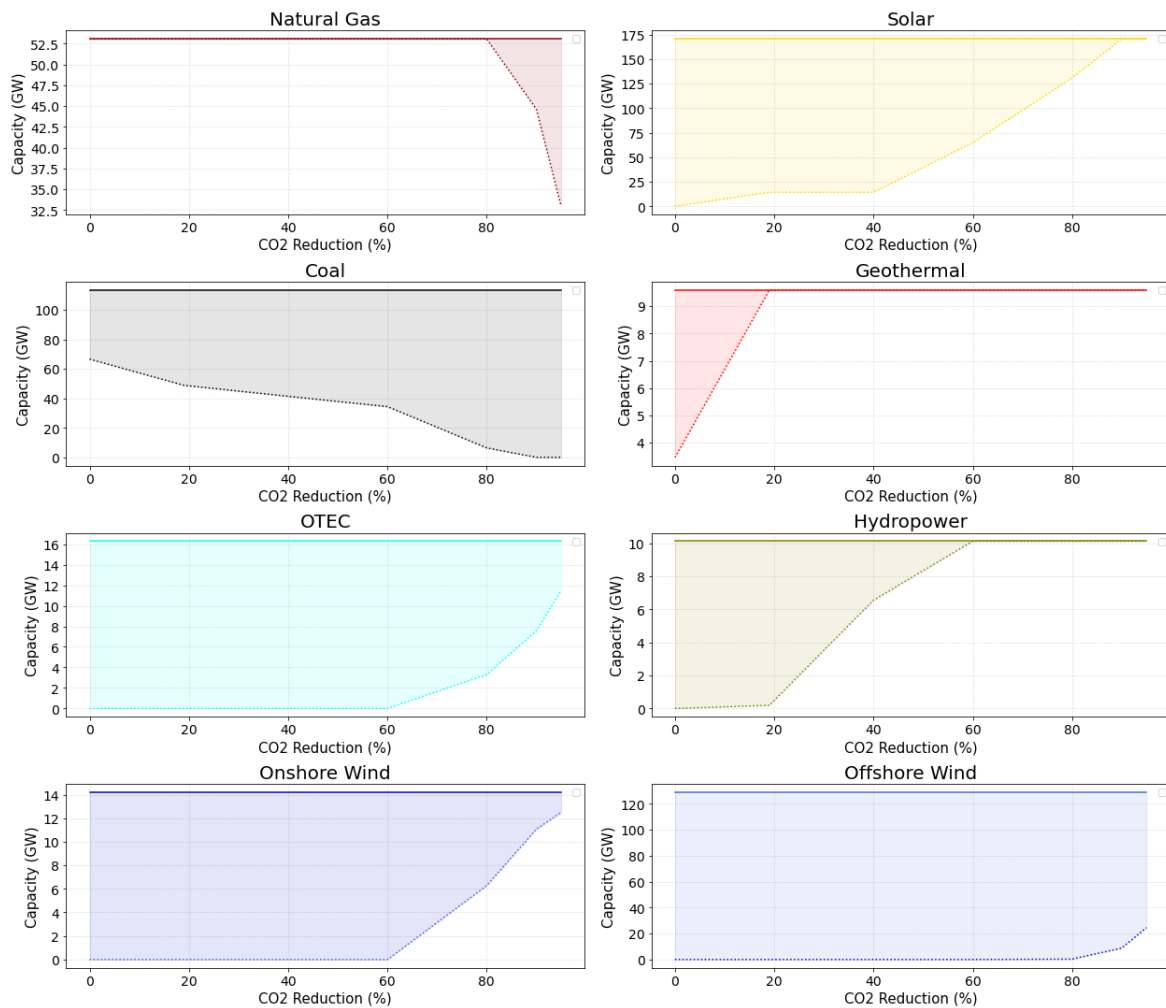


Figure 4.16: The solid line represent the maximum installable capacities of an energy technology. The surface represents the remaining available installable potential per technology. The dashed line indicates the capacity installed as a function of carbon emission reductions.

From Figure 4.16, logically, the available installable capacities for conventional technologies increase as a result of the carbon constraints and the renewable available potentials decrease. Interestingly, gas is used at its full available capacity and reduces after 80% carbon reductions, whereas coal is phased out at 90%. Coal is the largest installed capacity in the 'business as usual' scenario, although, it is not utilized at its cost-optimal capacity due to the carbon constraint. The reduction in coal capacity is first replaced by geothermal energy until it reaches its maximum installable capacity. Thereafter, the potentials for hydropower are deployed and solar capacities increase significantly. Interestingly, OTEC potentials are deployed when coal is phased out at 80% carbon reductions, whereas no offshore wind capacities are used. This can partly be explained by the site specific OTEC costs (discussed in section 4.5.3) and the high capacity factors of OTEC in combination with the scarce availability of wind in 2019 in Jamali and uniform capital cost in the model. This will extensively be debated in the discussion. When gas capacities start to reduce, solar reaches its maximum installable potential. Simultaneously, there is a considerable increase in OTEC capacities, which approaches its maximum installable potential. Thereby, a small part of the offshore wind potentials are utilized in the 95% reduction scenario, these are the potentials with the highest capacity factors.

In Figure 4.17 the capacity development of storage and the network are shown as a function of carbon emission reductions. Network capacities in cost-optimal configurations are higher in the high carbon reduction scenarios due to the concentrated distribution of conventional generator capacities, this will be evaluated in the sensitivity analysis in section 4.6. With lower carbon emissions (40% - 60%) solar, hydropower and geothermal resources are deployed, which are more distributed and therefore reduces the need for network

expansion. In the lower carbon cost-optimal systems the network capacity increases again, primarily due to the larger transmission line capacities between the regions on the northern and the southern coast of Java, which is visualized and discussed in section B.4. Lithium-ion batteries are not utilized in cost-optimal systems below 60% carbon reductions, thereafter, a large capacity increase is observed similar to the increase in solar capacities. From 80% carbon reductions on wards, the increase becomes more significant. This can be attributed to the decrease in gas capacity, therefore, more battery capacity is required to mitigate the solar variability. In the 95% carbon reduction scenario around 80 GW of battery power capacity is deployed, which is equivalent to 320 GWh. Small amounts of hydrogen storage are used in the lower carbon scenarios, which remains relatively constant until the 90% reduction scenario. The utilization of offshore wind in the 95% carbon reduction scenario is accompanied by an increase in hydrogen storage and network capacity.

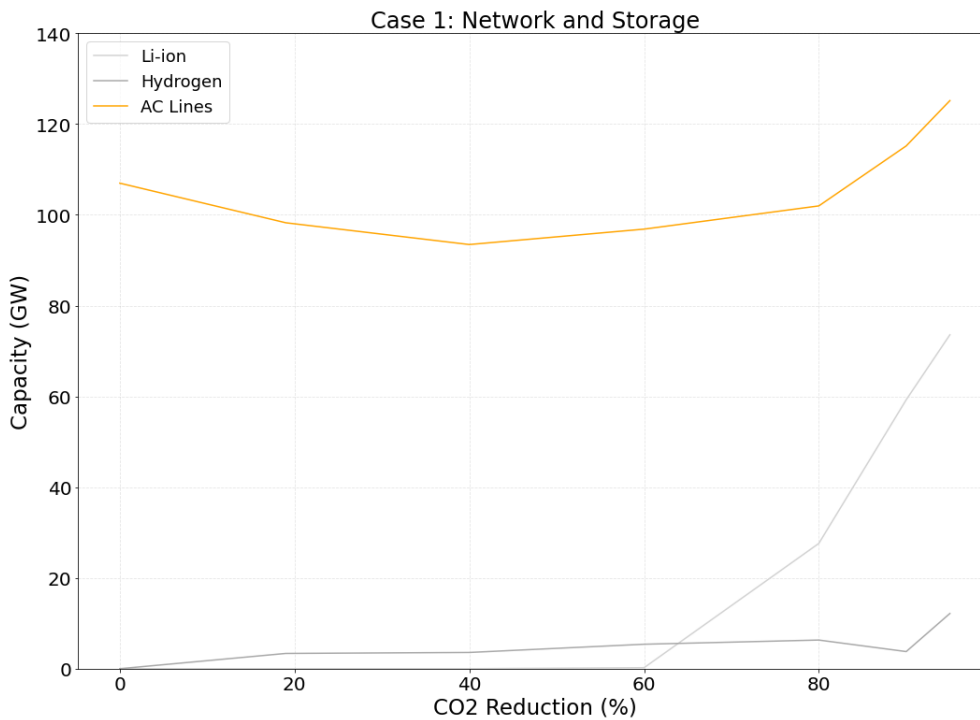


Figure 4.17: Capacity development of the network and storage as a function of carbon emissions reductions.

Although, the capacity developments do provide insight in the effect of the decreasing carbon constraint on the design of the system, it contains no information with regard to the costs and the spatial layout of the Jamali power system. In the next paragraph, the system costs per scenario are presented, with which the scenarios can be compared and conclusions can be drawn with regard to the economical feasibility of the low carbon cost-optimal outcomes.

In Figure 4.18 the average system costs as a function of carbon reductions is presented. The average system costs or levelized cost of the system are calculated by dividing the total system costs (the sum of the annualized investment costs per technology and the sum of variable costs per technology) by the total electricity produced in the system over the simulation period. The average system cost give an indication of the costs that were made for the production of one unit of electricity. In Figure 4.18 the average system costs are shown. The average cost of the components in the power system together accumulate to the average system cost, which are presented with different colors in Figure 4.18.

The results presented in Figure 4.18 show an exponential relation between average system cost and carbon reductions. In line with the capacity results presented in the previous section, in the high carbon scenarios the costs consist mainly of gas and coal. When the share of coal in the system starts to decrease, the share of solar and batteries in the average system cost increase, which results in a slight increase in the system costs. Thereafter, at 60% carbon emission reductions the utilization of OTEC and batteries significantly increases the average system cost. When gas capacities start to decrease at 80% carbon reductions, the use of solar,

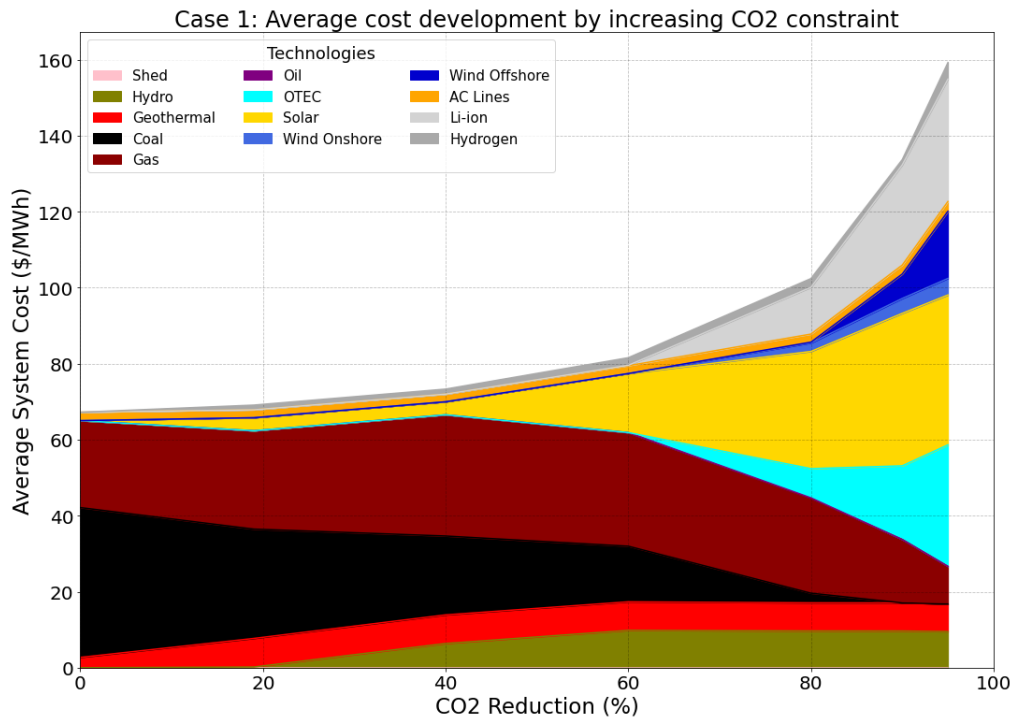


Figure 4.18: Case 1 average cost results. On the horizontal axis the carbon reduction target in percentages is shown. The vertical axis shows the average cost of the system per unit of electricity produced.

wind and OTEC drive up the system cost to above 150 \$/MWh, which is more than double the 'business as usual' scenario. This rise in renewable energy technology cost is accompanied by a large increase in storage.

Furthermore, one phenomenon stands out from the cost results presented in Figure 4.18. The average system costs consist mainly of generator costs, whereas network costs only make up a very small portion of the average costs. Generally, network costs only take up a small part of the total system cost. Thereby, the network costs depend strongly on the geographical size of a power system, the Jamali power system is relatively small and therefore the costs cover even a smaller portion of the total system costs compared to other power systems.

So far, aggregated system capacities were presented and the average system costs. Although, they give clear insight in how the cost-optimal system evolves over carbon emission limits, it does not provide any insight into the spatial design of the system. Therefore, the spatial design results of selected scenarios will be evaluated next.

The capacity and cost developments as a result of the carbon emission limits affect the spatial design of the system differently. To evaluate the effect three scenarios are visualized in Figure B.4. The 20%, 60% and 95% carbon reduction scenarios have been selected for analysis.

In the 20% reduction scenario coal generators are distributed throughout the system. Whereas, large gas power plant capacity is located in Jakarta. In section 4.2.2 the currently installed power plant capacities were presented, on which the potential conventional capacities are scaled. Most of the gas capacity is located in the Jakarta energy region. In the 60% reduction scenario, the gas capacity in Jakarta is unchanged, which is in line with the capacity development findings. Furthermore, along the southern coast coal capacities have partly been replaced by solar and in the central west part of the system by hydropower and geothermal. The spatial design of the 95% carbon reduction system is much different than the design of the lower presented scenarios. Along the southern coast of Java coal has been replaced by solar in combination with lithium-ion battery capacity and OTEC. Also, Bali has become an important energy region with significant solar and OTEC capacity. Thereby, most of the offshore wind capacity is connected to Madura.

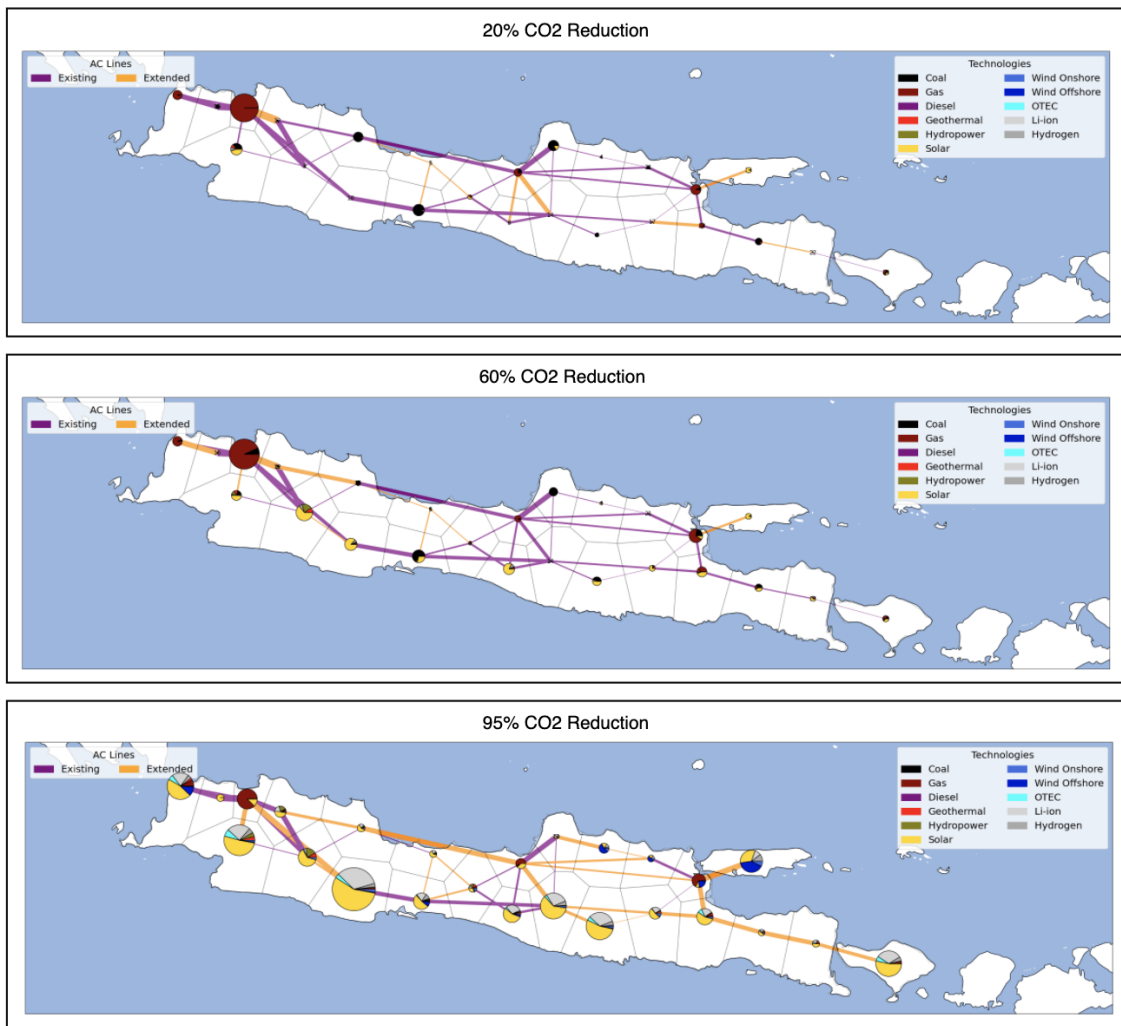


Figure 4.19: System designs as a result of different carbon reduction limits. The boxes indicate what carbon reduction limit is applied. The sizes of the pies indicate their capacities, the largest pie in the 95% reduction scenario equals approximately 38.4 GW.

Although, electricity demand has increased more than threefold compared to the electricity demand in 2018, in the first scenario network expansion is needed to deliver the produced electricity to the demand centers. This is likely caused by increasing the conventional generator capacities by five, as a result the generator capacities can be distributed throughout the system efficiently such that no network expansion is needed. In the second scenario the network capacity is more or less equal to the first presented scenario, although, very different lines were expanded. Also, the expansions are moderate, due to the spatial distribution of the renewable potentials. In the third scenario, the capacities of many transmission lines were increased. Due to the availability of solar and OTEC capacity in energy regions along the southern coast, most of the lines that connect the northern to the southern part of Java are expanded.

From the cost-optimal spatial layouts of the system in Figure B.4 it can be concluded that generator capacities are oriented differently in high carbon scenarios compared to the layout of the present system. In particular solar production has become an important source for electricity production, the capacities are concentrated along the Indian Ocean. Therefore, the system becomes more North-South oriented instead of the traditional East-West orientation.

Furthermore, with regard to both generator and network capacity expansion, there is no obvious sequence throughout the scenarios. This is, also, an expected result of the greenfield optimization approach, since investments in higher carbon scenarios are not taken into account in the lower reduction scenarios. This will be substantiated in more detail in the discussion.

4.5.2. Case 2: 2050 Forecast Cost

For the second case the cost reduction as a result of technological learning presented in section 3.4.3 are used. The scenarios follow the same carbon reduction targets as the scenarios in the previous case (except for an intermediate step (85% reduction scenario)), therefore, the results will be evaluated by comparing them to the results of case 1. For case 1 the trends were analyzed in detail, emphasis in this section will be on the differences that can be observed in case 2 rather than describing similar phenomenons. Similar to case 1 for all scenarios feasible solutions were found except for the 100% reduction scenario. In Figure 4.20 the system emissions over the carbon reduction targets are shown and the development of the shadow price of the carbon constraint. In contrast to case 1, the carbon constraint in the business as usual scenario are not binding, i.e. due to technology price reductions there is a cost-optimal solution that contains less carbon emissions than an extrapolation of the present system. In the sub-figure on the right this is reflected in a shadow price of 0 \$/tCO₂, thereafter, due to the cost reductions in renewable energy technologies the shadow price becomes significantly lower than in case 1. Only in the 95% carbon reduction scenario in case 2 higher cost reductions can be achieved by relaxing the constraint.

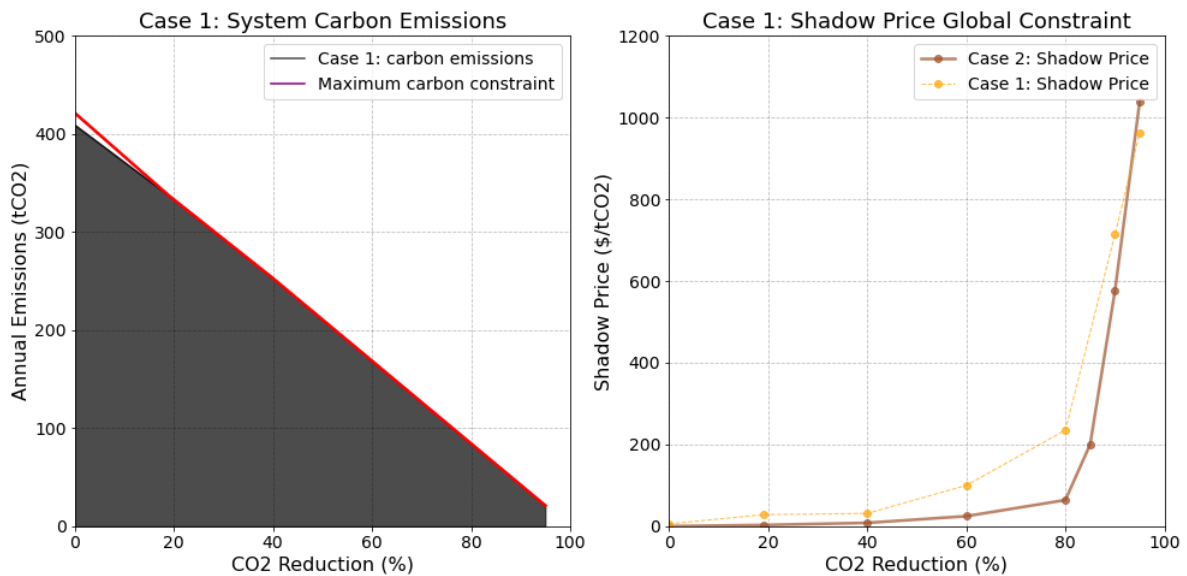


Figure 4.20: The vertical axis shows the annual system emissions in million metric tonnes, the horizontal axis represents the carbon reduction targets. The red line shows the maximum allowable emissions for the system, i.e. the global carbon constraint.

Similar to case 1 the power system capacities are visualized relative to their maximum installable potentials as a function of carbon emission reductions in Figure 4.21. Additionally, the development of network and storage capacities are illustrated in Figure 4.21. Again, the areas represent the remaining available installable potential, whereas a single solid line indicates that potentials are utilized to their full extent.

There are several striking differences in case 2 compared to case 1. Firstly, the gas capacity is not completely utilized in the high carbon scenario, while the coal capacity development is similar to that of case 1. Instead, geothermal potentials are completely deployed and solar capacity starts at about 25 GW, whereas no solar capacity was installed in case 1 in the business as usual case. Solar, also, reaches its full potential in a lower carbon reduction scenario than in case 1. Secondly, Hydropower is deployed much later due to the higher solar capacities throughout the scenarios. Accordingly, OTEC potentials are deployed only in the 90% carbon reduction scenario. Thirdly, no offshore wind capacities are used at all in case 2, instead more OTEC sites are deployed.

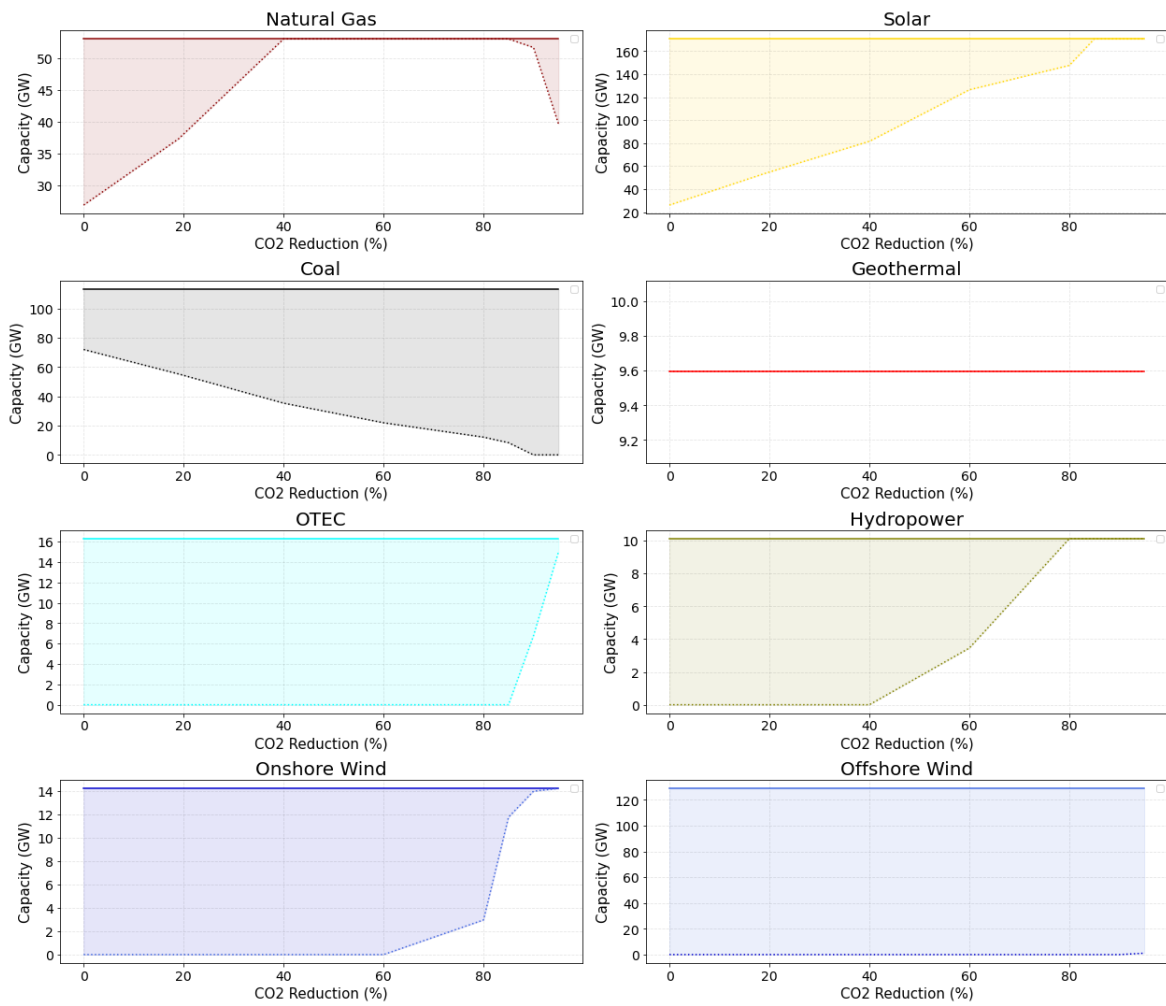


Figure 4.21: The solid line represent the maximum installable capacities of an energy technology. The surface represents the remaining available installable potential per technology and the dashed line shows the installed capacity of a technology.

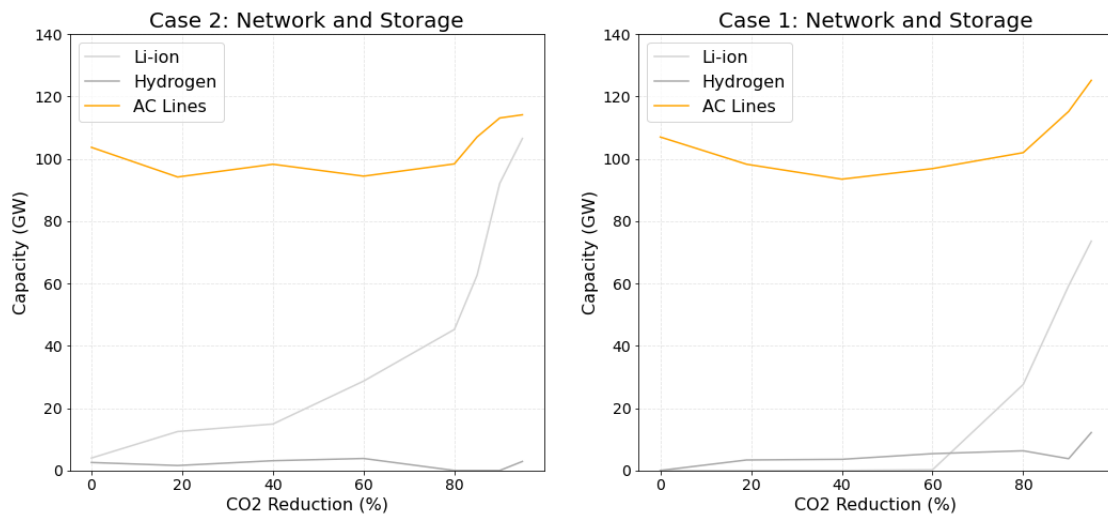


Figure 4.22: Capacity development of the network and storage as a function of carbon emissions reductions. The left sub-figure shows the capacity development in case 2, whereas the right sub-figure represents the development in case 1.

In Figure 4.22 the capacity development of storage and the network of case 2 is shown, for comparison purposes also the results for case 1 are included. There are several clear differences between the two scenarios that can be explained with the previous presented results. Firstly, the network capacities are similar, although, at 40% reductions in case 2 the capacities are slightly higher. In the higher carbon reduction scenarios (90% and 95%) in case 1 there is a larger increase in capacity. This increase can be attributed to the offshore wind capacities, which are zero in case 2. This applies to hydrogen storage as well. The most striking difference are the capacities of lithium-ion batteries, which are around 35 GW higher in case 2 in the 95% carbon reduction scenario. The lithium-ion battery capacities deployment starts in the business as usual scenario, after which the capacities show a steep increase. The battery capacity seem to be correlated to the solar capacity development until 85% carbon reductions. Afterwards, the capacities show an even larger increase due to the reduction of gas capacities. Finally, in the 95% carbon reduction scenario the lithium-ion battery capacities approach the network capacity. *Scenario Cost Development*

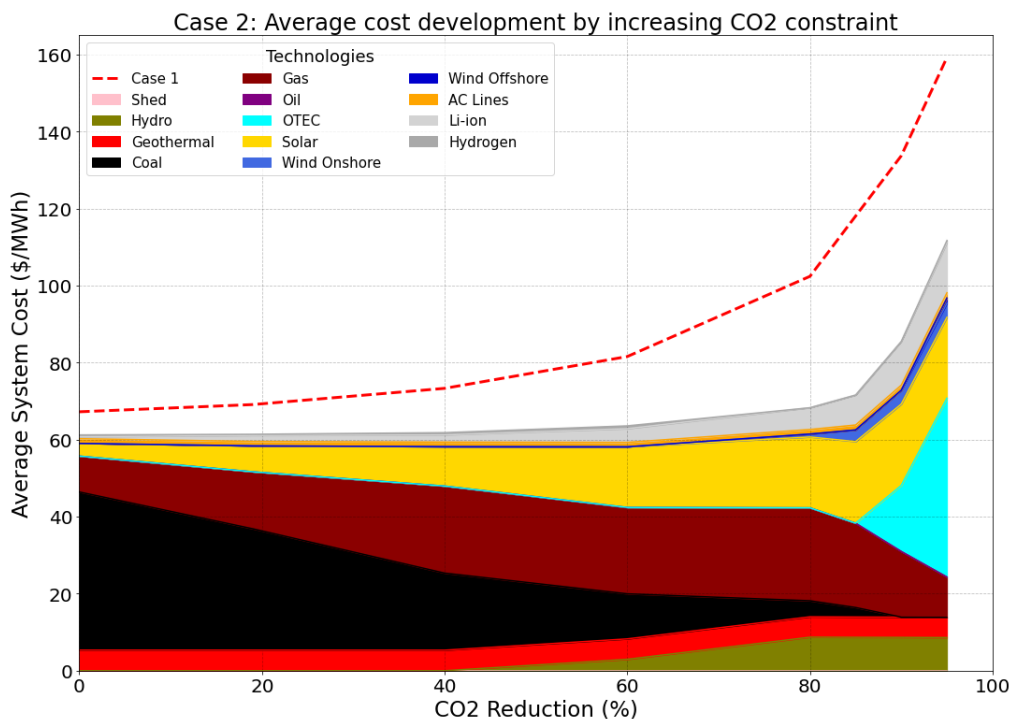


Figure 4.23: Case 2 cost results. On the horizontal axis the carbon reduction target in percentages is shown. The vertical axis shows the average cost of the system per unit of electricity produced. The dashed red line shows the cost development of case 1.

In Figure 4.24 the average cost developments as a function of carbon reductions is shown for case 2 per system component and set out against the cost results for case 1 (red dashed line). The average system costs in case 2 are lower than the costs of case 1 as a result of the technology cost reductions. A similar exponential relation is found between costs and carbon reductions, however, the cost-optimal solution space for case 2 is almost flat up to 40% carbon reductions and there is an increase of about 2 \$/MWh between the business as usual case and the 60% reduction scenario. The cost for the 80% carbon reduction scenario are 7 \$/MWh higher than the cost of the reference case. Additionally, the costs of all scenario up to 60% carbon reductions are lower than the costs of the business as usual scenario in case 1. The 80% reduction scenario in case 2 is less than 2 \$/MWh more expensive than the reference scenario in case 1. Similar to case 1, OTEC drives the system cost up in the lower carbon scenarios.

The capacity developments found in the section ?? are reflected in the spatial design of the Jamali power system. Similar to case 1, the cost-optimal system design for 20%, 60% and 95% reduction scenarios are shown in Figure 4.24 for case 2.

There are no major structural differences in the layout of the system in the 20% and 60% reduction scenarios between the two cases. In the 60% reduction scenario much more solar capacity is utilized, which is in line

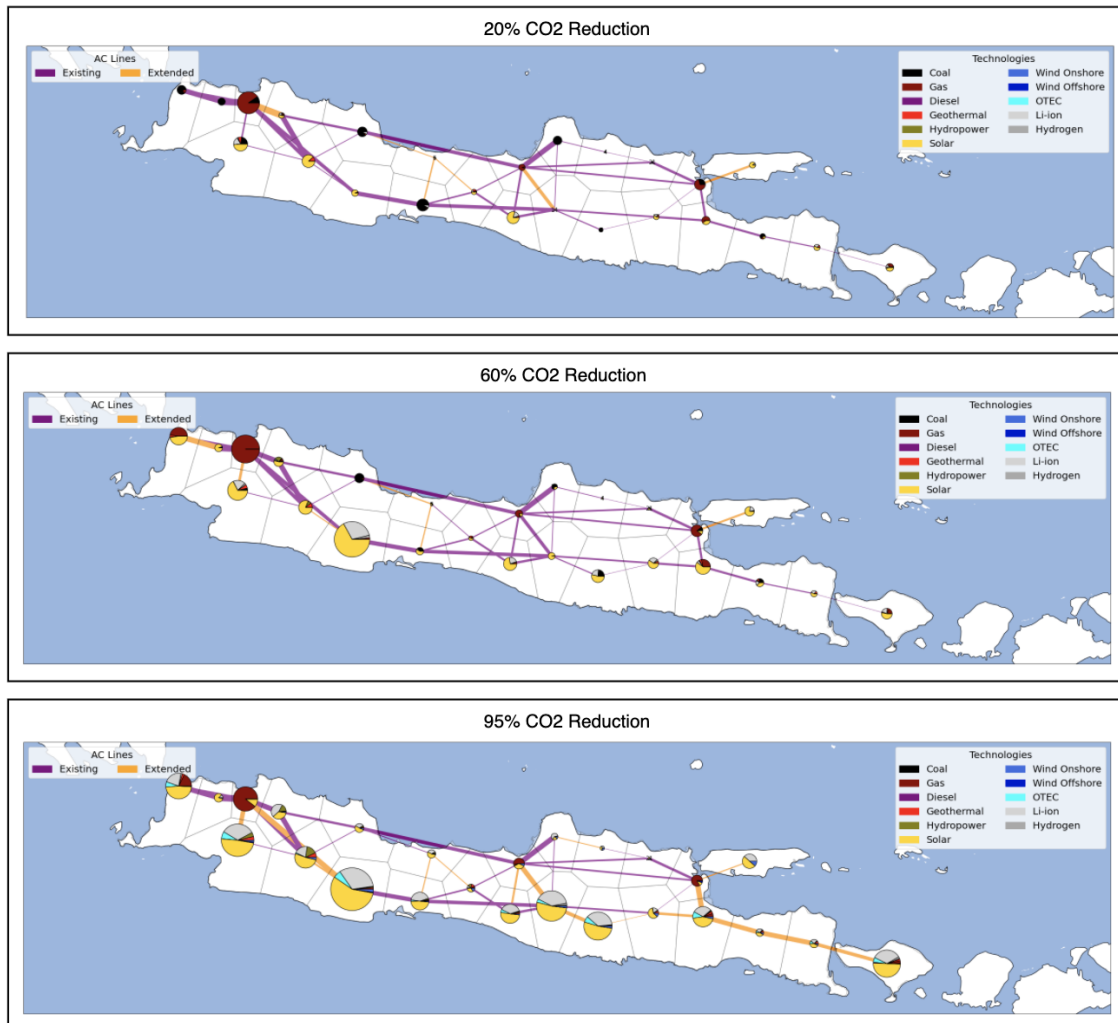


Figure 4.24: System designs as a result of different carbon reduction limits. The boxes indicate what carbon reduction limit is applied. The sizes of the pies indicate their capacities, the largest pie in the 95% reduction scenario equals approximately 38.4 GW.

with the findings presented in the previous sections. Especially, the 95% carbon reduction scenario in case 2 differs from the spatial design observed in 1, caused primarily by the replacement of offshore wind by OTEC, which requires significantly less network capacity. What is remarkable is that due to the relative constant availability of solar irradiance throughout the year, only little network expansion is needed in the cost-optimal system designs. Similar to case 1, mainly the north-south oriented lines are expanded to distribute the solar electricity production over the power system. Again, the sub-figures in Figure 4.24 cannot be read vertically due to the greenfield optimization approach.

In cases 1 and 2 a similar exponential relation between average system costs and carbon reductions was found. In case 2 average system costs are significantly lower as a result of cost reductions due to technological learning. Thereby, up to 60% carbon emission reductions in case 2 the solution space is almost flat, i.e. the cost do not increase significantly when reducing system carbon emissions up to 60%. Thereby, the cost of an optimal system with 80% carbon emissions reductions in case 2 is about 2 \$/MWh more expensive than the business as usual scenario in case 1. No major differences in spatial system designs were found between the two cases except for the scenarios with 95% carbon reductions. In case 1 the utilization of offshore wind led to significant network expansion in the Eastern half of the system (connection with Madura) and investments in hydrogen storage. In case 2 OTEC replaced the investments in offshore wind. Consequently, in the cost-optimal outcomes of the system less network expansion and hydrogen storage were included. This resulted in 35 GW more lithium-ion battery capacity that compensates for the reduction in gas capacities.

For both cases, it can be concluded that solar photovoltaics is an important renewable energy technology for electricity production in low and high carbon reduction scenarios with lithium-ion battery storage to compensate for its variability. The investments in solar capacity can be explained by its high availability throughout the year, which was illustrated in section 4.4.6 and the high estimated cost reductions of solar and lithium-ion batteries. Surprisingly, in high carbon reduction scenarios OTEC is preferred over offshore wind (especially in case 2) as was already mentioned this will be discussed extensively in the discussion. Also, major network expansion seems to be related to offshore wind production in the system. However, in the cost-optimal configuration solar dominates the energy mix, which results in transmission line expansion that interconnects regions from north to south and vice versa.

4.5.3. Case 3: The Role of OTEC

This case aims to analyze the role of OTEC in the Jamali power system in 2050. First, the investments in OTEC in the scenarios of case 2 are evaluated. Subsequently, the effect of OTEC in cost-optimal configurations of the Jamali power system on the average system cost and the spatial design is analyzed by running the 90% and 95% carbon reduction scenarios without OTEC.

OTEC is the only technology for which site specific data has been included in the model, which are presented by Langer et al. [53] and estimated by Langer et al. [54]. The potentials were not averaged or aggregated, they were solely connected to an energy region as single power plants with site specific capital cost. For other technologies uniform costs were assumed (aim of this section among others is to clarify the implications of using uniform costs). As discussed in section 3.4.1 the capital costs of OTEC power plants vary depending on the heat exchanger and power transfer costs (distance to an onshore connection point). The site specific investments per scenario are visualized in Figure 4.25.

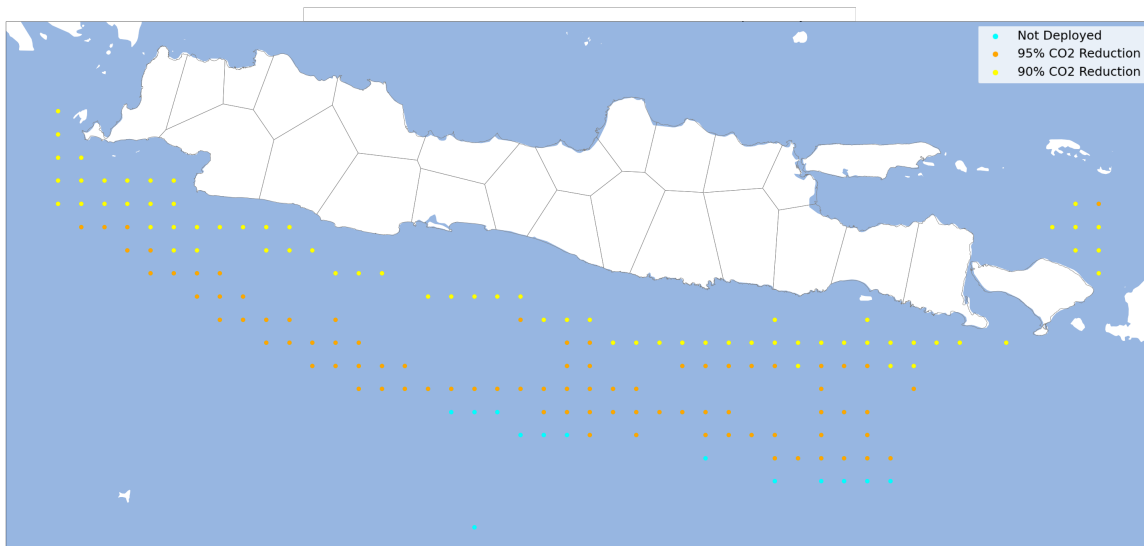


Figure 4.25: The Figure shows investments in OTEC power plants per carbon reduction scenario. The 90% scenario covers only the yellow potentials. The 95% scenario consists of the yellow and orange potentials. The sites labeled 'Not Deployed' are the remaining available potential sites.

In the 90% carbon reduction scenario about one third of the installable OTEC potential is used. As expected, these sites are located close to shore, which is cheaper compared to the sites located further away. In the 95% scenario much more of the available potential is used, also, the sites labeled 90% are included, these are cheaper and therefore invested in first. Only the sites that are the furthest away from shore are not invested in.

Although, the results are obvious, it is interesting to consider the distribution of the investments in the OTEC potentials. Especially, when considering the effect of aggregation of the latter into one energy region. Both potentials close to shore as well as the potentials further away that were included in the 95% scenario connect to the same energy regions. As a result the investments in OTEC would change when averaging these costs for a region, whereas the results show that their investment distribution is highly site specific. A similar effect for

other renewables is expected, i.e. investments in the cheaper locations before more expensive locations are deployed. And have an effect on the results, which will be mentioned in the discussion. Therefore, it would be beneficial to consider site specific data for more technologies in the model and analyze the effect of site specific technology costs and compare them to aggregated and uniform costs used in most power system models.

In order to estimate the effect of OTEC on the system costs the model was run for the 90% and 95% reduction scenarios without OTEC. With the assumptions for renewable energy potentials presented in section 4.4 this resulted in infeasible configurations. Therefore, the power density for offshore wind was set at 10 MW/km² to estimate the effect on the system costs (improvements in power/energy densities as a result of technological improvements are not considered in this thesis, however, in European models similar power densities were used). The average system costs as a function of carbon reductions is shown in Figure 4.26.

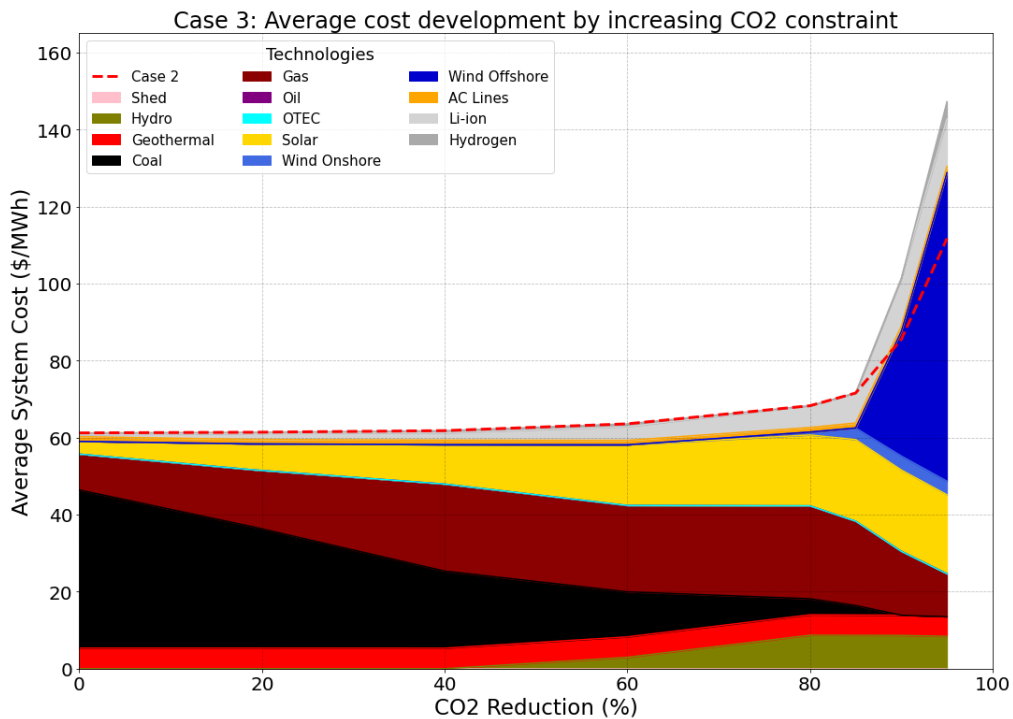


Figure 4.26: The Figure shows the development of average system costs by system components without OTEC as a function of carbon reductions. The dashed red line shows the average cost results of case 2 (with OTEC).

The average system costs till 85% carbon reductions are identical to the costs in case 2, because no OTEC was used in these scenarios. After 85% the average cost results show a much steeper increase compared to the average system costs from case 2. In case 2 solar and onshore wind capacities were at their maximum installable potential in the 85% carbon reduction scenario. Offshore wind was not used at all. To replace OTEC in the energy mix offshore wind is needed to cover the electricity demand throughout the year. As becomes apparent from Figure 4.26 offshore wind drives the average system costs up exponentially, which results in average system costs of about 146 \$/MWh for the 95% carbon reduction scenario. The costs found in case 3 for this scenario are approximately 36\$/MWh more expensive than the costs in case 2 with OTEC.

Although, less visible in Figure 4.26 the scenarios without OTEC also result in different network and storage capacities. In the next section the evolution of these capacities as a function of carbon emission reductions will be analyzed.

OTEC has a significant impact on maintaining reasonable costs in the low carbon scenarios, consequently without OTEC more capacity is required for storage and transmission lines to mitigate the variability of wind and distribute the electricity over the power system, in particular to the demand centres. The findings are shown in Figure 4.27.

Similar to the results in the previous section, the capacities in Figure 4.27 are the same until 85% carbon

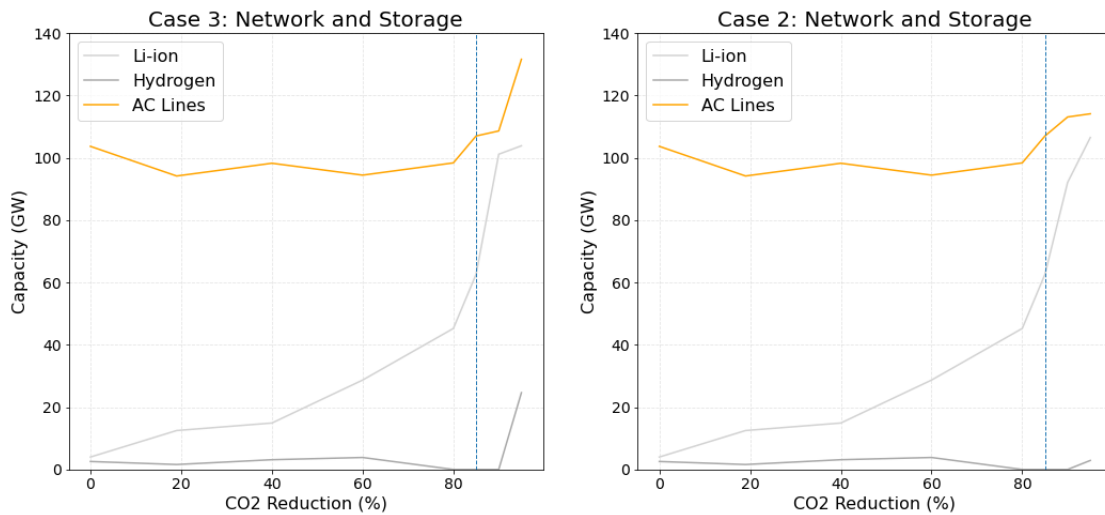


Figure 4.27: Network and storage capacities as a function of carbon reductions. In the left figure the capacities without OTEC are shown (case 3) and in the right figure the capacities with OTEC (case 2). The dashed blue line represents the 85% carbon reduction scenario, after which the cases start to diverge.

reductions, afterwards, different capacities can be observed. The capacities of lithium-ion batteries decrease slightly compared to the capacities in case 2. On the other hand, network capacities increase significantly without OTEC, whereas they only slightly increase with OTEC in the low carbon scenarios. Also, to mitigate the variability of offshore wind, significant investments in hydrogen storage capacities are made in case 3, but remain about a fifth of the lithium-ion capacities in the system.

The site specific data of OTEC provides clear insights in the optimal investment decisions made by the model. Although, the results are obvious, cheaper power plants are developed before the more expensive sites (further away from the coast), when aggregating and averaging these potentials and costs in an energy region the detail will be lost. As a result, different investment decisions will be made that lead to different (less realistic) system designs. This logic, therefore, implies the necessity of including spatial economic detail for renewable energy technologies in power system models. Spatial economic detail may result in less uniform optimal investment decisions over the energy regions. Investment decisions for offshore wind may be similar to OTEC, which also may result in earlier investments of cheaper sites close to shore. Additionally, there are large earthquake prone areas in Java, Bali and Madura, for onshore wind these were excluded. For solar panels, on the other hand, it was assumed that they can be constructed, but this would increase installment costs considerably, because higher quality support structures are needed. Which in turn decreases the uniformity in capital cost over the power system, thus resulting in different investment decisions.

In case 3 it was found that OTEC significantly reduces the average system costs in the lower carbon scenarios. If OTEC is not included as a renewable energy technology costs increase by about a quarter, because a lot of offshore wind capacity is needed to meet the electricity demand, which is highly intermittent. Here, it is useful to recall that the baseload power plants (geothermal and hydropower) are utilized to their maximum potentials and coal is almost phased out. Therefore, there is only about 20 GW baseload capacity against a peak demand of 82.4 GW. OTEC can fill this shortage in baseload (renewable) capacity well, whereas for variable technologies a lot of storage and or network expansion is needed to cover this shortage. This effect is clearly visible in Figure 4.27 in the 'case 3' sub-figure, due to the increased offshore wind capacities network and hydrogen capacities increase considerably.

4.5.4. Case 4: The Role of Storage and the High Voltage Network

In the previous cases the network and storage were unconstrained variables. In this case a single scenario from case 2 is selected to analyze the role of the high voltage network and storage capacities on the system design by varying the constraints on these variables. The 80% carbon emission reduction scenario from case 2 was selected as reference scenario for this case. This scenario was selected, because in this scenario high carbon emission reductions can be realized against moderate system cost increase relative to the business

as usual case. Different scenarios with and without network expansion and storage are evaluated in this case. Their average system cost results are visualized in Figure 4.28. The 80% carbon reduction scenario from case 2 without constraints on network expansion and storage is labeled as the 'Reference' scenario the average system costs equaled about 67 \$/MWh. In the next sections first the role of the high voltage network is discussed without constraints on storage. Thereafter, the role of storage is discussed in scenarios with constraints on storage capacities.

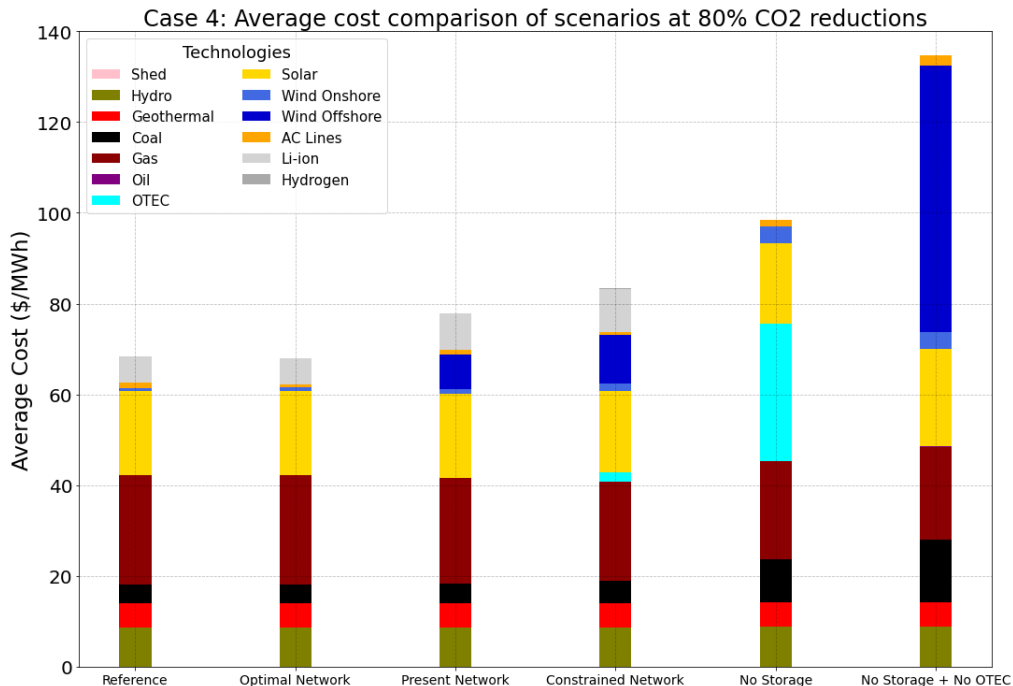


Figure 4.28: Average system cost results of scenarios in case 4.

In the previous cases the existing network was forced into the system design by a minimum constraint equal to the existing network capacities. The costs for the existing network capacities were not amortized and therefore contributed to the total system cost. In the 'Optimal Network' scenario this minimum capacity constraint on the transmission lines was removed, therefore, transmission line capacities could be optimized. No new connections between regions are included, only the existing interconnections were optimized. The optimal capacities resulted in average system cost that are a fraction lower than the reference case (0.7 \$/MWh). The cost reduction is moderate due to the small impact of network costs on the average system cost. The decrease is caused by lower capacities of transmission lines from the Eastern to the Western part of the system due to the different location of cost-optimal generator capacities in this scenario.

In the 'Present Network' scenario the high voltage network was not subject to optimization, the network capacities were fixed. A significant increase in average system cost was found as can be observed in Figure 4.28 of about 10 \$/MWh compared to the reference scenario. Due to the transmission capacities that limit the flow of power between energy regions, offshore wind capacities were needed to meet the electricity demand continuously throughout the simulation period. The spatial layout of of this scenario is visualized in Figure 4.29. As becomes apparent from the figure, the offshore wind capacity that drives up the cost is mainly installed on the island of Madura. As a result, large battery capacities are needed to balance the production and demand on the island.

To shed light on the impact of the availability of network capacities on the total system cost, a scenario without any network capacities was run, however, this led to an infeasible result. Therefore, in the 'Constrained Network' scenario, the optimal capacities of the 'Optimal Network' were reduced by 50%. This led to a cost increase of about 16 \$/MWh compared to the reference scenario.

All cases in the previous sections and the scenarios presented in this section have infinite storage capacity potential. These unconstrained capacities result in lithium-ion battery capacities of over 40 GW in the 'Refer-

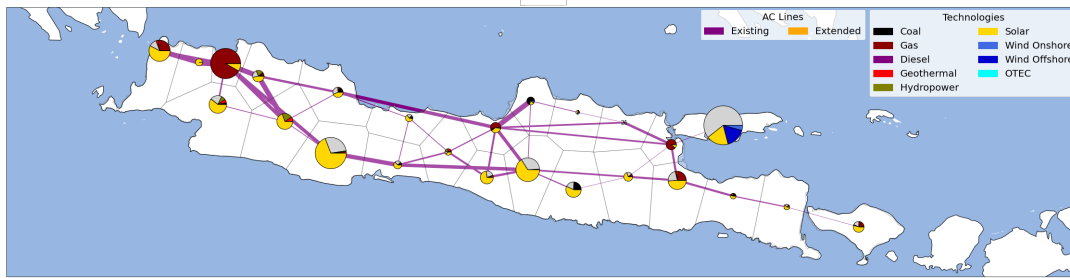


Figure 4.29: Spatial layout of the Jamali power system in scenario 'Present Network'. The largest pie equals about 35 GW

ence', 'Optimal Network' and 'Present Network' scenarios. These are considerable capacities considering the largest stationary battery facility in the world today has a power capacity of 100 MW. However, coupling to the transport sector could unleash large storage potential, this will be discussed in more detail in the discussion. Nevertheless, it is interesting to estimate what effect the battery capacities have on the system design and on the system costs. Therefore, in the scenarios 'No Storage' and 'No Storage + No OTEC' in Figure 4.28 storage capacity potentials were assumed zero. Immediately, it can be seen that the average system costs are considerably higher than the costs with unconstrained storage capacity potentials. OTEC covers a large portion of the average system costs, therefore, also a scenario without OTEC was run (with offshore wind densities of 10 MW/km^2), which results in a larger cost increase similar to the findings for case 3. Also, larger network capacities are needed, which is difficult to see in Figure 4.28. Therefore, the system layout of the 'No Storage' scenario is visualized in Figure 4.30.

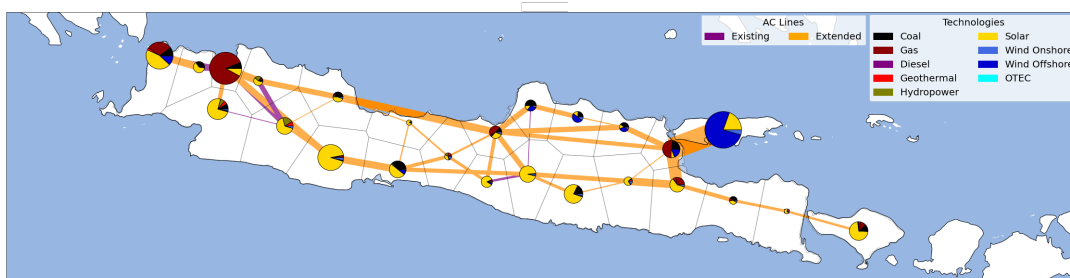


Figure 4.30: Spatial layout of the Jamali power system in scenario 'No Storage + No OTEC'. The largest pie equals about 33 GW

Figure 4.28 shows significant transmission line expansion in the 'No Storage + No OTEC' scenario. Without storage the network takes an important role in distributing electricity throughout the system to meet the load, however, it does not prevent a significant increase in system costs. This can mainly be attributed to the relatively uniform availability of solar and wind throughout the geographical extent of the Jamali power system. The network cannot provide the smoothing services it delivers in grids covering larger geographical systems such as the European grid, where it reduces the system cost up to 20% [80]. Nevertheless, a well functioning grid and line expansions remain very important factors to provide secure electricity in a future renewable Jamali power system.

For case 4 it was found that large lithium-ion battery storage capacity is essential in the establishment of an affordable low carbon Jamali power system. Moreover, system costs almost double when no storage and OTEC would be available. Furthermore, without network expansion (and with unconstrained storage capacities) average system cost increase, but remain in a plausible range with the cost-optimal reference scenario. Thereby, it is found that high voltage grid expansion cannot prevent the system costs from increasing when no storage would be included. On the other hand, network expansion is also important to prevent system costs from increasing.

4.6. Sensitivity Analysis

The model contains many different data inputs. Ideally, an one-at-a-time sensitivity analysis would be conducted to systematically investigate what parameters show the largest changes in outcomes, i.e. determine

the sensitivity of the model. In such an analysis every input parameter is changed individually, while the other parameters remain at their nominal values. However, due to the many inputs in the developed model as well as time limitations this was not an option in this thesis. Thereby, many scenarios have been computed to provide substantiated answers to the research questions, which already shows some of the model sensitivities. Therefore, only a few inputs were varied, which would provide extra insights. The focus of this narrow sensitivity analysis is on the generator capacity constraints and the estimated solar potentials and capital costs.

4.6.1. Conventional Generator Capacity Constraint

Conventional generators are constrained by five times their present installed capacities in all cases. In the cases network expansions were found in high carbon scenarios. Therefore, the capacity constrained was lifted in the 0% carbon reduction scenario to analyze what effect this constraint has on the results. The business as usual scenario was chosen, because the global carbon constraints is not binding. The spatial system layout results are shown in Figure 4.31. As can be observed without the constraint less network expansion is needed, due to the large coal capacity investments in the Jakarta region. Also, a small difference in average system cost is observed of a little under 1 \$/MWh. Therefore, it can be concluded that the generator capacity constraint is binding and that the network expansions in the higher carbon scenarios are attributable to this constraint.

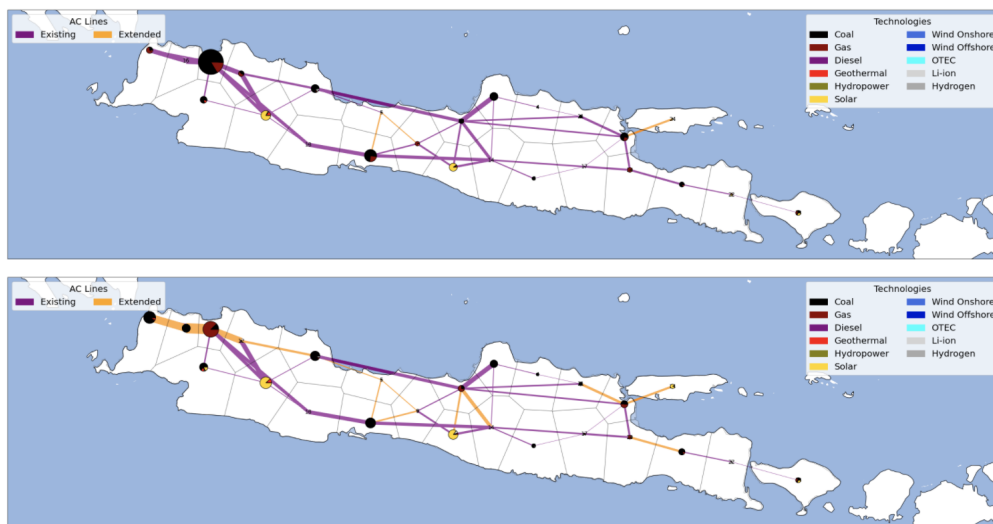


Figure 4.31: Business as usual scenario. Upper-figure represent the cost-optimal system layout without conventional generator capacity constraints. Lower-figure shows the results of business as usual scenario in case 2. The largest pie equals about 24.4 GW.

4.6.2. 100% Renewable Scenario

In the previous section it was found that given the installable renewable energy capacities a zero carbon system is infeasible. Therefore, in this section constraints are relaxed to estimate how a zero carbon system could look like and what the associated costs would be. Based on the results in the previous section, solar installable potentials were increased five fold, which means that 25% instead of 5% of their theoretical potential could be utilized. This resulted in a feasible solution for a zero carbon system, the resulting system design is depicted in Figure 4.32. The average system cost equal approximately 151 \$/MWh, which is a considerable increase from the costs found for the 95% carbon reduction scenario in case 2. Interestingly, not all available solar capacity is used (about 320 GW of the 850 GW total). Smaller increases in the available solar potential could, therefore, already result in a feasible solution. Battery power capacity surpasses 150 GW. OTEC deployed capacity is only half of the installable potential, therefore, it can be concluded that OTEC utilization depends on solar capacities. OTEC and solar potentials are mostly located in the same regions along the southern coast. Furthermore, in this scenario offshore wind capacities are utilized instead of OTEC (as was the case in the 95% carbon reduction scenario). Furthermore, especially the regions close to Jakarta have very large solar and battery capacity, since they have to supply the largest demand centers, which have little renewable energy capacity (which was in lower carbon scenarios fulfilled by gas power plants). In line with the results presented in the previous section the synergy between solar and batteries remains important when relaxing

the installable potential constraint. However, it is observed that in a cost-optimal configuration, besides solar, other energy technologies are also included, whilst there remains unused available solar capacity.

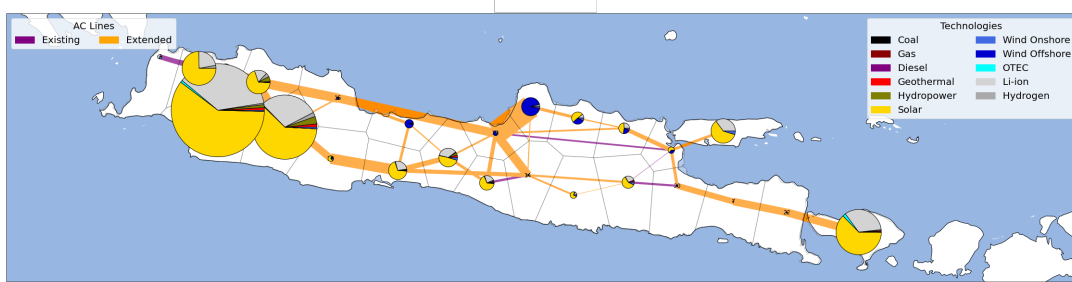


Figure 4.32: Zero carbon system layout with 25% solar capacity available for deployment of the estimated theoretical potential. The largest pie equals about 117.7 GW.

4.6.3. Solar Capital Cost

Similar to the previous section, this section also focuses on solar photovoltaics, because it was found to be an important energy technology throughout the carbon reduction scenarios. However, the focus here is on the sensitivity of the capital costs. In the 'Indonesian Power Technology' catalogue uncertainty ranges for fixed costs are included [19]. The uncertainty ranges are based on variety in costs found for 2020 and different experience indices (17.5% and 22.5% for solar). The average solar cost are 410 \$/kWh (used in case 2), whereas the lower estimate equals 310 \$/kWh and the higher estimate is 710 \$/kWh. To analyze the effect of these different cost assumptions the model was run for the 80% carbon reduction scenario. The average system cost results are shown in Figure 4.33.

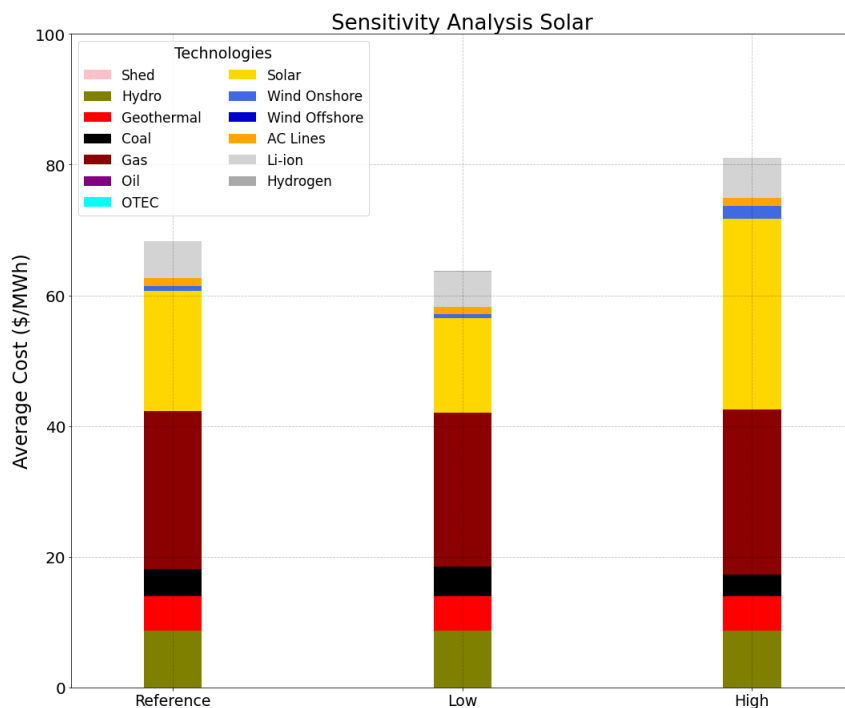


Figure 4.33: Cost sensitivity solar photovoltaics. The 'Average' bar represent the results for the 80% carbon reduction scenario found in case 2. The 'Low' bar uses the low cost assumptions and the 'High' bar the higher capital cost estimation.

Figure 4.33 shows that the cost variations do not result in different system designs, but do affect the average system costs. The lower cost estimation results in approximately 63 \$/MWh, which is in the same range as the business as usual scenario for case 2. With the higher cost estimations, the average system cost increase significantly and more onshore wind capacity is utilized. The average system cost exceed 80 \$/MWh.

5

Discussion

In this chapter the results are discussed, the chapter contains five sections. The first section starts with a comparison of the results of this thesis with results of models that applied a similar methodology for different power systems. Accordingly, differences and particularities in the results will be discussed. Thereafter, the outcomes are compared to models that focus on the Jamali power system, but did not consider the network, storage and/or renewable potentials (i). Then, the modeling assumptions and their implications are discussed (ii). Subsequently, the research approach and methodology are evaluated, shortcomings are identified and improvements are proposed. Accordingly, the implications of the simplifications on the results are discussed (iii). Then, the eligibility of the model and the results in this thesis for power system planning are mentioned by means of a critical appraisal. Thereafter, the implications of the model results for policy planning in Jamali (and more generally Indonesia) will be discussed (iv). The last section reflects on the scientific and societal contributions of this thesis (v).

5.1. Cost-Optimal Results

In case 1 and 2 a positive exponential relation was found between carbon emission reductions and system costs. First, the results are compared to model results of similar power system models that co-optimize generation, network expansion and storage. Thereafter, the results are compared to system costs found for the Jamali power system specifically. From the results two occurrences stood out in particular, the choice of OTEC over offshore wind and the need for a lot of battery capacity in the low carbon scenarios, these will be discussed.

5.1.1. Comparison to Power System Models

A similar relation between system costs and carbon reductions was found for the Chinese system [55]. On the other hand, for the European system a much more moderate relation between system costs and carbon reductions was observed [81]. Schlachtberger et al. [81], also, analyzed the effect of an increasing carbon constraint on the European system with limited network expansion, the resulting relation is comparable to the exponential increase in costs found in this thesis and by Liu et al. [55] in China. It can, therefore, be concluded that the Jamali grid cannot smooth the variability of renewable energy technologies (in particular wind) sufficiently to prevent large system cost increases in low carbon scenarios such as in the European grid.

For high carbon scenarios the costs found in this thesis are comparable to the cost found for China and higher than the costs found for the European power system [55] [81]. Interestingly, no coal power plants were invested in the Chinese model, although, the technology costs are in the same range as in this thesis, however, lower emissions were assumed due to the inclusion of open cycle gas power plants instead of the closed cycle gas power plant technology used here. In the zero carbon scenarios the costs for the Chinese system are around 100 \$/MWh and the costs for the European system below 80 \$/MWh with unconstrained network capacity. In the 95% carbon reduction scenario the costs in this thesis equal about 110 \$/MWh with OTEC and exceeds 140 \$/MWh without OTEC, whereas a zero carbon emission system was found to be infeasible with the renewable energy potentials presented in section 4.4. It should be noted that the systems are not one on one comparable, because costs assumptions by [81] Schlachtberger et al. and Liu et al. [55] are estimates for

2030, therefore, the system costs would be lower if estimates for 2050 would be used. Thereby, other authors made several different assumptions with regard to power densities of wind and solar, used different ratios for installable potentials, technologies and modeled different or more weather years. The high costs in low carbon scenarios are attributable to the maximum installable renewable potentials, solar and onshore wind reach a maximum at around 85% carbon reduction emissions compared to the business as usual scenario. As a result, investments are made in more expensive technologies like OTEC and offshore wind that drive up the average cost significantly. Interestingly, offshore wind does have a more prominent role throughout the carbon reduction scenarios in the Chinese, Vietnamese, European and systems, whereas it was not included for the South-African system. This is caused by the low availability of wind in the Jamali system, the uniform cost assumptions, the coarse resolution and the averaging of the time series at the energy regions in this thesis, this will be explained in more detail in section 5.1.3. Other authors modeled a single carbon reduction scenario for Europe, which led to similar results as found by Schlachberger et al. [81] depending on the model inputs.

Main difference between the results presented in this thesis and results from other power systems is the high use of solar photovoltaic capacity, which is favoured over wind throughout the Jamali power system due to its low seasonal variability. Accordingly, large lithium-ion battery capacity is needed to balance the diurnal cycles of solar photovoltaics. In the cost-optimal configurations of other systems much less battery capacity is needed and more hydrogen storage is used to balance the variability of on- and offshore wind, which was shown to be associated with wind production [94]. Thereby, battery capacity is needed to prevent the system costs from doubling. Only the Chinese power system model shows similar need for lithium-ion storage to maintain reasonable system costs [55].

5.1.2. Comparison to Jamali Models

Simaremare et al. [85] and Günther and Eichinger [31] modeled a 100% renewable Jamali power system, the system costs found were 83 \$/MWh and 65 \$/MWh respectively. Both models did not constrain renewable potentials instead they looked for a cost-optimal generation mix and large need for solar capacities were found. In this thesis it was shown that the maximum installable potentials cause the deployment of more expensive technologies in low carbon systems, which results in much higher system costs. Additionally, it was found that with the renewable potential assumptions and the estimated electricity demand growth a 100% renewable scenario as modeled by Simaremare et al. [85] and Günther and Eichinger [31] with the considered technologies is not feasible. On the other hand, Huber et al. [42] modeled an interconnected ASEAN (Association of East Asian Nations) system and found that all renewable technology shares should be balanced in a cost-optimal system. It was found that battery storage is only used in system with less than 100 gCO₂/kWh emissions. Thereby, the average system costs are lower than found in this thesis, because no maximum renewable capacity potentials were exceeded. More specifically, in the interconnected system Jamali became a net importer of electricity, whereas in this thesis it is modeled as an autonomous system.

The differences with the literature discussed in the previous paragraphs already indicate the value of the spatial dimension of the model, however, currently there are no 100% carbon reduction targets set by the Indonesian government [48]. Therefore, the lower carbon reduction scenarios are, also, of interest. Interesting research has been conducted by top-down modeling of the Jamali power system [34]. The authors model long-term power system planning (until 2030) of the Jamali power system while considering the impact of climate change. Several scenarios with regard to carbon reduction emissions (14% and 15%) were conducted to find out how the capacity mix would develop until 2030. Although, the results are not one on one comparable to the results found in this thesis due to different electricity demand growth, total emissions, cost assumptions and modeling approach, the carbon price for their 14% carbon reduction in the optimal scenario is in the range as the costs found in this thesis for 2020. Interestingly, they found that in the optimal scenario bio-electricity is preferred over solar and wind. Bio-electricity inclusion will be discussed in section 5.2.9.

5.1.3. OTEC and Offshore Wind

A result that can not easily be compared to previous power system modeling research are the investments in OTEC in the high carbon reduction scenarios. It was found that OTEC can prevent significant system cost increases in the low carbon scenarios. These findings correspond to the results of Fuchs Illoldi [25] who analyzed the role of OTEC in hybrid renewable energy systems on small islands and found that OTEC can con-

tribute to their energy transition in scenarios with more than 50% carbon reductions. However, considering the fact that OTEC is much more expensive than offshore wind the results in this thesis should be critically reviewed. Several reasons were identified and are discussed in the next paragraphs to evaluate what the reason for this occurrence is.

Firstly, only a single weather year is used in this thesis. As was shown in section 4.4.6 with the on- and offshore wind duration curves created from the averaged capacity factors there is a significant period during the year with little to no wind. Therefore, the weather year was validated based on wind speed data for twenty years and it can be concluded that the wind availability in 2019 does not deviate from other years the validation is added in appendix B.

Secondly, a uniform price was used for all technologies in this thesis except for OTEC. In the results it was shown that the location specific costs are a large factor in the investment decisions of the model. In fact, it is assumed that the costs for an offshore wind turbine 100 kilometer from shore are equal to a turbine very close to shore. To evaluate what effect this may have on the results the Levelized Cost Of Energy (LCOE) for offshore wind results found by Josef Sergio Simanjuntak [50] were compared to the LCOE of OTEC estimated by Langer et al. [53]. The LCOE of offshore wind is similar or lower along the south-western coast of Java than the LCOE for OTEC located within the Jamali provincial boundaries (between 0.2 USD/kWh and 0.3 USD/kWh). For the other locations (south-eastern coast and in the Indian Ocean) the LCOE for offshore wind is significantly higher between 0.35-0.45 USD/kWh close to shore and more than 0.45 USD/kWh further from shore. It can, therefore, be concluded that the uniform price used for offshore wind does have an effect on the results. Including site specific costs would, therefore, probably results in higher investments in offshore wind (close to shore). Nevertheless, most of the offshore wind capacity is located in the Java sea, the distances to shore are considerable and the wind availability is relatively low. It is, therefore, unlikely that capacities in those locations will outperform OTEC. Therefore, OTEC will still be present in the energy mix when site specific costs for offshore wind were to be included.

The last identified cause of the probable under performance of offshore wind in the model is the coarse spatial resolution used. A resolution of 25 by 25 km² was used with interpolated time series. Subsequently, the time series per grid cell were aggregated to the energy regions and averaged. As a result, the most western energy region borders both the Java sea (very low capacity factors) and the Indian Ocean (where the highest capacity factors are located), therefore, the most suitable sites disappear due to the coarse resolution and aggregation of the capacity factors.

Considering the role of OTEC in the results under the assumptions made in this thesis, it would be worthwhile to also estimate the potentials and costs of other renewable energy technologies in their early development stage and include them in bottom-up power system models (with sufficient technological detail) to assess their potential to contribute to the energy transition. Again, this differs per power system, OTEC for instance requires tropical sea surface temperatures and has, therefore, no to little potential in Europe. With the abundant availability of seawater in Indonesia, other marine technologies such as tidal and wave energy conversion may be interesting options that can contribute to the energy transition. It should be noted that OTEC is a renewable energy technology in its early development stage and there are several challenges with regard to its commercialization, therefore, also, scenarios without OTEC were conducted to assess how the cost-optimal system would develop less renewable baseload capacity. Significant cost increases due to higher deployment of offshore wind was found, which can be explained by the assumptions for offshore wind discussed in the previous paragraph.

5.1.4. Battery Capacity - Transport Sector Coupling

In the cost-optimal results of the low carbon scenarios the lithium-ion battery capacity is significant up to more than 100 GW power capacity and energy capacity of 400 GWh in the 95% carbon reduction scenario. Especially, considering that the largest stationary battery currently in operation has a power capacity of 100 MW [49]. However, an electric vehicle can have an energy capacity of 100 kWh, therefore, by conducting a back-on-the-envelope calculation the storage capacity in the 95% reduction scenario could be achieved with 4 million electric vehicles. Presently, there are around 18 million cars in use in Java. However, obviously, the electric vehicle batteries would not be dispatched as the stationary lithium-ion batteries in the model. In order to capture this more accurately coupling to the transport sector (and other sectors) could be included. For Europe it was shown that by coupling to the transport sector electric vehicles can balance the daily variations

of solar power [8], which would be ideal for the Jamali power system considering the low seasonal variability of solar irradiance throughout the year. Furthermore, for Europe it was also found that coupling to the heat sector reduces carbon emissions before any storage is needed [8]. In Indonesia with the increasing economic development the use of air-conditioning may increase significantly, which follows a similar pattern as the solar availability.

5.2. Model Discussion and Uncertainties

In this section several important modeling difficulties and uncertainties are evaluated and improvements are proposed. Within this thesis project the majority of the time has gone into the development of the model. A detailed description of all components demands a multi-disciplinary approach, therefore, simplifications and assumptions were made. In the following sections several model components and their simplifications are discussed based, thereby improvements are proposed.

5.2.1. Electricity Demand

The electricity demand profile used is a proxy scaled to the Jamali total annual power demand. An obvious improvement is the use of the actual hourly electricity demand of the Jamali power system. Except for the usage of this proxy, electricity demand has experienced insufficient attention within this thesis due to time limitations. There are several possible improvements to increase the accuracy of demand modeling.

Firstly, the demand scaling over the energy regions should be conducted not only on the population density, but also on the electricity demand of the services and industrial sector. As a result, the electricity demand will be distributed differently over the system. More specifically, demand centers will become larger, because most industry is concentrated in specific areas. Secondly, ideally demand patterns should be obtained for regions individually instead of forcing a single profile on all the regions. Bali will have a completely different electricity demand pattern than Jakarta due to its large tourism industry. Thirdly, changes in demand profiles by 2050 should be considered, although, highly uncertain. An example is adapting the demand pattern for the use of more air-conditioning in the future, the pattern might become more similar to a country such as Singapore.

5.2.2. Energy Regions

The construction of the demand regions is based on the geographical locations of the electrical substations throughout Java. Borders of regencies or provinces were not taken into account. In this thesis the choice was made to create the energy regions by the locations of the electrical buses, because no detailed spatially resolved information on demand regions could be found. PLN [73] provides information on the electricity demand per province, however, with the seven provinces the transmission network would not be properly presented in the model. The main drawback of the applied methodology is that the energy regions cover areas that may in reality not be interconnected by a distribution grid. Therefore, areas are aggregated together, which in reality have to use the transmission grid to exchange electricity. As a result, the power flow may be underestimated. The regions can be adapted by clustering within provincial boundaries.

5.2.3. Spatial Resolution

In section 5.1.3 the implications of the spatial resolution on the results (which in particular affect offshore wind) have been explained. Difficulty with the resolution is the data availability, currently there are to the author's knowledge no hourly time series openly available with higher spatial resolution. On the other hand, spatially resolved capacity factors can be obtained with tools such as PVGIS and the Global Wind Atlas, which can be used to correct the Renewables.Ninja hourly output profiles to obtain higher spatial resolution.

5.2.4. Availability Factors

Wind and solar energy have low energy densities compared to other energy technologies. As a result, they require a lot of land that can be used for other activities as well and they pollute the environment, which results in public opposition. Therefore, in this thesis land availability factors have been used to account for the land that cannot be used for the deployment of solar and wind or may by 2050 be used for different purposes. The factors are arbitrary to a certain extent, because of the uncertainty involved in the development of land use and public opposition towards solar and wind in the future. Therefore, they are also highly location dependent. As a result, estimated capacities may be considerably higher or lower. This affects the results, since

especially in low carbon scenarios maximum installable potentials have a large impact on the results.

5.2.5. Spatial-Economic Resolution

As already mentioned in section 5.1.3 and in the results, site specific data may have a large impact on cost-optimal system outcomes and on the spatial system layout. In this thesis it has a considerable impact on the offshore wind investments. Therefore, it would increase the accuracy of the model when instead of uniform prices site specific economics would be included for all technologies. However, this requires the estimation of site specific data of renewable energy resources, which is generally not widely available and may be difficult to estimate for certain technologies. Additionally, this increases the computational burden of the model, since the number of variables increases significantly.

5.2.6. Technological Learning

The assumption with regard to the uniform experience indices is very rough and may not be very accurate. Rubin et al. [78] analyzed experience indices for different technologies and found varying estimates, however, generally the experience indices for conventional technologies are lower than for renewable technologies. Nevertheless, due to the estimated accumulative predicted capacities in 2050, cost reductions between renewable and conventional technologies were large. By using technology specific learning rates the technology capital cost may become different, which affects the investment decision of the model.

Thereby, the accumulative capacities used in estimating the technological cost reductions depend on predicted global installation rates. This implies that Indonesia will be open to the global power technology market by 2050. Even if this were true, the capital costs of technologies develop over time (due to accumulated capacity) on a national level in Indonesia. Therefore, it would be better practice to model the technological cost reduction as an endogenous variable, which is determined by the power plant capacities in the system, which is more often done in bottom-up models [51]. And was implemented in the LEAP energy model for the Jamali power system [35]. However, this would require simulation periods of multiple years, i.e. a multi-horizon optimization and results in a concave optimization problem. This is discussed in more detail in section 5.3.1.

Nevertheless, the comparison between spatial system design with current costs and the design with forecast costs provides valuable insight in the potential renewable energy technologies have and will have in the future. The findings correspond to the findings of Schlachtberger et al. [81] who explored the impact of cost reductions on the system design of single generation technology components in Europe.

5.2.7. Weather Data

For wind and solar historical time series were used to determine their hourly availability throughout a year, however, variations between different years exist in particular for wind production. Therefore, multiple years should be considered to optimize a more robust power system by including the inter-year variability of weather occurrences. This increases the size of the problem and the computational burden, Pfenninger [68] described the difficulties as well as methods to include inter-year variability into energy system models. This may have a significant impact on the results, since wind availability it especially scarce in the first half of 2019. By including the previous year more electricity can be stored and may be used instead of investing in other technologies that can provide baseload electricity to meet the demand.

5.2.8. Variability OTEC and Hydropower

Wind and solar are not the only variable renewable energy technologies. Hydropower depends on precipitation occurrences and water availability, whereas OTEC's electricity production depends on sea surface and deep sea water temperatures. Temperature as well as water availability exhibits seasonal cycles, therefore, for more accurate modeling time series should be used for both technologies instead of modeling them as baseload power plants.

5.2.9. Technology Selection

Several articles in the literature review included bio-electricity as a sustainable electricity source as well as Handayani et al. [34] for the Jamali power system. In this thesis bio-electricity was not considered, which is a conservative assumptions. Considering the relatively low baseload included in the energy mix, it would likely be beneficial to use biomass as a source of electricity. With the inclusion of bio-electricity the 100% renewable

energy scenarios may become feasible. Considering the potential for solar photovoltaics, it would be interesting to also include concentrated solar power, which can complement the renewable baseload capacity in the system.

5.2.10. Temporal Resolution

The model has an hourly temporal resolution and due to hardware restrictions the results were computed with timesteps of three hours. Although, not the aim of this research, a lower temporal resolution would provide more insights in the ability of the conventional generators to ramp up and down. Thereby, the model considers the power system in its steady-state. However, also the stability of the power system on shorter time intervals is of interest and its ability to return to the steady-state after disturbances. This would require, a much more detailed modeling of the power system components, which is out of the scope of this research. However, the performance of batteries and their potential to provide ancillary services to the transmission system would be an interesting direction for research in the Jamali power system.

5.2.11. Electrical Characteristics and Power Flow

The data assumptions with regard to the electrical characteristics (reactance and thermal limits) of the transmission lines and their expansion costs have not been validated, because there is no openly official data available from PLN on types of lines currently in use in the Jamali power system. Also, when evaluating the model validation only a couple lines are loaded to their maximum value (with the 70% congestion limit) during peak demand. Additionally, only relatively small capacity extensions are necessary in the 2050 business as usual case, although, electricity demand has increased by more than 350%. Therefore, it could be that the line capacities have been overestimated (when considering the latter), either through clustering of the transmission lines or by the thermal capacity limit assumptions presented in chapter 4.

5.3. Research Approach and Methodology

This thesis followed the research approach loosely described in chapter 1. However, with the insights and experiences gained throughout this thesis, the approach is evaluated and alternatives are proposed.

5.3.1. Greenfield Optimization and Transition Pathways

This thesis adopts a greenfield optimization approach, i.e. building the system from scratch without considering installed capacities at the start of the simulation. With this approach optimal system designs can be found and with the linear optimal power flow methodology a high temporal resolution can be included that captures the variability of variable renewable energy technologies well. However, throughout this thesis the advantages of transition pathways to assist in policy planning became more apparent. Hybrid model such as Integrated Assessment Models can, for instance, be used to model transition pathways. They take a much wider approach, which includes among others several sectors and climate models, but lack sufficient temporal detail to model integration of variable renewable energy technologies [20]. Modeling transition pathways with bottom-up models (with high temporal resolution) can, on the other hand, be accomplished by including a longer temporal horizon that covers the evolution of the energy system to the target year. A longer time horizon can be included by optimizing the model on (for instance) five year intervals to determine the optimal capacity mix, network expansion and investments in storage and provide insight in the optimal pathway to a least cost system in the target year [75]. Furthermore, this can be accomplished simultaneously (perfect foresight) or with a myopic approach. Although, the results found in this thesis throughout carbon reduction scenarios show some resemblance they contain no information for the construction of a pathway to a low carbon system. The cost-optimal system outcomes as a result of different carbon emission reduction targets does not provide insight in when to start the transition and how the resulting costs relate to a rapid, slow or gradual transition to low carbon power system.

5.3.2. Deterministic Approach and Optimization

The model takes a deterministic approach, i.e. it assumes a system operator with perfect foresight and with actors behaving rationally. Presently, the Indonesian power system is a vertically integrated utility, therefore, the assumptions of a centralized social planner could be accurate if PLN aims to maximise the social welfare [93]. However, PLN has no perfect foresight and may not at all times maximise social welfare. This is reflected in the power purchase agreements in which coal generators are paid a fixed price regardless of external circumstances [76], which may create lock-ins. These kind of phenomena already undermine the

deterministic approach, because it results in PLN not being able to maximize the social welfare and minimize the cost of electricity. Additionally, both electricity demand, solar and wind availability are not known beforehand and have to be forecast, which increases the uncertainty and thus unpredictability of the system, which is completely ignored in a deterministic approach.

Furthermore, the approach and methodology contains no mechanism to test for social feasibility of the cost-optimal outcomes. Moreover, sub cost-optimal solutions as modeled by [60] may contain solutions that are more expensive, but more realistic when taking social concerns into consideration with regard to network expansion and installment of large wind and solar production facilities.

5.3.3. Consideration of Non-Technological Factors

The model takes a bottom-up approach, which describes the relations between different technologies and their interactions through the transmission system well. However, it does not cover the interaction between technical, economical, environmental and social aspects of the system, although, they may have large impact on the eventual design of the system. The model represents a future optimal state of the system, which can be used in for example backcasting to construct pathways to modeled cost-optimal system by assessing what policies are needed to get there. Another option is the use of Integrated Assessment Models, also agent based models could cover these interactions to a certain extent.

5.4. Implications for Policy Planning

The focus of the previous sections was primarily on the model and the implications of assumptions, methodology and approach on the results. However, purpose of this thesis is also to provide an independent view on the power system and if possible recommend a power system planning direction for the Jamali system based on the results. Aim of this section is to 'zoom out' and adopt a broader view. Therefore, first, the model and the results are critically appraised by considering how the results could potentially be used in policy planning. Thereafter, the implications of the presented results in this thesis are discussed for the present renewable energy targets and policies in Indonesia.

5.4.1. Critical Appraisal

The model demonstrates the techno-economic feasibility of several low carbon scenarios in the Jamali power system. The model does not tell how to get to a certain power system state in the future. By adopting a longer time horizon as discussed in section 5.3.1 insights in the optimal pathway can be generated, while maintaining a high temporal resolution [95]. On the other hand, it does tell what the costs related to these states are. As a matter of fact, through cost reductions in renewable energy technologies significant carbon reductions can be realized with very little system cost increases compared to the business as usual scenario even without considering the negative externalities of conventional power plants. Additionally, with the spatial model results trade-offs can be made with regard to network investments or storage deployment. Therefore, the results can give direction to policy makers, assist in substantiating the design of policies and the formulation of targets that envision a low carbon power system in Jamali. Although, the model is subject to simplifications and subjective judgement with regard to its inputs, it is a valuable tool to analyze future state of the system. Thereby, it exposes system dynamics, which cannot be deduced from the data components alone. However, similar to other energy economic models its accurateness remains questionable [21], because the modeled worlds cannot be benchmarked against real world occurrences (until 2050). Therefore, the model results should be used to provide insights to policy makers with regard to system dynamics and designs. Valuable insights are, for instance, that solar is favoured over wind in the Jamali power system and that there is a strong incentive to deploy solar in combination with lithium-ion batteries, whereas the costs significantly increase without such synergies. Rather than using the outcomes as predictions of future system states.

Furthermore, there is the issue of quantification of models in general and the many non-technical developments that they do not cover [26]. Although, quantification has many advantages there are factors that cannot easily or accurately be quantified. Such factors exist in the technical and economic domain (fast unexpected technology breakthroughs and/or cost reductions) and to a larger extent in the social, political and environmental domains, which are not reflected in the model at all.

The present institutions and protectionist mechanisms in Indonesia are one of the main barriers for the integration of renewable energy technologies [10]. Josef Sergio Simanjuntak [50] identified several institutional

barriers and proposed three institutional recommendations for the uptake of wind energy in Indonesia; implementation of supportive economic structures, independent regulatory body for the electricity sector and reallocation of PLN subsidies. The model does not have the ability to test and/or address such instruments accurately, because it does not consider the position of PLN as a monopolistic (non-social) central planner, in contrast it assumes perfect competition or an independent central authority that maximizes social welfare already.

Nevertheless, the model presented in this thesis and the accompanying results will be valuable resources to explore future states of the Jamali power system and provide insights to policy planners. But, the model and its results should not be used in isolation due to the limitations with regard to validation, inclusion of non-technical factors and data input subjectivity. In fact, when the model is used to assist in policy planning it should be used in combination with other quantitative and qualitative methods to create a range of possible future scenarios as described by Gambhir [26].

5.4.2. Implications for Present Targets and Policies

In the introduction the renewable energy targets set by the Indonesian government were discussed. Also, their formulation as well as how the Indonesian government aims to achieve them was explained, namely by investing in hydropower and geothermal energy. It is important to note that these targets apply to Indonesia and not to the Jamali system only. Nevertheless, Jamali is the largest power system and therefore considerable progress can be made by phasing out conventional generators and replacing them with renewable energy technologies. In this thesis it is shown that against small cost increases 80% carbon reductions can be achieved in the Jamali power system mainly by phasing out coal power plants and utilizing the solar potential in combination with batteries in 2050. In the following paragraphs, first, the findings of these implications for the renewable energy targets are discussed. Thereafter, the implications for the application of policy instruments is presented.

The importance and potential of solar energy found in this thesis contradicts with both the short- and long-term generation mix plans in RUEN and RUPTL, where solar is not considered a major renewable energy source to achieve the target set for 2050. Considering the worldwide developments and wide application of solar and wind energy in combination with the results presented this thesis it can be concluded that the present target for 2050 is sub-optimal or outdated.

The Indonesian energy system contains sufficient potential to achieve the present target for 2050 by 2030 [48]. Considering the latter in combination with the results presented in this thesis indicates that more ambitious goals for 2050 can be formulated. Especially, when taking into account that negative externalities of conventional energy resources on society are not considered. However, the 25% target will likely not be achieved by 2025 [58] [5]. Therefore, higher transparency in the methodology of setting targets is imperative. More specifically, the targets should be substantiated by the results of multiple models and thorough scenario analyses to create public support in achieving the targets, i.e. the targets should not be aspirational, but achievable. The model and results in this thesis can be perceived as a proof of concept to substantiate the formulation of more ambitious renewable energy targets. Moreover, in this thesis it was shown that it is cost-optimal to reduce coal capacities significantly, while maintaining gas capacities in the system under increasingly stringent carbon reduction targets. Therefore, carbon reduction targets for the power sector may result in lower emissions against lower prices than renewable energy targets.

To prevent aspirational targets accurate strategies and policy instruments should be selected and applied to achieve the formulated goals. However, among others unclear strategies and contradicting policies are the reason that the 2025 target will not be realized [58] [10] [5]. Important barriers are the subsidization of coal power plants (for a large part owned by PLN) and the fixed power purchase prices, which simply make renewable generated electricity not profitable [5] [58]. Even with the extrapolated technology costs for 2050 in the business as usual scenario coal remains an important technology in the cost-optimal configuration of the Jamali power system without considering any subsidies. In fact, the application and/or shift of policy instruments that focus on renewable energy technologies is of paramount importance to achieve the 31% target or more ambitious targets.

Also, large investment capital is needed to cover the costs of required renewable energy capacities. Foreign and private investors will be important actors to provide such capital [58]. Apart from a reliable regulatory

framework they will also need a grid that can accommodate the variability of renewable energy technologies. In this thesis it is shown that with higher renewable capacities in the generation mix of the Jamali system a lot of battery capacity is required as well as a reorientation of the high-voltage system. Therefore, PLN has to take a facilitating role in providing sufficient network capacity and ensure the presence and proper usage of flexibility options to provide secure electricity supply in the future. Furthermore, it was shown that without battery capacity system cost increase significantly and almost all existing transmission lines have to be expanded. Therefore, careful planning with regard to battery/network capacity is required as well as efficient and adequate operation of the latter.

In summary, although, the results of this thesis may motivate the formulation of more ambitious renewable energy targets for the Jamali power system, transparency in the creating such targets is essential. Thereby, policy instruments have to be focused on renewable energy technologies in order to achieve such targets. From the results presented in this thesis it can be concluded that renewables will not outperform conventional generators with the estimated technology costs for 2050, therefore, supportive policies are necessary.

5.5. Reflection Contributions

In this section the outcomes of this thesis are evaluated based on their scientific and societal contribution.

5.5.1. Scientific Contribution

As explicated in chapter 1 the main contribution of this thesis is the development of a power system model of the Jamali system with multiple nodes, includes the existing high-voltage network, renewable energy potentials and high temporal resolution. It can be concluded that the results of the cost-optimal Jamali power systems generate new insights into the design of a low carbon power systems, which is different from the power systems that have been modeled before. Moreover, another novelty in this thesis is the comparison of carbon reduction scenarios with and without technological learning and the inclusion of OTEC as a renewable baseload power plant in a large power system. In this thesis insights in both phenomena have been generated. And a methodology is proposed to transform georeferenced topological power system into a mathematical graph.

The power system model uses the linear optimal power flow methodology, which is implemented in the PyPSA modeling toolbox [6]. In the previous section several improvements with regard to the application of the methodology were proposed. The improvements are focused mainly on generating more valuable results for policy planning rather than on difficulties with the well developed linear optimal power flow methodology.

In hindsight the development of a complete (simplified) power system model was a time consuming process, especially, due to the data requirements related to power system components and renewable energy potentials in Indonesia. Which in itself required detailed analyses, data curation, computations and implementation of methods before the optimization could be executed. However, the Python Pandas software is excellent for the former assignments and connects seamlessly with PyPSA, which is built on Pandas.

For other research or thesis projects it is worth mentioning that in particular the availability of data is an important factor when aiming to develop a similar model as has been developed in this thesis. Without the GIS maps provided by the ESDM one map project, the development of this model would not have been possible or had to be simplified. DeCarolis et al. [21] described energy economic optimization models as 'ambitious in scope and data-intensive in nature', therefore, significant computational resources are recommended for researchers aiming to conduct a similar project. Furthermore, although, several interesting ideas for scenarios and model runs were in the making due to time limitations caused by the time intensive development of the model these could not be executed, these will be addressed in section 6.3.

5.5.2. Societal Contribution

Climate change is more pressing than ever before with the release of the sixth IPCC report. In order to prevent drastic changes in climate and the more frequent and severe weather occurrences actions have to be taken. The power sector can contribute significantly to the reduction of carbon emissions by phasing out power plants that rely on conventional fuels. More specifically, taking into consideration the large electricity demand growth in Indonesia and other developing countries, it is of paramount importance that sustainable energy technologies instead of conventional generators are deployed to cover the future demand to at least

stabilize emissions. Moreover, in this thesis it was shown that renewable energy technologies will be cost competitive by 2050, while unexpected developments that may cause rapid technology cost reductions were not taken into account. Based on these results the Jamali power system should consider a shift from the traditional coal oriented system towards a system that utilizes its abundant solar potentials and battery capacity (potentially from electric vehicles) to balance the intermittency. Thereby, the grid will have to be redesigned, since the renewable potentials are differently distributed over the islands than the conventional generation capacity as was shown in this thesis as well. Decisions related to grid operation and planning are therefore of high importance when supplying the millions of electricity consumers in Java and Bali in a renewable future and to maintain system adequacy. The results presented in this research are highly relevant for policy planning and exploring possibilities for future low carbon systems, the implications were addressed in 5.4.2. Therewith, based on cost-optimal system configurations targets can be set to realize systems that remain affordable, become clean and increase the security of supply of the Jamali power system.

6

Conclusion and Outlook

This thesis has investigated the effect of carbon constraints on the design of the Jamali power system in 2050, while considering generators, storage and the high-voltage network simultaneously. This was done by evaluating promising renewable energy and storage technologies in Java and Bali as well as the role of the transmission network. For this purpose data was collected for the potentials of renewable energy technologies and estimated if they were not available (or not suitable for use in this thesis). Thereafter, a model was developed of the Jamali power system with the PyPSA modeling toolbox and co-optimized to find the minimum system costs subject to a global carbon constraint. In this chapter, answers to the research questions presented in chapter 2 will be formulated. Thereafter, the main conclusion is formulated and a recommendation is done with regard to the (sustainable) development of the Jamali power system. Lastly, recommendations for future research are proposed.

6.1. Research Questions Revisited

This section formulates answers to each subquestion individually and closes by answering the main research question.

6.1.1. Power System Conceptualization

SQ 1: *"How can the Jamali power system be conceptualized? And how can the system be divided into energy regions?"*

The Jamali power system is conceptualized based on georeferenced maps of its transmission system, which includes locations of electrical substations and transmission lines. Energy regions could be created by clustering the electrical substations and creating a Voronoi diagram with regions closest to the clustered substations. Since, the islands of Madura and Bali are connected to one point in Java, they are conceptualized as separate regions.

6.1.2. Renewable Energy Potentials

SQ 2: *"What are spatial energy potentials of geothermal, hydropower, solar, wind and ocean thermal energy conversion in Java, Bali and Madura? And what are their hourly production profiles?"*

Only for OTEC georeferenced potentials were taken from [53] [54], which amount to 16.3 GW. For geothermal and hydropower total potentials are reported, but not georeferenced [64] [19]. The potentials are 8.64 GW and 7.1 GW respectively. The potentials for geothermal were evenly distributed over the Jamali power system based on maps with georeferenced volcanic occurrences. The hydropower potentials were located with the global hydropower gross theoretical potential database [36]. Only large potentials (larger than 30 MW) were included. For solar and on- and offshore wind potentials were estimated, the potentials that were found are 170.6 GW, 14.2 GW and 161.1 GW respectively. It can therefore be concluded that there are abundant renewable energy potentials in Java, Bali and Madura. Solar and wind time series were generated with Renewables.ninja. Solar showed little seasonal variation throughout the year, whereas wind availability is (compared to solar) relatively scarce. Hydropower and OTEC were modeled as baseload power plants, their variability has been neglected in this thesis.

6.1.3. Effect of Technological Learning

SQ 3: *"How may technology costs develop until 2050? What effect do they have on the cost-optimal configurations of the Jamali power system subject to carbon constraints?"*

Estimated technology cost reductions as a result of learning-by-doing were presented in chapter 2, accumulative capacities by 2050 are based on the technology capacity estimations in the Stated Policies and Sustainable Development scenarios developed by the International Energy Agency [43]. Based on the results of case 1 and 2 it can be concluded that technology cost reductions lead to lower system cost for all scenarios, which is an expected and obvious result. More interestingly, it was found that due to the cost reductions incurred by technological learning the system cost remain relatively stable up to 60% carbon emission reductions, whereas without cost reductions a cost increase of approximately 22% is observed. There are no major effects on the power system design (except for higher solar penetration). However, in the 95% carbon reduction scenario the model with learning cost reductions invests in OTEC (the more expensive sites) instead of offshore wind capacity, this results in considerably different expansions of the network and different need for storage capacity. It can be concluded that cost reductions have a large impact on the system costs development as a function of carbon reductions.

6.1.4. Role of OTEC

SQ4: *What is the role of OTEC potentials in the cost-optimal configuration of the Jamali power system? Under what carbon constraints and at what locations does OTEC penetrate the energy mix?*

In cost-optimal configurations of the Jamali power system in 2050 OTEC potentials are deployed in system with carbon emission reduction target of 90% and higher. Whereas, in a system without cost reductions several OTEC sites are used already at the 80% emission reduction scenario due to less lithium-ion battery capacity deployment. It is shown that the sites closest to shore are deployed before the more expensive sites, which provides valuable insights and motivation to research the spatial economic dimension of power system models. Furthermore, it was found that the deployment of OTEC as a baseload power plant can prevent considerable system cost increases, because other renewable baseload technologies are at their maximum installable potentials. Additionally, these findings relate to a system with unconstrained storage capacity potentials and network expansion. When assuming constrained storage and network capacities OTEC becomes an important baseload power plant to secure electricity production, which was shown for the 80% carbon reduction scenario and may also apply to the 60% carbon reduction scenario. Therefore, it can be concluded that OTEC can potentially contribute to the energy transition in Java, Bali and Madura as a baseload power plant and therewith prevent significant increases in the total system costs. However, as mentioned in the discussion the simplifications for offshore wind (uniform price, aggregation and averaging capacity factors, coarse spatial resolution) should be considered when interpreting the results for OTEC, which has an impact on the investment decision of the model.

6.1.5. Network and Storage

SQ 5: *How does the need for storage and network expansion evolve under increasing carbon constraints in 2050? And how do they affect the costs of the system?*

From the results in case 2 it can be concluded that network capacities remain relatively constant up to 80% carbon reductions and increase in cost-optimal configurations with higher emission reduction targets. Furthermore, without OTEC the required network expansion in the low carbon scenarios is much more significant. Thereby, it was found that an optimal network decreases the system costs only slightly. If the network capacities would not be expanded, system cost increase. A higher increase was observed when the network is constrained to 50% of its optimal capacity.

On the other hand, lithium-ion short-term storage capacity is already deployed in 0% cost-optimal carbon reduction scenarios to balance the variability of solar photovoltaics. The capacities increase significantly surpassing 100 GW total power capacity in scenarios with 90% carbon reduction targets or higher in 2050. The need for storage and transmission depends a lot on the energy mix. In case 3 where no OTEC is included, a lot of offshore wind capacity is deployed, as a result the network capacity is more than doubled and long-term hydrogen storage capacities increase accordingly. Furthermore, it was found that storage capacity in particular is necessary to maintain reasonable system cost in low carbon systems. With constrained battery capacities or no capacity at all, the system cost almost double.

It can be concluded that storage has a more significant role in maintaining reasonable system cost than the network in low carbon systems in 2050. Nevertheless, without any network capacity unfeasible solutions were found in the 80% reduction scenario, in particular due to the high demand in and around Jakarta and the low renewable potential in those regions.

6.1.6. Effect of Carbon Reductions

RQ: *"How do system cost and generation, network and storage capacities develop in cost-optimal configurations of a co-optimized Jamali power system under increasing carbon constraints moving to zero emissions in 2050?"*

Based on the answers on the previous questions and the results of case 2 it can be concluded that there is a positive exponential relation between carbon reductions and system costs. From 0% reduction emissions to a system with 60% carbon emission reductions there is little structural change in the system design and the system cost remain relatively constant. Thereafter, system cost increase exponentially due to the use of OTEC as a baseload power plant, higher short-term storage capacities and offshore wind that replaces coal and gas in the energy mix. Due to the large scale deployment of solar photovoltaics the system design changes. Large capacities of lithium-ion battery storage are needed to maintain reasonable system costs and the North-South oriented transmission lines become more important and are expanded in a cost-optimal layout of the system in contrast to the traditional East-West orientation of the power system. Furthermore, a 100% decarbonized Jamali power system was found to be infeasible given the assumptions with respect to the renewable energy potentials assumptions and the extrapolated electricity demand growth.

It can be concluded that a low carbon system (up to 80% carbon reductions) in Java, Bali and Madura can be realized in 2050 against moderate cost increases compared to the business as usual scenario. In such a system in particular the synergy between solar photovoltaics and lithium-ion batteries is important to maintain reasonable system costs. At the same time, the network cannot smooth the variability of renewables sufficiently to maintain reasonable system costs in low carbon scenarios. However, the network remains important in a system with high solar and battery capacities to distribute electricity to regions with less renewable energy capacity.

6.2. General Conclusion and Recommendation

In this section a general conclusion is formulated. Thereafter, a recommendation is done with regard to the renewable energy targets, strategies to achieve the latter and present policies related to the Jamali power system.

6.2.1. General Conclusion

In this thesis it was found that in the Jamali power system the on- and offshore wind variability cannot be smoothed spatially, i.e. there are periods during the year with little to no wind, which is likely caused by the presence of a single weather system over the geographical area of Jamali. On the other hand, due to its location in the tropics solar availability is relatively stable throughout the year. This is reflected in the results where solar is an important renewable energy technology in all scenarios. Furthermore, to balance the solar variability it was found that large lithium-ion battery capacities are needed. As a result of the battery usage the existing network does not require significant expansions. Nevertheless, the network orientation changes from East-West to North-South due to the location of renewable potentials in the low carbon systems. It was, also, found that this depends on the presence of storage, without storage considerable expansions of almost all transmission lines in the existing network were made. Due to the high estimated demand growth in low carbon systems the maximum installable potentials of renewables is an important factor in the design of the power system. This results, for instance, in high utilization of OTEC potentials. It can be concluded that significant carbon reductions in the Jamali power system can be realized against little or moderate system cost increases in 2050, which are close to the system costs of the business as usual scenario with 2020 technology costs.

6.2.2. Recommendation Power System Planning

In the discussion in section 5.4 a broader view on the results was adopted. The results generate new insights on the renewable energy targets formulated in RUEN. The results cannot be abstracted to the entire Indonesian power system, therefore, the recommendations in this section are focused on the Jamali power system

specifically. First, considering the low additional cost of carbon reductions up to 80% in the Jamali power system, renewable energy targets can be reformulated to more ambitious targets for 2050. Importantly, the targets have to be substantiated by transparent use of multiple models and scenario analyses. Additionally, solar was shown to be an important renewable energy technology. Therefore, solar photovoltaics should get a more prominent position in the present strategies to achieve the targets next to hydropower and geothermal energy. Especially, considering its high capacity potential compared to hydropower and geothermal, its modularity, short lead times and its dominance in the low carbon scenarios modeled in this thesis. Consequently, flexibility options become important, the results show that it is cost-optimal to balance solar diurnal variability with lithium-ion batteries. The high capacity for batteries found in this thesis may be unrealistic for stationary systems, however, electric vehicles may provide such capacity. Moreover, it was shown that in low carbon scenarios sufficient battery capacity is needed, otherwise network expansions are required, which results in a significant increase of the total system costs. Therefore, careful capacity planning and operation of such flexibility options is important, an independent network operator may be required to guarantee the latter and attract the necessary private investments. Flexibility options should become a fundamental part of the strategies in achieving the renewable energy targets. Although, an in depth policy analysis of the power system is not within the scope of this thesis, based on the results it can be concluded that a reconsideration of strategy and policy instruments is necessary to achieve the renewable energy targets. From a cost-optimal perspective in 2050 coal still remains an important energy source, therefore, policy instruments are necessary that promote renewable energy and conflicting policy instruments should be reconsidered such as the present subsidies on coal.

6.3. Outlook

In this thesis several interesting options for research have been identified, some of which were explored to a certain extent, but did not deliver tangible results within the time frame of this project. Thereby, not all the knowledge gaps identified in chapter 2 have been covered or were only partly addressed. Several directions are discussed and substantiated in the following sections. Notably, most of these directions arise from issues identified in the discussion in chapter 5.

6.3.1. Spatial economic Detail

The lack of spatial economic detail in power system models was identified in the literature review in 2. And has been discussed in the results and discussion. Although, with the site specific data of OTEC some insights have been developed with regard to the effect of including spatial economic detail in a power system model, no fundamental analysis was conducted. The expected effect has been discussed in the results and the discussion. To make a comparison between the modeled system dynamics of aggregated data and site specific data two issues arise. Firstly, to conduct such an analysis site specific economic data similar to that of OTEC has to be estimated for the other renewable energy technologies. Secondly, this will result in an increase of variables in the model, which is complicated by the computational burden. However, these barriers can be overcome with the correct resources.

6.3.2. Sector Coupling

An interesting option for future research would be the coupling to other sectors in the Jamali power system. Especially, with the high battery capacity found in the lower carbon scenarios, which can potentially be covered by electric vehicles in 2050. Coupling to other sectors led to interesting and valuable results in Europe [6] [94] [95]. However, as has been shown in this thesis the energy system in Java, Bali and Madura is fundamentally different than the European system due to the different geographical scale, different weather conditions, demand, spatial availability of renewable energy sources and the spatial locations of electricity demand and generation. Therefore, sector coupling will likely result in different insights as well, especially, because the European heating and transport sectors are not one on one comparable to those in Indonesia.

6.3.3. Interconnecting the Indonesian Grids

With the methodology developed in chapter 4 for the conceptualization of the power system from georeferenced data [63], also, other grids in Indonesia can be modeled. Taking into consideration the different results found by Huber et al. [42] for the ASEAN countries, the advantages of coupling the large power systems in Indonesia may result in lower system costs and more efficient usage of renewable energy potentials. Thereby, it may be of particular interest which system designs (interconnected islands) result in the highest cost savings,

while taking into consideration the costs of submarine transmission cables.

6.3.4. Indonesian Power System Modeling and System Robustness

Indonesia is prone to natural disasters, which affect the power system. As a result the Indonesian power system has to perform under harsh conditions. Therefore, it is of high interest to design a power system that has high robustness against disasters such as earthquakes, landslides, volcanic eruptions and flooding. Logically, more local solutions such as system designs with high storage capacities will be more robust against such catastrophes. However, as was shown in this thesis large demand centers such as Jakarta cannot be self-proficient in low carbon systems. Therefore, it would be beneficial to quantify the vulnerability of the network and the power system in general. In order to do so two directions are proposed.

Firstly, the natural occurrences can be modeled as a disruption in the system at a specific time instant. Subsequently, the effect can be measured by identifying where in the system load needs to be shed without optimizing the capacities of the system. Another option would be the exclusion of the system parts from the optimization to find what amount and more specifically where additional generation, storage or network capacities are needed to prevent the system from collapsing. This can also be investigated with the security constrained optimal power flow methodology in PyPSA [6].

Another direction is the use of algebraic connectivity to assess the robustness of the network. The algebraic connectivity is the second smallest eigenvalue of a graph, this was described in chapter 3. The second smallest eigenvalue of a graph indicates the degree of connectedness of a graph and the robustness of a network [23]. This measure can be used to identify critical connections in the system. Based on the critical lines the largest system disruptions can potentially be found, which can be used to simulate system network disruptions efficiently and assess the effect on load shedding or extra capacity investments.

6.3.5. Combination of Methods

In this thesis a future state of the Jamali power system is modeled. In order to do so, several simplifications were conducted such as the extrapolation of the demand by a fixed factor, a similar demand pattern as in 2018 was assumed, extrapolation of system emissions, greenfield optimization and fixed fuel prices. In the discussion the shortcomings of the approach have been discussed and it has been emphasized that the model should not be used in isolation. In fact, it should be used in combination with other quantitative modeling methods and qualitative methods that might cover unexpected future developments in society that capture technological and economical impacts better. In future research this model could be used in combination with quantitative methods such as Integrated Assessment Models or qualitative methods, which cover broader aspects of the actual world, while the techno-economic model can be used to describe the technological system dynamics.

6.3.6. El Niño

Without going into this topic in depth, it would be very interesting to estimate what the effect is of El Niño occurrences on the design of the power systems in general and more specifically in Indonesia. However, it should first be determined if El Niño occurrences are reflected in NASA MERRA-2 Reanalysis datasets, because the El Niño occurrences affect the power system through weather deviations and different demand patterns. The between 2004-2005 there was a strong El Niño event, however, from the weather year comparison in appendix B, these years do not show large deviations from other years.

Bibliography

- [1] H. Z. Al Garni and A. Awasthi. Solar pv power plants site selection: a review. *Advances in renewable energies and power technologies*, pages 57–75, 2018.
- [2] A. Blakers, M. Stocks, B. Lu, K. Anderson, and A. Nadolny. An atlas of pumped hydro energy storage. *Victoria*, 4400(11,000):300, 2017.
- [3] K. Blok and E. Nieuwlaar. *Introduction to energy analysis*. Routledge, 2017.
- [4] J. Bosch, I. Staffell, and A.D. Hawkes. Temporally-explicit and spatially-resolved global onshore wind energy potentials. *Energy*, 131:207–217, 2017.
- [5] R. Bridle. *Missing the 23 per cent target: Roadblocks to the development of renewable energy in Indonesia*. International Institute for Sustainable Development, 2018.
- [6] T. Brown, J. Hörsch, and D. Schlachtberger. Pypsa: Python for power system analysis. *arXiv preprint arXiv:1707.09913*, 2017.
- [7] T. Brown, T. Bischof-Niemz, K. Blok, C. Breyer, H. Lund, and B.V. Mathiesen. Response to ‘burden of proof: A comprehensive review of the feasibility of 100% renewable-electricity systems’. *Renewable and sustainable energy reviews*, 92:834–847, 2018.
- [8] T. Brown, D. Schlachtberger, A. Kies, S. Schramm, and M. Greiner. Synergies of sector coupling and transmission reinforcement in a cost-optimised, highly renewable european energy system. *Energy*, 160:720–739, 2018.
- [9] C. Budischak, D. Sewell, H. Thomson, L. Mach, D.E. Veron, and W. Kempton. Cost-minimized combinations of wind power, solar power and electrochemical storage, powering the grid up to 99.9% of the time. *journal of power sources*, 225:60–74, 2013.
- [10] P.J. Burke, J. Widnyana, Z. Anjum, E. Aisbett, B. Resosudarmo, and K.G.H. Baldwin. Overcoming barriers to solar and wind energy adoption in two asian giants: India and indonesia. *Energy Policy*, 132:1216–1228, 2019.
- [11] L. Byers, J. Friedrich, R. Hennig, A. Kressig, X. Li, C. McCormick, and L.M. Valeri. A global database of power plants. *World Resour. Inst*, 18, 2018.
- [12] A.A. Cahyaningwidi. Assessment of economic potential of ocean thermal energy conversion in indonesia: A spatial approach. 2018.
- [13] C. Chalkiadakis. Otec resource potential mapping: A spatial assessment, including" state of the art" practicable criteria by using geo-information systems (gis). 2017.
- [14] E.J.L. Chappin, G.P.J. Dijkema, K.H. van Dam, and Z. Lukszo. Modeling strategic and operational decision-making an agent-based model of electricity producers. In *Proceedings of the 21st annual European Simulation and Modelling Conference (ESM2007)*, St. Julian's, Malta, pages 22–24, 2007.
- [15] S. Chatzivasileiadis. Lecture notes on optimal power flow (opf). *arXiv preprint arXiv:1811.00943*, 2018.
- [16] Tokyo Electric Power Services Co. Preparatory Survey on Central and West Java 500kV Transmission Line Project. Technical report, Japan International Cooperation Agency, 2012.
- [17] S. Collins, J.P. Deane, and B. Gallachóir. Adding value to eu energy policy analysis using a multi-model approach with an eu-28 electricity dispatch model. *Energy*, 130:433–447, 2017.
- [18] National Energy Council. Indonesia energy outlook - 2019, 2019.

- [19] National Energy Council. Technology data for the Indonesian power sector: Catalogue for generation and storage of electricity, 2021.
- [20] F. Creutzig, P. Agoston, J.C. Goldschmidt, G. Luderer, G. Nemet, and R.C. Pietzcker. The underestimated potential of solar energy to mitigate climate change. *Nature Energy*, 2(9):1–9, 2017.
- [21] J.F. DeCarolis, K. Hunter, and S. Sreepathi. The case for repeatable analysis with energy economy optimization models. *Energy Economics*, 34(6):1845–1853, 2012.
- [22] Energy Exemplar. Plexos® simulation software. <https://energyexemplar.com/products/plexos-simulation-software/>. Accessed: 2021-01-30.
- [23] M. Fiedler. Algebraic connectivity of graphs. *Czechoslovak mathematical journal*, 23(2):298–305, 1973.
- [24] M.M. Frysztacki, J. Hörsch, V. Hagenmeyer, and T. Brown. The strong effect of network resolution on electricity system models with high shares of wind and solar. *Applied Energy*, 291:116726, 2021.
- [25] J. Fuchs Illoldi. Optimal configuration of hybrid renewable energy systems for islands’ energy transition. 2017.
- [26] A. Gambhir. Planning a low-carbon energy transition: what can and can’t the models tell us? *Joule*, 3(8):1795–1798, 2019.
- [27] H.C. Gils, Y. Scholz, T. Pregger, D.L. de Tena, and D. Heide. Integrated modelling of variable renewable energy-based power supply in Europe. *Energy*, 123:173–188, 2017.
- [28] R.S. Go, F.D. Munoz, and J.P. Watson. Assessing the economic value of co-optimized grid-scale energy storage investments in supporting high renewable portfolio standards. *Applied Energy*, 183:902–913, 2016.
- [29] S. Gross. Renewables, land use, and local opposition in the United States. *Brookings Institution*, January, 2020.
- [30] N. Gunningham. Managing the energy trilemma: The case of Indonesia. *Energy Policy*, 54:184–193, 2013.
- [31] M. Günther and M. Eichinger. Cost optimization for the 100% renewable electricity scenario for the Java-Bali grid. *International Journal of Renewable Energy Development*, 7(3), 2018.
- [32] A. Hagberg, P. Swart, and D. Chult. Exploring network structure, dynamics, and function using networkx. Technical report, Los Alamos National Lab. (LANL), Los Alamos, NM (United States), 2008.
- [33] D. Hakam. Nodal pricing: The theory and evidence of Indonesia power system. *International Journal of Energy Economics and Policy*, 8(6):135–147, 2018.
- [34] K. Handayani, Y. Krozer, and T. Filatova. Trade-offs between electrification and climate change mitigation: An analysis of the Java-Bali power system in Indonesia. *Applied Energy*, 208:1020–1037, 2017.
- [35] K. Handayani, Y. Krozer, and T. Filatova. From fossil fuels to renewables: An analysis of long-term scenarios considering technological learning. *Energy Policy*, 127:134–146, 2019.
- [36] O. Hoes, L.J.J. Meijer, R.J. Van Der Ent, and N.C. Van De Giesen. Systematic high-resolution assessment of global hydropower potential. *PLoS One*, 12(2):e0171844, 2017.
- [37] Y. Hofman, D. de Jager, E. Molenbroek, F. Schilig, and M. Voogt. The potential of solar electricity to reduce CO₂ emissions. *Utrecht, Ecofys*, 106, 2002.
- [38] J. Hörsch and T. Brown. The role of spatial scale in joint optimizations of generation and transmission for European highly renewable scenarios. In *2017 14th International Conference on the European Energy Market (EEM)*, pages 1–7. IEEE, 2017.
- [39] J. Hörsch and J. Calitz. Pypsa-za: Investment and operation co-optimization of integrating wind and solar in South Africa at high spatial and temporal detail. *arXiv preprint arXiv:1710.11199*, 2017.

- [40] J. Hörsch, F. Hofmann, D. Schlachtberger, and T. Brown. Pypsa-eur: An open optimisation model of the european transmission system. *Energy Strategy Reviews*, 22:207–215, 2018.
- [41] J. Hörsch, H. Ronellenfitsch, D. Witthaut, and T. Brown. Linear optimal power flow using cycle flows. *Electric Power Systems Research*, 158:126–135, 2018.
- [42] M. Huber, A. Roger, and T. Hamacher. Optimizing long-term investments for a sustainable development of the asean power system. *Energy*, 88:180–193, 2015.
- [43] IEA. World energy outlook 2019. *International Energy Agency*, 2019.
- [44] IESR. A roadmap for indonesia’s power sector: How renewable energy can power java-bali and sumatra. *Institute for Essential Services Reform*, 2019.
- [45] IESR. Beyond 207 gigawatts: Unleashing indonesia’s solar potential. *Institute for Essential Services Reform*, 2021.
- [46] IRENA. Ocean thermal energy conversion, technology brief. 2014.
- [47] IRENA. Battery storage for renewables: Market status and technology outlook. *International Renewable Energy Agency, Abu Dhabi*, 2015.
- [48] IRENA. Renewable energy prospects: Indonesia, a remap analysis. 2017.
- [49] IRENA. Innovation landscape brief: Utility-scale batteries. 2019.
- [50] S. Josef Sergio Simanjuntak. Techno-economic and institutional assessment of wind energy in indonesia: A spatial evaluation of wind energy potential and its pertinent institutions. 2021.
- [51] S. Kahouli-Brahmi. Technological learning in energy–environment–economy modelling: A survey. *Energy policy*, 36(1):138–162, 2008.
- [52] V. Krishnan, J. Ho, B.F. Hobbs, A.L. Liu, J.D. McCalley, M. Shahidehpour, and Q.P. Zheng. Co-optimization of electricity transmission and generation resources for planning and policy analysis: review of concepts and modeling approaches. *Energy Systems*, 7(2):297–332, 2016.
- [53] J. Langer, A.A. Cahyaningwidi, C. Chalkiadakis, J. Quist, O. Hoes, and K. Blok. Plant siting and economic potential of ocean thermal energy conversion in indonesia a novel gis-based methodology. *Energy*, 224:120121, 2021.
- [54] J. Langer, J. Quist, and K. Blok. Upscaling scenarios for ocean thermal energy conversion in indonesia including technological learning. *Unpublished manuscript*, 2021.
- [55] H. Liu, T. Brown, G.B. Andresen, D.P. Schlachtberger, and M. Greiner. The role of hydro power, storage and transmission in the decarbonization of the chinese power system. *Applied Energy*, 239:1308–1321, 2019.
- [56] X. Luo, J. Wang, M. Dooner, and J. Clarke. Overview of current development in electrical energy storage technologies and the application potential in power system operation. *Applied energy*, 137:511–536, 2015.
- [57] B.V. Mathiesen, H. Lund, D. Connolly, H. Wenzel, P.A. Østergaard, B. Möller, S. Nielsen, I. Ridjan, P. Karnøe, and K. Sperling. Smart energy systems for coherent 100% renewable energy and transport solutions. *Applied Energy*, 145:139–154, 2015.
- [58] M. Maulidia, P. Dargusch, P. Ashworth, and F. Ardiansyah. Rethinking renewable energy targets and electricity sector reform in indonesia: A private sector perspective. *Renewable and Sustainable Energy Reviews*, 101:231–247, 2019.
- [59] A. Molod, L. Takacs, M. Suarez, and J. Bacmeister. Development of the geos-5 atmospheric general circulation model: Evolution from merra to merra2. *Geoscientific Model Development*, 8(5):1339–1356, 2015.

- [60] F. Neumann and T. Brown. The near-optimal feasible space of a renewable power system model. *Electric Power Systems Research*, 190:106690, 2021.
- [61] I. Nikolic, Z. Lukszo, E.J.L. Chappin, M. Warnier, J.H. Kwakkel, P.W.G. Bots, and F.M. Brazier. Guide for good modelling practice in policy support. 2019.
- [62] Y. Noorollahi, R. Ghasempour, and S. Jalilinasrabady. A gis based integration method for geothermal resources exploration and site selection. *Energy Exploration & Exploitation*, 33(2):243–257, 2015.
- [63] Ministry of Energy and Mineral Resources (MEMR). Arcgis rest services of memr geoportal. https://geoportal.esdm.go.id/monaresia/rest/services/4.GEOLOGI/Kebencanaan_Geologi/MapServer, n.d.
- [64] Ministry of Energy and Mineral Resources Republic of Indonesia. Handbook of energy and economic statistics of indonesia, 2019.
- [65] Ministry of Environment and Forestry (MoEF). Arcgis rest services of moef geoportal. https://geoportal.menlhk.go.id/arcgis/rest/services/KLHK_EN, 2017.
- [66] Gurobi Optimization. Gurobi optimizer. <http://www.gurobi.com>. Accessed: 2021-03-30.
- [67] R. Pelc and R.M. Fujita. Renewable energy from the ocean. *Marine Policy*, 26(6):471–479, 2002.
- [68] S. Pfenninger. Dealing with multiple decades of hourly wind and pv time series in energy models: A comparison of methods to reduce time resolution and the planning implications of inter-annual variability. *Applied energy*, 197:1–13, 2017.
- [69] S. Pfenninger and J. Keirstead. Renewables, nuclear, or fossil fuels? scenarios for great britain’s power system considering costs, emissions and energy security. *Applied Energy*, 152:83–93, 2015.
- [70] S. Pfenninger and B. Pickering. Calliope: a multi-scale energy systems modelling framework. *Journal of Open Source Software*, 3(29):825, 2018.
- [71] S. Pfenninger and I. Staffell. Long-term patterns of european pv output using 30 years of validated hourly reanalysis and satellite data. *Energy*, 114:1251–1265, 2016.
- [72] S. Pfenninger, A. Hawkes, and J. Keirstead. Energy systems modeling for twenty-first century energy challenges. *Renewable and Sustainable Energy Reviews*, 33:74–86, 2014.
- [73] PLN. Pln statistics 2018. *Perusahaan Listrik Negara*, 2018.
- [74] PLN. Rencana usaha penyediaan tenaga listrik (ruptl) pln. *Perusahaan Listrik Negara*, 2019.
- [75] M.G Prina, G. Manzolini, D. Moser, B. Nastasi, and W. Sparber. Classification and challenges of bottom-up energy system models-a review. *Renewable and Sustainable Energy Reviews*, 129:109917, 2020.
- [76] PWC. Power in indonesia: Investment and taxation guide. *Price Waterhouse Coopers*, 2017.
- [77] H.K. Ringkjøb, P.M. Haugan, and I.M. Solbrekke. A review of modelling tools for energy and electricity systems with large shares of variable renewables. *Renewable and Sustainable Energy Reviews*, 96:440–459, 2018.
- [78] E.S. Rubin, I.M.L. Azevedo, P. Jaramillo, and S. Yeh. A review of learning rates for electricity supply technologies. *Energy Policy*, 86:198–218, 2015.
- [79] P. Schavemaker and L. Van der Sluis. *Electrical power system essentials*. John Wiley & Sons, 2017.
- [80] D.P. Schlachtberger, T. Brown, S. Schramm, and M. Greiner. The benefits of cooperation in a highly renewable european electricity network. *Energy*, 134:469–481, 2017.
- [81] D.P. Schlachtberger, T. Brown, M. Schäfer, S. Schramm, and M. Greiner. Cost optimal scenarios of a future highly renewable european electricity system: Exploring the influence of weather data, cost parameters and policy constraints. *Energy*, 163:100–114, 2018.

- [82] M. Schlott, B. Schyska, D.T. Viet, V. Van Phuong, D.M. Quan, M.P. Khanh, F. Hofmann, L. von Bremen, D. Heinemann, and A. Kies. Pypsa-vn: An open model of the vietnamese electricity system. In *2020 5th International Conference on Green Technology and Sustainable Development (GTSD)*, pages 253–258. IEEE, 2020.
- [83] D. Setyawan. Assessing the current indonesia's electricity market arrangements and the opportunities to reform. *Int. Journal of Renewable Energy Development*, 3(1):2014, 2013.
- [84] H.A. Setyowati, M.P. Dwinugroho, B.S. Sigit Heru Murti, A Yulianto, N.E. Ajiwihanto, J. Hadinata, and A.K. Sanjiwana. Esdm one map indonesia indonesia: Opportunities and challenges to support one map policy based on applied web-gis. In *IOP Conference Series: Earth and Environmental Science*, volume 165, page 012021. IOP Publishing, 2018.
- [85] A.A. Simaremare, A. Bruce, and I. MacGill. Least cost high renewable energy penetration scenarios in the java bali grid system. In *Proceedings of 2017 Asia Pacific Solar Research Conference*, pages 1–13, 2017.
- [86] D. Spielman. Spectral graph theory. *Combinatorial scientific computing*, 18, 2012.
- [87] I. Staffell and S. Pfenninger. Using bias-corrected reanalysis to simulate current and future wind power output. *Energy*, 114:1224–1239, 2016.
- [88] M. Stocks, A. Blakers, C. Cheng, and B. Lu. Towards 100% renewable electricity for indonesia: the role for solar and pumped hydro storage. In *2019 International Conference on Technologies and Policies in Electric Power & Energy*, pages 1–4. IEEE, 2019.
- [89] H.G. Svendsen and O. Spro. Powergama: A new simplified modelling approach for analyses of large interconnected power systems, applied to a 2030 western mediterranean case study. *Journal of Renewable and Sustainable Energy*, 8(5):055501, 2016.
- [90] T. Tröndle, J. Lilliestam, S. Marelli, and S. Pfenninger. Trade-offs between geographic scale, cost, and infrastructure requirements for fully renewable electricity in europe. *Joule*, 4(9):1929–1948, 2020.
- [91] A.J. Veldhuis and A.H.M.E. Reinders. Reviewing the potential and cost-effectiveness of grid-connected solar pv in indonesia on a provincial level. *Renewable and Sustainable Energy Reviews*, 27:315–324, 2013.
- [92] A.J. Veldhuis and A.H.M.E. Reinders. Reviewing the potential and cost-effectiveness of off-grid pv systems in indonesia on a provincial level. *Renewable and Sustainable Energy Reviews*, 52:757–769, 2015.
- [93] M. Ventosa, P. Linares, and I.J. Pérez-Arriaga. Power system economics. In *Regulation of the Power Sector*, pages 47–123. Springer, 2013.
- [94] M. Victoria, K. Zhu, T. Brown, G.B. Andresen, and M. Greiner. The role of storage technologies throughout the decarbonisation of the sector-coupled european energy system. *Energy Conversion and Management*, 201:111977, 2019.
- [95] M. Victoria, K. Zhu, T. Brown, G.B. Andresen, and M. Greiner. Early decarbonisation of the european energy system pays off. *Nature communications*, 11(1):1–9, 2020.
- [96] D.B. West. *Introduction to graph theory*, volume 2. Prentice hall Upper Saddle River, 2001.
- [97] WorldPOP. Indonesia 100m population. alpha version 2010, 2015 and 2020 estimates of numbers of people per pixel (ppp) with national totals adjusted to match un population division estimates. <https://www.worldpop.org/doi/10.5258/SOTON/WP00114>, 2014.

A

A1

Manually Combines Lines by 'objet ID'			
150 kV Lines		500 kV Lines	
396	848	4	296
742	743	11	110
742 (Connection Java - Madura)	735	113	757
740 (Connection Java - Bali)	743	114	800
750	751	330	458
774	810	811	100
790	791		
895	903		
901	876		

B

B1

The 2019 wind weather year was validated by comparing it to twenty weather years. For an onshore location Longitude: 107.67096 and Latitude: -7.35483 and an offshore location Longitude: 114.64508 and Latitude: -6.38694. A duration curve was created and mean, median, variance, maximum and minimum wind speeds were calculated for each wind year.

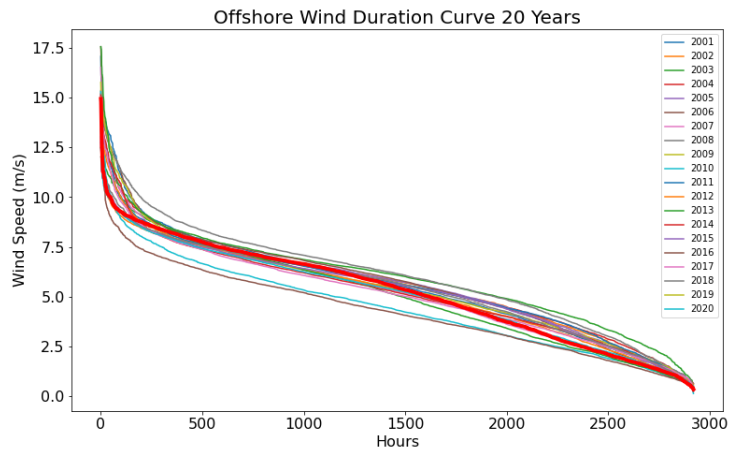


Figure B.1: Duration curve offshore wind. The thick red line represent the 2019 weather year.

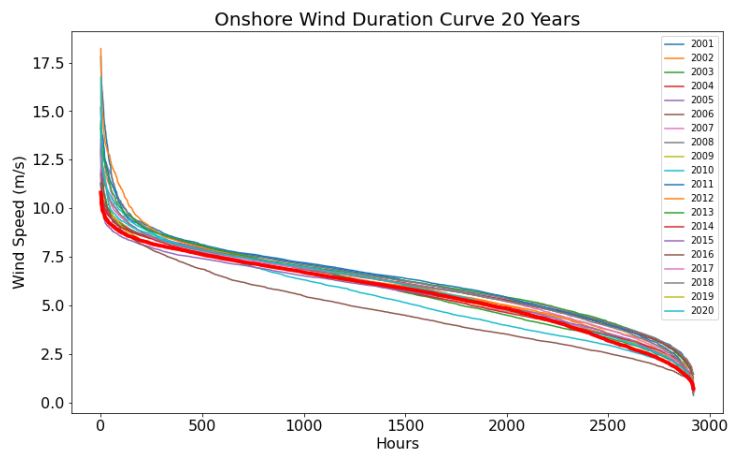


Figure B.2: Duration curve onshore wind. The thick red line represent the 2019 weather year.

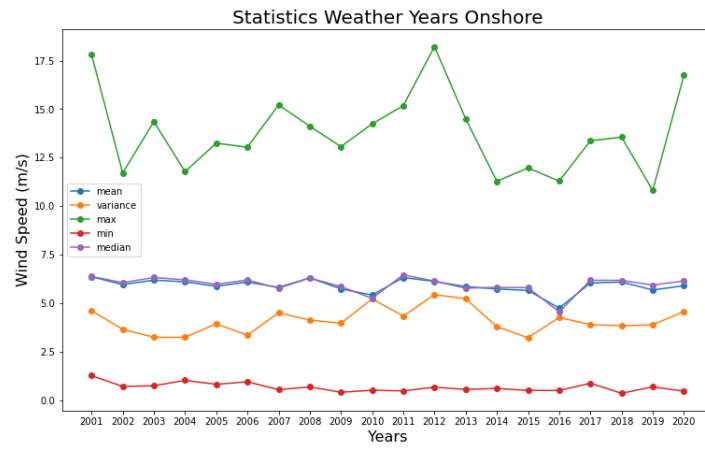


Figure B.3: Statistics offshore wind.

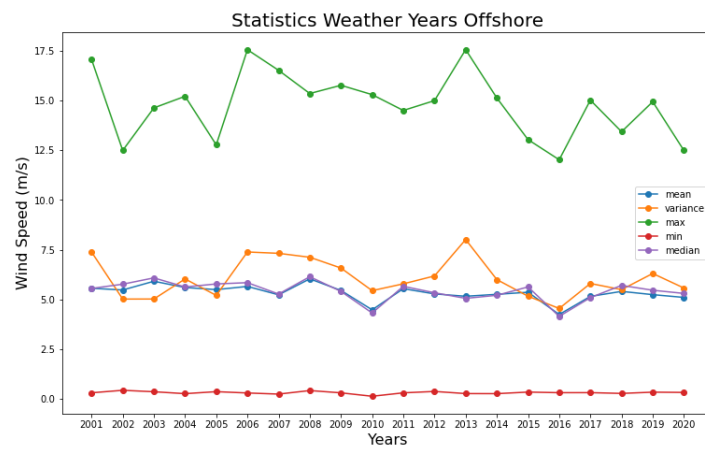


Figure B.4: Statistics onshore wind.